FOSSIL ENERGY

DOE/BC/14994-7
OSTI ID: 9319

WATER INFLUX, AND ITS EFFECT ON OIL RECOVERY: PART 1. AQUIFER FLOW

SUPRI TR 103

By
William E. Brigham

June 1997

Work Performed Under Contract No. DE-FG22-96BC14994

Stanford University
Stanford, California

National Petroleum Technology Office
U. S. DEPARTMENT OF ENERGY
Tulsa, Oklahoma

DISCLAIMER

Portions of this document may be illegible in electronic image products. Images are produced from the best available original document.

DOE/BC/14994-7
Distribution Category UC-122

Water Influx, and Its Effect on Oil Recovery:
Part 1. Aquifer Flow

SUPRI TR 103

By
William E. Brigham

June 1997

Work Performed Under Contract DE-FG22-96BC14994

Prepared for
U.S. Department of Energy
Assistant Secretary for Fossil Energy

Thomas Reid, Project Manager
National Petroleum Technology Office
P.O. Box 3628
Tulsa, OK 74101

Prepared by
Stanford University
Petroleum Engineering Department
65 Green Earth Sciences Bldg.
Stanford, CA 94305

Table of Contents

List of Tables

List of Figures

Abstract

Natural water encroachment is commonly seen in many oil and gas reservoirs. In fact, overall, there is more water than oil produced from oil reservoirs worldwide. Thus it is clear that an understanding of reservoir/aquifer interaction can be an important aspect of reservoir management to optimize recovery of hydrocarbons. Although the mathematics of these processes are difficult, they are often amenable to analytical solution and diagnosis. Thus this will be the ultimate goal of a series of reports on this subject.

This first report deals only with aquifer behavior, so it does not address these important reservoir/aquifer issues. However, it is an important prelude to them, for the insight gained gives important clues on how to address reservoir/aquifer problems.

In general when looking at aquifer flow, there are two convenient inner boundary conditions that can be considered; constant pressure or constant flow rate. There are three outer boundary conditions that are convenient to consider; infinite, closed and constant pressure. And there are three geometries that can be solved reasonably easily; linear, radial and spherical. Thus there are a total of eighteen different solutions that can be analyzed.

The information in this report shows that all of these cases have certain similarities that allow them to be handled fairly easily; and, though the solutions are in the form of infinite series, the effective results can be put into very simple closed form equations. Some equation forms are for shorter time results, and others are for longer time results; but, remarkably, for all practical purposes, the solutions switch immediately from one to the other. The times at which they switch depend on the sizes of the systems being considered; and these, too, can be defined by simple equations. These simple equation forms provide great insight on the nature of the behavior of these systems.

Real field aquifer data are never at constant pressure or constant flow rate. This fact, however, can be handled easily using the superposition integral. This report also discusses this idea and its application, and shows how the simpler analytic solutions make this superposition process considerably easier to perform.

Acknowledgements

This work was supported by the U.S. Department of Energy, under contract No. DE-FG22-93BC14994 to Stanford University and from the SUPRI A Industrial Affiliates Program. This financial and technical support is greatly appreciated.

Introduction

The recovery from many oil reservoirs is affected by water influx, either from the perimeters of the oil reservoirs, or from below, or from both. In fact, worldwide, there is far more water produced from oil reservoirs than oil. Much of this is natural water influx. It is clear then, that an understanding of the interplay between aquifers and the oil reservoirs needs to be understood to properly perform oil recovery calculations. I mentioned bottom water earlier, and it is often important, but the material here will concentrate on peripheral water influx -- for even that subject can become quite complex to understand and analyze. We'll have to defer discussion of bottom water for later notes.

Typically, when one looks at discussions of water influx in reservoir engineering texts, the subject is treated as though only the aquifer needs to be looked at. With this view, the various inner and outer boundary conditions and geometries are addressed, and solutions on the behavior of the aquifers are discussed. From these, various ways of solving these problems are presented, assuming one knows the inner boundary rate or pressure history.

This approach is useful academically, for it is relatively easy to do, and it also is useful to give insight into the nature of aquifer flow. For these reasons it will be discussed here in some detail. Unfortunately, it is "not" very useful for real reservoir problems, for typically we cannot define the inner boundary condition for the oil reservoir/aquifer system in any meaningful way.

These boundary condition dilemmas arise in two different ways. One is when trying to history match past performance of an oil reservoir/aquifer system, and from this match, to infer the reservoir and aquifer properties. The other is to predict the future behavior of the reservoir/aquifer system under various assumed operating scenarios. Both of those problems are important from a reservoir engineering and reservoir management point of view. These should be the ultimate goal of the reservoir engineer. Fortunately, methods have been devised to solve these problems in an analytic manner. Thus these problems, though difficult, are amenable to solution as will be shown in later notes.

In these notes I will discuss these various problems in the order of their complexity of solution rather than in the chronological order in which they would be used by a reservoir engineer. The reason for this is simple. The ideas from one group of concepts can thus be built upon for the next group. In this set of notes, I'll address aquifer flow solutions. Later notes will address reservoir/aquifer interaction.

Aquifer Flow

The equation we use for aquifer flow is the diffusivity equation; the same one we use in well testing theory for undersaturated oil reservoirs. Also the geometries used are the same; linear, radial and spherical flow. Although these equations are well known, I'll repeat them here for later reference.

Linear Flow

$$\frac{\partial^2 p}{\partial x^2} = \frac{\phi \mu c_t}{k} \frac{\partial p}{\partial t} \tag{1}$$

Radial Flow

$$\frac{\partial^2 p}{\partial r^2} + \frac{1}{r} \frac{\partial p}{\partial r} = \frac{\phi \mu c_t}{k} \frac{\partial p}{\partial t} \tag{2}$$

Spherical Flow

$$\frac{\partial^2 p}{\partial r^2} + \frac{2}{r} \frac{\partial p}{\partial r} = \frac{\phi \mu c_t}{k} \frac{\partial p}{\partial t}. \tag{3}$$

Those who are familiar with well testing useage know that in oil reservoirs, all the terms; ϕ, μ, c_t, and k in the diffusivity term can be a problem in practical application. In aquifer flow this problem is far simpler, for the only fluid flowing is water, thus both μ and c_t remain nearly constant. Usually in aquifer flow, the variation of k/ϕ with pressure is ignored, for it does not change nearly as much as it does in oil reservoirs. The effect of k/ϕ variation was discussed in considerable detail by Samaniego *et al.* (1979).

As is done for reservoir systems, Eqs. 1 - 3 are usually changed to dimensionless parameters. These following equations result for linear flow,

$$\frac{\partial^2 p_D}{\partial x_D^2} = \frac{\partial p_D}{\partial t_D} \tag{4}$$

where the dimensionless terms used are as follows:

$$x_D = x / L \tag{5a}$$

and

$$t_D = \frac{kt}{\phi \mu c_t L^2} \tag{5b}$$

where

L = The length of the linear aquifer

And, as in well testing, the definition of p_D depends on the inner boundary conditions chosen. If a constant rate inner boundary is used, p_D is defined as,

$$p_D = \frac{kA(p - p_i)}{q\mu L} \tag{5c}$$

where

p_i = initial aquifer pressure

A = cross sectional area of the aquifer

If a constant pressure inner boundary is used, then the definition for p_D is,

$$p_D = \frac{p - p_i}{p_w - p_i} \tag{5d}$$

where p_w = inner boundary constant pressure

Note that the subscript, w, is usually used at the inner boundary just as it is in well testing, even though the inner boundary is not a well; rather, it is at the original boundary of the oil reservoir/aquifer system.

The dimensionless equation for radial flow is,

$$\frac{\partial^2 p_D}{\partial r_D^2} + \frac{1}{r_D}\frac{\partial p_D}{\partial r_D} = \frac{\partial p_D}{\partial t_D} \tag{6}$$

where some of the dimensionless terms are,

$$r_D = r / r_w \tag{7a}$$

$$t_D = \frac{kt}{\phi \mu c_t r_w^2} \tag{7b}$$

These equations should look familiar to well testing engineers. Note that the term, r_w, is commonly used to define the original oil reservoir/aquifer radius. It's handy, for it emphasizes the similarity of the two systems; but it is also confusing, for one has to be careful to remember which radius is actually being considered in the equation.

The dimensionless pressure for the constant rate inner boundary of a radial system is,

$$p_D = \frac{2\pi kh(p - p_i)}{q\mu} \tag{7c}$$

and for the constant pressure inner boundary, it is Eq. 5d again. Note that these, too, are the same as commonly used in well testing.

Spherical flow is not very common in aquifers; but it can occur whenever there is an oil reservoir "bubble" surrounded on all sides and at the bottom by a very large aquifer.

So this equation will also be addressed briefly in these notes. The dimensionless equation is,

$$\frac{\partial^2 p_D}{\partial r_D^2} + \frac{2}{r_D}\frac{\partial p_D}{\partial r_D} = \frac{\partial p_D}{\partial t_D} \tag{8}$$

In this case, r_D and t_D are defined the same as in radial flow, Eqs. 7a and 7b. Dimensionless pressure at constant rate is defined as follows,

$$p_D = \frac{4\pi k r_w (p - p_i)}{q\mu} \tag{9}$$

Note the similarity to Eq. 7c. The constant is 4π because of the changed geometry, and the distance term in the numerator is r_w. For the constant pressure inner boundary, Eq. 5d is again used.

The spherical flow equation can be simplified in an interesting way. Suppose that we define a new dimensionless variable, b_D, as follows,

$$b_D = r_D p_D \tag{10}$$

When we do this, Eq. 8 simplifies to,

$$\frac{\partial^2 b_D}{\partial r_D^2} = \frac{\partial b_D}{\partial t_D} \tag{11}$$

Thus the spherical flow equation becomes identical in form to the linear equation. This transformation always can be made for the diffusivity equation, and for its steady state equivalents, the LaPlace Equation, or Poisson's Equation. The boundary conditions will be expressed somewhat differently, as we will see in our later discussion of this geometry.

We turn now to solutions of these equations for various geometries, starting with the radial geometry, for that is the most commonly used in reservoir engineering evaluations.

Radial Geometry

In general, for all aquifer geometries there are two convenient inner boundary conditions that can be used: constant pressure or constant flow rate. If there is a known pressure or flow rate history, the idea of superposition can be used. This is an effective procedure, and it will be discussed in some detail later; but first, we will discuss the nature of the various solutions that can arise from these boundary conditions.

There are also reasonable assumptions that can be made for the outer boundary: constant pressure, closed or infinite. Thus there are a total of six possible solutions available which should be considered in some detail. These will be discussed and grouped together in a logical manner to show their differences in behavior, and the reasons for these differences.

Constant Rate Inner Boundary

We will look at the results obtained for all three outer boundary conditions for the constant rate case, compare them, see how they behave at short and long time, and write simplified equations for their short and long time behavior. To do all this, we will rely heavily on Chatas' tables from the Petroleum Engineer series which started in May 1953, of which the important part is duplicated and attached. Chatas' tables borrowed heavily from work originally done by Van Everdingen and Hurst (1949), but are more compact than their work was. Chatas' nomenclature is different from the nomenclature we commonly use in petroleum engineering today (as was Van Everdingen and Hurst), so I will clarify these differences as they arise.

Infinite Aquifer

The first constant rate solution we will look at is for an infinite aquifer. The solutions are shown in Table 1 by Chatas. His nomenclature in the table refers to dimensionless time, and labels it, t. We now use t_D. The heading labeled pressure

A Practical Treatment of Nonsteady-State Flow Problems in Reservoir Systems

Part 3 (Appendix) Practical information is presented in the form of tables, definitions, and a complete resume of the Hurst-van Everdingen equations

ANGELOS T. CHATAS*

Definitions

1. *Annulus Problem.* The determination of the flowing bottom-hole pressure history of a flowing well, undergoing a flow test, that produces through tubing at a constant surface-rate of production. During the test some of the oil comes from the pay formation, but some is also unloaded from the annulus between the tubing and casing.

2. *Annulus Volume Adjustment.* In the "annulus problem" the volume of fluid unloaded from the annulus per unit pressure drop per unit sand thickness. It may be expressed approximately by

$$\frac{\pi (r_c^2 - r_T^2)}{\rho_o g h}$$

which in dimensionless form becomes

$$C = \frac{r_c^2 - r_T^2}{2 g \phi h \rho_o c_o r_w^2}.$$

3. *Boundary Conditions.* The location of the interior and exterior boundaries and the specification of pressure and/or flow at these boundaries at a given instant of time.

4. *Boundary Variations.* The changes in the boundary conditions of a reservoir system undergoing exploitation.

5. *Continuous Succession of Steady States.* A method of solving flow problems in a reservoir system that suffers boundary variations but fulfills instantaneous steady-state conditions. The history of such a system is divided into an appropriate number of stages, each of which is treated by steady-state analysis.

6. *Dimensionless Time Ratio.* The dimensionless ratio defined by the following relations:

Radial System

$$t = \frac{k\,\theta}{\phi\,\mu\,c_f r_w^2}$$

Linear System

$$t = \frac{k\theta}{\Phi\,\mu\,c_f x_c^2} = \frac{K\theta}{\rho M C_f}$$

7. *Fluid-Influx Terms.* Terms that appear in the Hurst-van Everdingen equation which treats the "pressure case." Such a term, denoted by $q(t)$, is a dimensionless, numerical quantity representing the total volume of fluid per unit thickness that passes the interior boundary of a reservoir system over the time span $t = t_M - t_i$, which is caused by a unit pressure drop at this boundary at time t_i.

8. *Infinite Reservoir System.* A reservoir system analyzed over a period of time during which the presence of an exterior boundary is not felt.

9. *Linear Reservoir System.* A system defined by two parallel planes, which serve as boundaries, over which pressure and flow are specified according to prescribed conditions, and whose physical properties of interest vary only with the perpendicular distance x between the two planes.

10. *Nonsteady-State Flow.* In reservoir systems undergoing exploitation, fluid flow that is characterized predominately by time variations and necessitates the formal introduction of time as an explicit variable in the basic flow equations.

11. *Oil Field Equivalent.* An oil field lumped together such that its outer limits serve as the interior boundary of a reservoir system, with a pressure equal to the average oil field pressure, and with a flux equal to the sum of the fluxes of the individual wells.

12. *Pressure Case.* In the analysis of a reservoir system the situation that presumes knowledge of the pressure history and predicts the cumulative fluid influx.

13. *Pressure Change Terms.* Terms that appear in the Hurst-van Everdingen equation which treats the "rate case." Such a term, denoted by $p(t)$, is a dimensionless, numerical quantity representing the change in pressure at the interior boundary of a reservoir system over the time span $t = t_M - t_i$, which is caused by a unit rate of production per unit thickness at time t_i.

14. *Pressure Correction Terms.* Terms that appear in the Hurst-van Evendingen equation which treats the "annulus problem." Such a term, denoted by $p'(t)$, is a diminsionless numerical quantity representing the total pressure drop in the well bore, which is caused by a unit rate of production at the surface and is corrected for the unloading of fluid from the annulus.

15. *Radial Reservoir System.* A system defined by two concentric circular cylinders, which serve as boundaries, over which pressure and flow are specified according to prescribed conditions, and whose physical properties of interest vary only with the distance r from the axis of symmetry.

16. *Rate Case.* In the analysis of a reservoir system the situation that presumes knowledge of the production or fluid-influx rate history and predicts the cumulative pressure-drop for a reservoir at its interior boundary.

17. *Steady-State Flow.* In reservoir systems undergoing exploitation, fluid flow whose time variations are insignificant, and, which permit the formal neglect of time as an explicit variable in the basic flow equations.

18. *Time of Readjustment.* The approximate time required for the readjustment of the internal pressure distribution in a reservoir system to a steady-state distribution when pressure variations occur at the boundaries. For radial systems this time is given by

$$\theta_R = \frac{\phi c_f r_e^2}{4 k/\mu}$$

while for linear systems it is

TABLE 1. Infinite radial system — Rate case.

Dimensionless time t	Pressure change p(t)	Dimensionless time t	Pressure change p(t)	Dimensionless time t	Pressure change p(t)	Dimensionless time t	Pressure change p(t)
0	0	.06	.2500	3.0	1.1685	150.0	2.9212
.005	.0250	.07	.2680	4.0	1.2750	200.0	3.0636
.001	.0352	.08	.2845	5.0	1.3625	250.0	3.1726
.002	.0495	.09	.2999	6.0	1.4362	300.0	3.2630
.003	.0603	.1	.3144	7.0	1.4997	350.0	3.3394
.004	.0694	.15	.3750	8.0	1.5557	400.0	3.4057
.005	.0774	.2	.4241	9.0	1.6057	450.0	3.4641
.006	.0845	.3	.5024	10.0	1.6509	500.0	3.5164
.007	.0911	.4	.5645	15.0	1.8294	550.0	3.5643
.008	.0971	.5	.6167	20.0	1.9601	600.0	3.6076
.009	.1028	.6	.6622	30.0	2.1470	650.0	3.6476
.01	.1081	.7	.7024	40.0	2.2824	700.0	3.6842
.015	.1312	.8	.7387	50.0	2.3884	750.0	3.7184
.02	.1503	.9	.7716	60.0	2.4758	800.0	3.7505
.025	.1669	1.0	.8019	70.0	2.5501	850.0	3.7805
.03	.1818	1.2	.8572	80.0	2.6147	900.0	3.8088
.04	.2077	1.4	.9160	90.0	2.6718	950.0	3.8355
.05	.2301	2.0	1.0195	100.0	2.7233	1000.0	3.8584

*Magnolia Petroleum Company.

$$\theta_M = \frac{\phi c_t x_M^2}{2k/\mu}$$

Hurst-Van Everdingen Equations

A. Radial Systems.

1. *Rate Case.* The rate case presumes knowledge of the production or fluid-influx rate history and predicts the cumulative pressure drop for a reservoir system at its interior boundary. This pressure drop is given by the simple algebraic equation

$$P_o - (r_w, \theta_M) = \frac{\mu}{2\pi kh}$$
$$\{Q(\theta_o)\, p(t_M) + [Q(\theta_1) - Q(\theta_o)] \times p(t_M - t_1) + [Q(\theta_2) - Q(\theta_1)] \times p(t_M - t_2) + \ldots + [Q(\theta_n) - Q(\theta_{n-1})]\, p(t_M - t_n)\}$$

where it can be noted that P_o, μ, k, h, and $Q(\theta_i)$ are obtained from field data[1]. Thus, to obtain $P(r_w, \theta_M)$, the pressure at the interior boundary of a system at time θ_M, one need only further determine the pressure change terms p(t) with $t = t_M - t_i$. These terms may be determined for the ensuing types of systems as follows:

Infinite system.

$t < 0.01$ $\quad p(t) = 2\sqrt{t/\pi}$

$0.01 < t < 100$ see Fig. 1 or Table 1

$t > 100$ $\quad p(t) = 1/2(\ln t + 0.80907)$

Finite system with closed exterior boundary

$t < 0.01$ $\quad p(t) = 2\sqrt{t/\pi}$

$t > 0.01$ see Fig. 9 or Table 4

$$\text{large } t \quad p(t) \approx \frac{(1/2 + 2t)}{[(r_e/r_w)^2 - 1]} - \frac{[3(r_e/r_w)^4 - 4(r_e/r_w)^4 \ln r_e/r_w - 2(r_e/r_w)^2 - 1]}{4[(r_e/r_w)^2 - 1]^2}$$

Finite system with fixed constant pressure at exterior boundary.

$t < 0.01$ $\quad p(t) = 2\sqrt{t/\pi}$

$t > 0.01$ see Figs. 10, 11, 12, and 13 or Table 5

large t $\quad p(t) \approx \ln r_e/r_w$

2. *Pressure Case.* The pressure case treats the inverse problem of determining the cumulative fluid influx, and presumes knowledge of the pressure history at the interior boundary of a reservoir system. This cumulative fluid influx is given by the similar algebraic equation

$$F_c(\theta_M) = 2\pi \phi c_t r_w^2 h$$
$$\{[P_o - P(\theta_1)]\, q(t_M) + [P(\theta_1) - P(\theta_2)]\, q(t_M - t_1) + [P(\theta_2) - P(\theta_3)]\, q(t_M - t_2) + \ldots + [P(\theta_{n-1}) - P(\theta_n)]\, q(t_M - t_{n-1})\}$$

[1] Sometimes these quantities are not directly available from field data, and the empirical approach of examining and treating the past history of a system proves necessary for their determination.

TABLE 2. Infinite radial system — Pressure case.

Dimensionless time t	Fluid influx q(t)	Dimensionless time t	Fluid influx q(t)	Dimensionless time t	Fluid influx q(t)	Dimensionless time t	Fluid influx q(t)	Dimensionless time t	Fluid influx q(t)	Dimensionless time t	Fluid influx q(t)
0.00	0.000	79	35.697	455	150.249	1190	340.843	3250	816.090	35,000	6780.247
0.01	0.112	80	36.058	460	151.640	1200	343.308	3300	827.088	40,000	7650.096
0.05	0.278	81	36.418	465	153.029	1210	345.770	3350	838.067	50,000	9363.099
0.10	0.404	82	36.777	470	154.416	1220	348.230	3400	849.028	60,000	11,047.299
0.15	0.520	83	37.136	475	155.801	1225	349.460	3450	859.974	70,000	12,708.358
0.20	0.606	84	37.494	480	157.184	1230	350.688	3500	870.903	75,000	13,531.457
0.25	0.689	85	37.851	485	158.565	1240	353.144	3550	881.816	80,000	14,350.121
0.30	0.758	86	38.207	490	159.945	1250	355.597	3600	892.712	90,000	15,975.389
0.40	0.898	87	38.563	495	161.322	1260	358.048	3650	903.594	100,000	17,586.284
0.50	1.020	88	38.919	500	162.698	1270	360.496	3700	914.459	125,000	21,560.732
0.60	1.140	89	39.272	510	165.444	1275	361.720	3750	925.309	1.5(10)^5	2.538(10)^4
0.70	1.251	90	39.626	520	168.183	1280	362.942	3800	936.144	2.0 "	3.308 "
0.80	1.359	91	39.979	525	169.549	1290	365.386	3850	946.966	2.5 "	4.066 "
0.90	1.469	92	40.331	530	170.914	1300	367.828	3900	957.773	3.0 "	4.817 "
1	1.569	93	40.684	540	173.639	1310	370.267	3950	968.566	4.0 "	6.267 "
2	2.447	94	41.034	550	176.357	1320	372.704	4000	979.344	5.0 "	7.699 "
3	3.202	95	41.385	560	179.069	1325	373.922	4050	990.108	6.0 "	9.113 "
4	3.893	96	41.735	570	181.774	1330	375.139	4100	1000.858	7.0 "	1.051(10)^5
5	4.539	97	42.084	575	183.124	1340	377.572	4150	1011.595	8.0 "	1.189 "
6	5.153	98	42.433	580	184.473	1350	380.003	4200	1022.318	9.0 "	1.326 "
7	5.743	99	42.781	590	187.166	1360	382.432	4250	1033.028	1.0(10)^6	1.462 "
8	6.314	100	43.129	600	189.852	1370	384.859	4300	1043.724	1.5 "	2.126 "
9	6.869	105	44.858	610	192.533	1375	386.070	4350	1054.409	2.0 "	2.781 "
10	7.411	110	46.574	620	195.208	1380	387.283	4400	1065.082	2.5 "	3.427 "
11	7.940	115	48.277	625	196.544	1390	389.705	4450	1075.743	3.0 "	4.064 "
12	8.457	120	49.968	630	197.878	1400	392.125	4500	1086.390	4.0 "	5.313 "
13	8.964	125	51.648	640	200.542	1410	394.543	4550	1097.024	5.0 "	6.544 "
14	9.461	130	53.317	650	203.201	1420	396.959	4600	1107.646	6.0 "	7.761 "
15	9.949	135	54.976	660	205.854	1425	398.167	4650	1118.257	7.0 "	8.965 "
16	10.434	140	56.625	670	208.502	1430	399.373	4700	1128.854	8.0 "	1.016(10)^6
17	10.913	145	58.265	675	209.825	1440	401.786	4750	1139.439	9.0 "	1.134 "
18	11.386	150	59.895	680	211.145	1450	404.197	4800	1150.012	1.0(10)^7	1.252 "
19	11.855	155	61.517	690	213.784	1460	406.606	4850	1160.574	1.5 "	1.828 "
20	12.319	160	63.131	700	216.417	1470	409.013	4900	1171.125	2.0 "	2.398 "
21	12.778	165	64.737	710	219.046	1475	410.214	4950	1181.666	2.5 "	2.961 "
22	13.233	170	66.336	720	221.670	1480	411.418	5000	1192.198	3.0 "	3.517 "
23	13.684	175	67.928	725	222.980	1490	413.820	5100	1213.222	4.0 "	4.610 "
24	14.131	180	69.512	730	224.259	1500	416.220	5200	1234.203	5.0 "	5.689 "
25	14.573	185	71.090	740	226.904	1525	422.214	5300	1255.141	6.0 "	6.758 "
26	15.013	190	72.661	750	229.514	1550	428.196	5400	1276.037	7.0 "	7.816 "
27	15.450	195	74.226	760	232.120	1575	434.168	5500	1296.893	8.0 "	8.866 "
28	15.883	200	75.785	770	234.721	1600	440.128	5600	1317.709	9.0 "	9.911 "
29	16.313	205	77.338	775	236.020	1625	446.077	5700	1338.486	1.0(10)^8	1.095(10)^7
30	16.742	210	78.886	780	237.318	1650	452.016	5800	1359.225	1.5 "	1.604 "
31	17.167	215	80.428	790	239.912	1675	457.945	5900	1379.927	2.0 "	2.108 "
32	17.590	220	81.965	800	242.501	1700	463.863	6000	1400.593	2.5 "	2.607 "
33	18.011	225	83.497	810	245.086	1725	469.771	6100	1421.224	3.0 "	3.100 "
34	18.429	230	85.023	820	247.668	1750	475.669	6200	1441.820	4.0 "	4.071 "
35	18.845	235	86.545	825	248.957	1775	481.558	6300	1462.383	5.0 "	5.032 "
36	19.259	240	88.062	830	250.245	1800	487.437	6400	1482.912	6.0 "	5.984 "
37	19.671	245	89.575	840	252.819	1825	493.307	6500	1503.408	7.0 "	6.928 "
38	20.080	250	91.084	850	255.388	1850	499.167	6600	1523.872	8.0 "	7.865 "
39	20.488	255	92.589	860	257.953	1875	505.019	6700	1544.305	9.0 "	8.797 "
40	20.894	260	94.090	870	260.515	1900	510.861	6800	1564.706	1.0(10)^9	9.725 "
41	21.298	265	95.588	875	261.795	1925	516.695	6900	1585.077	1.5 "	1.429(10)^8
42	21.701	270	97.081	880	263.073	1950	522.520	7000	1605.418	2.0 "	1.880 "
43	22.101	275	98.571	890	265.629	1975	528.337	7100	1625.729	2.5 "	2.328 "
44	22.500	280	100.057	900	268.181	2000	534.145	7200	1646.011	3.0 "	2.771 "
45	22.897	285	101.540	910	270.729	2025	539.945	7300	1666.265	4.0 "	3.645 "
46	23.291	290	103.019	920	273.274	2050	545.737	7400	1686.490	5.0 "	4.510 "
47	23.684	295	104.495	925	274.545	2075	551.522	7500	1706.688	6.0 "	5.368 "
48	24.076	300	105.968	930	275.815	2100	557.299	7600	1726.859	7.0 "	6.220 "
49	24.466	305	107.437	940	278.353	2125	563.068	7700	1747.002	8.0 "	7.066 "
50	24.855	310	108.904	950	280.888	2150	568.830	7800	1767.120	9.0 "	7.909 "
51	25.244	315	110.367	960	283.420	2175	574.585	7900	1787.212	1.0(10)^10	8.747 "
52	25.633	320	111.827	970	285.948	2200	580.332	8000	1807.278	1.5 "	1.288(10)^9
53	26.020	325	113.284	975	287.211	2225	586.072	8100	1827.319	2.0 "	1.697 "
54	26.405	330	114.738	980	288.473	2250	591.806	8200	1847.336	2.5 "	2.103 "
55	26.791	335	116.189	990	290.995	2275	597.532	8300	1867.329	3.0 "	2.505 "
56	27.174	340	117.638	1000	293.514	2300	603.252	8400	1887.298	4.0 "	3.299 "
57	27.555	345	119.083	1010	296.030	2325	608.965	8500	1907.243	5.0 "	4.087 "
58	27.935	350	120.526	1020	298.543	2350	614.672	8600	1927.166	6.0 "	4.868 "
59	28.314	355	121.966	1025	299.799	2375	620.372	8700	1947.065	7.0 "	5.643 "
60	28.691	360	123.403	1030	301.053	2400	626.066	8800	1966.942	8.0 "	6.414 "
61	29.068	365	124.838	1040	303.560	2425	631.755	8900	1986.796	9.0 "	7.183 "
62	29.443	370	126.270	1050	306.065	2450	637.437	9000	2006.628	1.0(10)^11	7.948 "
63	29.818	375	127.699	1060	308.567	2475	643.113	9100	2026.438	1.5 "	1.17(10)^10
64	30.192	380	129.126	1070	311.066	2500	648.781	9200	2046.227	2.0 "	1.55 "
65	30.565	385	130.550	1075	312.314	2550	660.098	9300	2065.995	2.5 "	1.92 "
66	30.937	390	131.972	1080	313.562	2600	671.379	9400	2085.744	3.0 "	2.29 "
67	31.308	395	133.391	1090	316.055	2650	682.640	9500	2105.473	4.0 "	3.02 "
68	31.679	400	134.808	1100	318.545	2700	693.877	9600	2125.184	5.0 "	3.75 "
69	32.048	405	136.223	1110	321.032	2750	705.090	9700	2144.878	6.0 "	4.47 "
70	32.417	410	137.635	1120	323.517	2800	716.280	9800	2164.555	7.0 "	5.19 "
71	32.785	415	139.045	1125	324.760	2850	727.449	9900	2184.216	8.0 "	5.89 "
72	33.151	420	140.453	1130	326.000	2900	738.598	10,000	2203.861	9.0 "	6.58 "
73	33.517	425	141.859	1140	328.480	2950	749.725	12,500	2688.967	1.0(10)^12	7.28 "
74	33.883	430	143.262	1150	330.958	3000	760.833	15,000	3164.780	1.5 "	1.08(10)^11
75	34.247	435	144.664	1160	333.433	3050	771.922	17,500	3633.368	2.0 "	1.42 "
76	34.611	440	146.064	1170	335.906	3100	782.992	20,000	4095.800		
77	34.974	445	147.461	1175	337.142	3150	794.042	25,000	5005.726		
78	35.336	450	148.856	1180	338.376	3200	805.075	30,000	5899.508		

where again all the terms on the right hand side of the equation, except the fluid-influx terms q(t), may be obtained from field data[1]. The fluid-influx terms may be determined similarly as follows:

Infinite system

$t < 0.01$ $\quad q(t) = 2\sqrt{t/\pi}$

$t > 0.01$ See Figs. 2, 3, and 4 or Table 2.

Finite system with closed exterior boundary

$t < 0.01$ See $q(t) = 2\sqrt{t/\pi}$

$t > 0.01$ See Figs. 5, 6, 7, and 8 or Table 3

large t $\quad q(t) \approx [(r_e/r_w)^2 - 1]/2$

EXPLANATION OF SYMOLS.

A = proven area of oil field

A' = estimated area of aquifer

B = bulk modulus of reservoir fluid

C = dimensionless "annulus volume adjustment term"

C_1 = arbitrary constant

F_c = cumulative influx of fluid

G = mass rate of flow

I_o = modified Bessel function of the first kind and order zero

J_n = Bessel function of the first kind and order n

K_o = modified Bessel function of the second kind and order zero

P = pressure

P_T = transform of pressure

P_B = pressure at a boundary

P_{BP} = bubble point pressure

P_e = pressure at exterior boundary; effective reservoir pressure

P_F = flowing bottom hole pressure

P_o = original reservoir pressure

P_w = pressure at interior boundary;

Q = volume rate of flow; average rate of production

Q_T = transform of production

Q_s = volume rate of flow measured at the stock tank

W_e = cumulative water influx into oil field

X = arbitrary function

Y_n = Bessel function of the second kind and order n

a = cross-sectional area perpendicular to the direction of flow in linear system

c = speed of sound

c_f = compressibility of fluid

c_o = compressibility of oil

c_w = compressibility of water

g = gravitational acceleration

h = net effective formation thickness

TABLE 3. Finite radial system with closed exterior boundary—Pressure case.

re/rw=1.5

Dimensionless time t	Fluid influx q(t)
$5.0(10)^{-2}$	0.276
6.0 "	0.304
7.0 "	0.330
8.0 "	0.354
9.0	0.376
$1.0(10)^{-1}$	0.395
1.1 "	0.414
1.2 "	0.431
1.3 "	0.446
1.4 "	0.461
1.5 "	0.474
1.6 "	0.486
1.7 "	0.497
1.8 "	0.507
1.9 "	0.517
2.0 "	0.525
2.1 "	0.533
2.2 "	0.541
2.3 "	0.548
2.4 "	0.554
2.5 "	0.559
2.6 "	0.565
2.8 "	0.574
3.0 "	0.582
3.2 "	0.588
3.4 "	0.594
3.6 "	0.599
3.8 "	0.603
4.0 "	0.606
4.5 "	0.613
5.0 "	0.617
6.0 "	0.621
7.0 "	0.623
8.0 "	0.624

re/rw=2.0

Dimensionless time t	Fluid influx q(t)
$5.0(10)^{-2}$	0.278
7.5 "	0.345
$1.0(10)^{-1}$	0.404
1.25 "	0.458
1.50 "	0.507
1.75 "	0.553
2.00 "	0.597
2.25 "	0.638
2.50 "	0.678
2.75 "	0.715
3.00 "	0.751
3.25 "	0.785
3.50 "	0.817
3.75 "	0.848
4.00 "	0.877
4.25 "	0.905
4.50 "	0.932
4.75 "	0.958
5.00 "	0.983
5.50 "	1.028
6.00 "	1.070
6.50 "	1.108
7.00 "	1.143
7.50 "	1.174
8.00 "	1.203
9.00 "	1.253
1.00	1.295
1.1	1.330
1.2	1.358
1.3	1.382
1.4	1.402
1.6	1.432
1.7	1.444
1.8	1.453
2.0	1.468
2.5	1.487
3.0	1.495
4.0	1.499
5.0	1.500

re/rw=2.5

Dimensionless time t	Fluid influx q(t)
$1.0(10)^{-1}$	0.408
1.5 "	0.509
2.0 "	0.599
2.5 "	0.681
3.0 "	0.758
3.5 "	0.829
4.0 "	0.897
4.5 "	0.962
5.0 "	1.024
5.5 "	1.083
6.0 "	1.140
6.5 "	1.195
7.0 "	1.248
7.5 "	1.299
8.0 "	1.348
8.5 "	1.395
9.0 "	1.440
9.5 "	1.484
1.0	1.526
1.1	1.605
1.2	1.679
1.3	1.747
1.4	1.811
1.5	1.870
1.6	1.924
1.7	1.976
1.8	2.022
2.0	2.106
2.2	2.178
2.4	2.241
2.6	2.294
2.8	2.340
3.0	2.380
3.4	2.444
3.8	2.491
4.3	2.525
4.6	2.551
5.0	2.570
6.0	2.599
7.0	2.613
8.0	2.619
9.0	2.622
10.0	2.624

re/rw=3.0

Dimensionless time t	Fluid influx q(t)
$3.0(10)^{-1}$	0.755
4.0 "	0.895
5.0 "	1.023
6.0 "	1.143
7.0 "	1.256
8.0 "	1.363
9.0 "	1.465
1.00	1.563
1.25	1.791
1.50	1.997
1.75	2.184
2.00	2.353
2.25	2.507
2.50	2.646
2.75	2.772
3.00	2.886
3.25	2.990
3.50	3.084
2.75	3.170
4.00	3.247
4.25	3.317
4.50	3.381
4.75	3.439
5.00	3.491
5.50	3.581
6.00	3.656
6.50	3.717
7.00	3.767
7.50	3.809
8.00	3.843
9.00	3.894
10.00	3.928
11.00	3.951
12.00	3.967
14.00	3.985
16.00	3.993
18.00	3.997
20.00	3.999
22.00	3.999
24.00	4.000

re/rw=3.5

Dimensionless time t	Fluid influx q(t)
1.00	1.571
1.20	1.761
1.40	1.940
1.60	2.111
1.80	2.273
2.00	2.427
2.20	2.574
2.40	2.715
2.60	2.849
2.80	2.976
3.00	3.098
3.25	3.242
3.50	3.379
3.75	3.507
4.00	3.623
4.25	3.742
4.50	3.850
4.75	3.951
5.00	4.047
5.50	4.222
6.00	4.378
6.50	4.516
7.00	4.639
7.50	4.749
8.00	4.846
8.50	4.932
9.00	5.009
9.50	5.078
10.00	5.128
11	5.241
12	5.321
13	5.385
14	5.435
15	5.476
16	5.506
17	5.531
18	5.551
20	5.579
25	5.611
30	5.621
35	5.624
40	5.625

re/rw=4.0

Dimensionless time t	Fluid influx q(t)
2.00	2.442
2.20	2.598
2.40	2.748
2.60	2.893
2.80	3.034
3.00	3.170
3.25	3.334
3.50	3.493
3.75	3.645
4.00	3.792
4.25	3.932
4.50	4.068
4.75	4.198
5.00	4.323
5.50	4.560
6.00	4.779
6.50	4.982
7.00	5.169
7.50	5.343
8.00	5.504
8.50	5.653
9.00	5.790
9.50	5.917
10	6.035
11	6.246
12	6.425
13	6.580
14	6.712
15	6.825
16	6.922
17	7.004
18	7.076
20	7.189
22	7.272
24	7.332
26	7.377
30	7.434
34	7.464
38	7.481
42	7.490
46	7.494
50	7.497

re/rw=4.5

Dimensionless time t	Fluid influx q(t)
2.5	2.835
3.0	3.196
3.5	3.537
4.0	3.859
4.5	4.165
5.0	4.454
5.5	4.727
6.0	4.986
6.5	5.231
7.0	5.464
7.5	5.684
8.0	5.892
8.5	6.089
9.0	6.276
9.5	6.453
10	6.621
11	6.930
12	7.208
13	7.457
14	7.680
15	7.880
16	8.060
18	8.365
20	8.611
22	8.809
24	8.968
26	9.097
28	9.200
30	9.283
34	9.404
38	9.481
42	9.532
46	9.565
50	9.586
60	9.612
70	9.621
80	9.623
90	9.624
100	9.625

re/rw=5.0

Dimensionless time t	Fluid influx q(t)
3.0	3.195
3.5	3.542
4.0	3.875
4.5	4.193
5.0	4.499
5.5	4.792
6.0	5.074
6.5	5.345
7.0	5.605
7.5	5.854
8.0	6.094
8.5	6.325
9.0	6.547
9.5	6.760
10	6.965
11	7.350
12	7.706
13	8.035
14	8.339
15	8.620
16	8.879
18	9.338
20	9.731
22	10.07
24	10.35
26	10.59
28	10.80
30	10.98
34	11.26
38	11.46
42	11.61
46	11.71
50	11.79
60	11.91
70	11.96
80	11.98
90	11.99
100	12.00
120	12.00

re/rw=6.0

Dimensionless time t	Fluid influx q(t)
6.0	5.148
6.5	5.440
7.0	5.724
7.5	6.002
8.0	6.273
8.5	6.537
9.0	6.795
9.5	7.047
10.0	7.293
10.5	7.533
11	7.767
12	8.220
13	8.651
14	9.063
15	9.456
16	9.829
17	10.19
18	10.53
19	10.85
20	11.16
22	11.74
24	12.26
25	12.50
31	13.74
35	14.40
39	14.93
51	16.05
60	16.56
70	16.91
80	17.14
90	17.27
100	17.36
110	17.41
120	17.45
130	17.46
140	17.48
150	17.49
160	17.49
180	17.50
200	17.50
220	17.50

re/rw=7.0

Dimensionless time t	Fluid influx q(t)
9.00	6.861
9.50	7.127
10	7.389
11	7.902
12	8.397
13	8.876
14	9.341
15	9.791
16	10.23
17	10.65
18	11.06
19	11.46
20	11.85
22	12.58
24	13.27
26	13.92
28	14.53
30	15.11
35	16.39
40	17.49
45	18.43
50	19.24
60	20.51
70	21.45
80	22.13
90	22.63
100	23.00
120	23.47
140	23.71
160	23.85
180	23.92
200	23.96
500	24.00

re/rw=8.0

Dimensionless time t	Fluid influx q(t)
9	6.861
10	7.398
11	7.920
12	8.431
13	8.930
14	9.418
15	9.895
16	10.351
17	10.82
18	11.26
19	11.70
20	12.13
22	12.95
24	13.74
26	14.50
28	15.23
30	15.92
34	17.22
38	18.41
40	18.97
45	20.26
50	21.42
55	22.46
60	23.40
70	24.98
80	26.26
90	27.28
100	28.11
120	29.31
140	30.08
160	30.61
180	30.91
200	31.12
240	31.34
280	31.43
320	31.47
360	31.49
400	31.50
500	31.50

re/rw=9.0

Dimensionless time t	Fluid influx q(t)
10	7.417
15	9.945
20	12.26
22	13.13
24	13.98
26	14.79
28	15.59
30	16.35
32	17.10
34	17.82
36	18.52
38	19.19
40	19.85
42	20.48
44	21.09
46	21.69
48	22.26
50	22.82
52	23.36
54	23.89
56	24.39
58	24.88
60	25.36
65	26.48
70	27.52
75	28.48
80	29.36
85	30.18
90	30.93
95	31.63
100	32.27
120	34.39
140	35.92
160	37.04
180	37.85
200	38.44
240	39.17
280	39.38
320	39.77
360	39.88
400	39.94
440	39.97
480	39.98

re/rw=10.0

Dimensionless time t	Fluid influx q(t)
15	9.965
20	12.32
22	13.32
24	14.09
26	14.95
28	15.75
30	16.59
32	17.38
34	18.16
36	18.91
38	19.65
40	20.37
42	21.07
44	21.78
46	22.42
48	23.07
50	23.71
52	24.33
54	24.94
56	25.53
58	26.11
60	26.67
65	28.02
70	29.29
75	30.49
80	31.61
85	32.67
90	33.66
95	34.60
100	35.48
120	38.51
140	40.89
160	42.75
180	44.21
200	45.36
240	46.95
280	47.94
320	48.54
360	48.91
400	49.14
440	49.28
480	49.36

3. *Rate of Fluid Influx.* The rate of fluid influx has been presented as a function of the fluid-influx terms and, therefore, is a modification of the "pressure case." Thus the rate of fluid-influx at the interior boundary of a radial reservoir system is given at time θ_M by the algebraic equation

$$Q(\theta_M) = 2\pi\phi c_f r_w^2 h \{ [P_o' - P(\theta_1)] \frac{[q(t_M) - q(t_M - t_1)]}{\theta_1} + [P(\theta_1) - P(\theta_2)]$$

TABLE 4. Finite radial system with closed exterior boundary—Rate case.

re/rw=1.5		re/rw=2.0		re/rw=2.5		re/rw=3.0		re/rw=3.5		re/rw=4.0	
Dimension-less time	Pressure change	Dimension-less time	Pressure change	Dimension-less time	Pressure change	Dimension-less time	Pressure change	Dimension-less time	Pressure change	Dimension-less time	Pressure change
t	p(t)	t	p(t)	t	p(t)	t	p(t)	t	p(t)	t	p(t)
6.0(10)$^{-2}$	0.251	2.2(10)$^{-1}$	0.443	4.0(10)$^{-1}$	0.565	5.2(10)$^{-1}$	0.627	1.0	0.802	1.5	0.927
8.0 "	0.288	2.4 "	0.459	4.2 "	0.576	5.4 "	0.636	1.1	0.830	1.6	0.948
1.0(10)$^{-1}$	0.322	2.6 "	0.476	4.4 "	0.587	5.6 "	0.645	1.2	0.857	1.7	0.968
1.2 "	0.355	2.8 "	0.492	4.6 "	0.598	6.0 "	0.662	1.3	0.882	1.8	0.988
1.4 "	0.387	3.0 "	0.507	4.8 "	0.608	6.5 "	0.683	1.4	0.906	1.9	1.007
1.6 "	0.420	3.2 "	0.522	5.0 "	0.618	7.0 "	0.703	1.5	0.929	2.0	1.025
1.8 "	0.452	3.4 "	0.536	5.2 "	0.628	7.5 "	0.721	1.6	0.951	2.2	1.059
2.0 "	0.484	3.6 "	0.551	5.4 "	0.638	8.0 "	0.740	1.7	0.973	2.4	1.092
2.2 "	0.516	3.8 "	0.565	5.6 "	0.647	8.5 "	0.758	1.8	0.994	2.6	1.123
2.4 "	0.548	4.0 "	0.579	5.8 "	0.657	9.0 "	0.776	1.9	1.014	2.8	1.154
2.6 "	0.580	4.2 "	0.593	6.0 "	0.666	9.5 "	0.791	2.0	1.034	3.0	1.184
2.8 "	0.612	4.4 "	0.607	6.5 "	0.688	1.0	0.806	2.25	1.083	3.5	1.255
3.0 "	0.644	4.6 "	0.621	7.0 "	0.710	1.2	0.865	2.50	1.130	4.0	1.324
3.5 "	0.724	4.8 "	0.634	7.5 "	0.731	1.4	0.920	2.75	1.176	4.5	1.392
4.0 "	0.804	5.0 "	0.648	8.0 "	0.752	1.6	0.973	3.0	1.221	5.0	1.460
4.5 "	0.884	6.0 "	0.715	8.5 "	0.772	2.0	1.076	4.0	1.401	5.5	1.527
5.0 "	0.964	7.0 "	0.782	9.0 "	0.792	3.0	1.328	5.0	1.579	6.0	1.594
5.5 "	1.044	8.0 "	0.849	9.5 "	0.812	4.0	1.578	6.0	1.757	6.5	1.660
6.0 "	1.124	9.0 "	0.915	1.0	0.832	5.0	1.828			7.0	1.727
		1.0	0.982	2.0	1.215					8.0	1.861
		2.0	1.649	3.0	1.596					9.0	1.994
		3.0	2.316	4.0	1.977					10.0	2.127
		5.0	3.649	5.0	2.358						

re/rw=4.5		re/rw=5.0		re/rw=6.0		re/rw=7.0		re/rw=8.0		re/rw=9.0		re/rw=10.0	
Dimension-less time	Pressure change	Dimension-less time	Pressure change	Dimension-less time	Pressure change	Dimension-less time	Pressure change	Dimension-less time	Pressure change	Dimension-less time	Pressure change	Dimension-less time	Pressure change
t	p(t)	t	p(t)	t	p(t)	t	p(t)	t	p(t)	t	p(t)	t	p(t)
2.0	1.023	3.0	1.167	4.0	1.275	6.0	1.436	8.0	1.556	10.0	1.651	12.0	1.732
2.1	1.040	3.1	1.180	4.5	1.322	6.5	1.470	8.5	1.582	10.5	1.673	12.5	1.750
2.2	1.056	3.2	1.192	5.0	1.364	7.0	1.501	9.0	1.607	11.0	1.693	13.0	1.768
2.3	1.072	3.3	1.204	5.5	1.404	7.5	1.531	9.5	1.631	11.5	1.713	13.5	1.784
2.4	1.087	3.4	1.215	6.0	1.441	8.0	1.559	10.0	1.653	12.0	1.732	14.0	1.801
2.5	1.102	3.5	1.227	6.5	1.477	8.5	1.586	10.5	1.675	12.5	1.750	14.5	1.817
2.6	1.116	3.6	1.238	7.0	1.511	9.0	1.613	11.0	1.697	13.0	1.768	15.0	1.832
2.7	1.130	3.7	1.249	7.5	1.544	9.5	1.638	11.5	1.717	13.5	1.786	15.5	1.847
2.8	1.144	3.8	1.259	8.0	1.576	10.0	1.663	12.0	1.737	14.0	1.803	16.0	1.862
2.9	1.158	3.9	1.270	8.5	1.607	11.0	1.711	12.5	1.757	14.5	1.819	17.0	1.890
3.0	1.171	4.0	1.281	9.0	1.638	12.0	1.757	13.0	1.776	15.0	1.835	18.0	1.917
3.2	1.197	4.2	1.301	9.5	1.668	13.0	1.810	13.5	1.795	15.5	1.851	19.0	1.943
3.4	1.222	4.4	1.321	10.0	1.698	14.0	1.845	14.0	1.813	16.0	1.867	20.0	1.968
3.6	1.246	4.6	1.340	11.0	1.757	15.0	1.888	14.5	1.831	17.0	1.897	22.0	2.017
3.8	1.269	4.8	1.360	12.0	1.815	16.0	1.931	15.0	1.849	18.0	1.926	24.0	2.063
4.0	1.292	5.0	1.378	13.0	1.873	17.0	1.974	17.0	1.919	19.0	1.955	26.0	2.108
4.5	1.349	5.5	1.424	14.0	1.931	18.0	2.016	19.0	1.986	20.0	1.983	28.0	2.151
5.0	1.403	6.0	1.469	15.0	1.988	19.0	2.058	21.0	2.051	22.0	2.037	30.0	2.194
5.5	1.457	6.5	1.513	16.0	2.045	20.0	2.100	23.0	2.116	24.0	2.090	32.0	2.236
6.0	1.510	7.0	1.556	17.0	2.103	22.0	2.184	25.0	2.180	26.0	2.142	34.0	2.278
7.0	1.615	7.5	1.598	18.0	2.160	24.0	2.267	30.0	2.340	28.0	2.193	36.0	2.319
8.0	1.719	8.0	1.641	19.0	2.217	26.0	2.351	35.0	2.499	30.0	2.244	38.0	2.360
9.0	1.823	9.0	1.725	20.0	2.274	28.0	2.434	40.0	2.658	34.0	2.345	40.0	2.401
10.0	1.927	10.0	1.808	25.0	2.560	30.0	2.517	45.0	2.817	38.0	2.446	50.0	2.604
11.0	2.031	11.0	1.892	30.0	2.848					40.0	2.496	60.0	2.806
12.0	2.135	12.0	1.975							45.0	2.621	70.0	3.008
13.0	2.239	13.0	2.059							50.0	2.746		
14.0	2.343	14.0	2.142										
15.0	2.447	15.0	2.225										

$$\times\left[\frac{q(t_M-t_1)-q(t_M-t_2)}{\theta_2-\theta_1}\right]+\dots+[P(\theta_{n-1})-P(\theta_n)]\left[\frac{q(t_M-t_{n-1})-q(t_M-t_n)}{\theta_n-\theta_{n-1}}\right]\Bigg\}$$

where the fluid-influx terms, $q(t)$, are determined for the various boundary conditions in the manner prescribed above for the "pressure case."

B. Linear Systems. The corresponding expressions for the rate case, pressure case, and rate of fluid influx for infinite linear systems are as follows:

1. *Rate Case*

$$P_o-P(O,\theta_M)=\frac{2}{a}\sqrt{\frac{\mu}{\pi\phi k c_e}}\{Q(\theta o)\sqrt{\theta_M}+[Q(\theta_1)-Q(\theta_o)]\sqrt{\theta_M-\theta_1}+$$
$$[Q(\theta_2)-Q(\theta_1)]\sqrt{\theta_M-\theta_2}+\dots+[Q(\theta_n)-Q(\theta_n-1)]\sqrt{\theta_M-\theta_n}\}$$

2. *Pressure Case*

$$F_e(\theta_M)=2a\sqrt{\frac{\phi c_e k}{\pi\mu}}\quad\{[P_o-P(\theta_1)]\sqrt{\theta_M}+$$
$$[P(\theta_1)-P(\theta_2)]\sqrt{\theta_M-\theta_1}+\dots+[P(\theta_{n-1})-P(\theta_n)]\sqrt{\theta_M-\theta_{n-1}}\}$$

3. *Rate of Fluid Influx*

$$Q(\theta_M)=a\sqrt{\frac{\phi c_e k}{\pi\mu}}\left\{\frac{[P_o-P(\theta_1)]}{\sqrt{\theta_M}}+\frac{[P(\theta_1)-P(\theta_2)]}{\sqrt{\theta_M-\theta_1}}\right.$$
$$\left.+\frac{[P(\theta_2)-P(\theta_3)]}{\sqrt{\theta_M-\theta_2}}+\dots+\frac{[P(\theta_n-1)-P(\theta_n)]}{\sqrt{\theta_M-\theta_{n-1}}}\right\}$$

i — subscript: represents any positive integer from the set 1, 2, 3, ..., n

k — average permeability

m — mass

n — arbitrary positive integer

p — dimensionless pressure change term

p' — dimensionless pressure correction term

q — dimensionless fluid-influx term

r — radial distance

r_c — internal radius of casing

r_e — equivalent radius of exterior boundary; effective producing radius

r_T — external radius of tubing

r_w — equivalent radius of interior boundary; well radius

s — arbitrary variable

t — dimensionless time ratio

t_M — corresponds to total period of time under consideration

v_M — maximum velocity

w — variable of integration

x — linear distance

x_M — distance between exterior and interior boundaries of a linear system

x_r — counting element of distance in linear system

α — central angle of circular sector

β — average formation volume factor

δ — mathematical root

θ — time

θ_M — total period of time under consideration

θ_R — time of readjustment

κ — mathematical root

μ — viscosity

ζ — mathematical root

ρ — average density

ρ_o — average density of oil at bottom-hole conditions

ϕ — average effective porosity

TABLE 5. Finite radial system with fixed constant pressure at exterior boundary—Rate case. . .

re/rw=1.5

Dimensionless time t	Pressure change p(t)
$5.0(10)^{-2}$	0.230
5.5 "	0.240
6.0 "	0.249
7.0 "	0.266
8.0 "	0.282
9.0 "	0.292
$1.0(10)^{-1}$	0.307
1.2 "	0.328
1.4 "	0.344
1.6 "	0.356
1.8 "	0.367
2.0 "	0.375
2.2 "	0.381
2.4 "	0.386
2.6 "	0.390
2.8 "	0.393
3.0 "	0.396
3.5 "	0.400
4.0 "	0.402
4.5 "	0.404
5.0 "	0.405
6.0 "	0.405
7.0 "	0.405
8.0 "	0.405

re/rw=2.0

Dimensionless time t	Pressure change p(t)
$2.0(10)^{-1}$	0.424
2.2 "	0.441
2.4 "	0.457
2.6 "	0.472
2.8 "	0.485
3.0 "	0.498
3.5 "	0.527
4.0 "	0.552
4.5 "	0.573
5.0 "	0.591
5.5 "	0.606
6.0 "	0.619
6.5 "	0.630
7.0 "	0.639
7.5 "	0.647
8.0 "	0.654
8.5 "	0.660
9.0 "	0.665
9.5 "	0.669
1.0	0.673
1.2	0.682
1.4	0.688
1.6	0.690
1.8	0.692
2.0	0.692
2.5	0.693
3.0	0.693

re/rw=2.5

Dimensionless time t	Pressure change p(t)
$3.0(10)^{-1}$	0.502
3.5 "	0.535
4.0 "	0.564
4.5 "	0.591
5.0 "	0.616
5.5 "	0.638
6.0 "	0.659
7.0 "	0.695
8.0 "	0.728
9.0 "	0.755
1.0	0.778
1.2	0.815
1.4	0.842
1.6	0.861
1.8	0.876
2.0	0.887
2.2	0.895
2.4	0.900
2.6	0.905
2.8	0.908
3.0	0.910
3.5	0.913
4.0	0.915
4.5	0.916
5.0	0.916
5.5	0.916
6.0	0.916

re/rw=3.0

Dimensionless time t	Pressure change p(t)
$5.0(10)^{-1}$	0.617
5.5 "	0.640
6.0 "	0.662
7.0 "	0.702
8.0 "	0.738
9.0 "	0.770
1.0	0.799
1.2	0.850
1.4	0.892
1.6	0.927
1.8	0.955
2.0	0.980
2.2	1.000
2.4	1.016
2.6	1.030
2.8	1.042
3.0	1.051
3.5	1.069
4.0	1.080
4.5	1.087
5.0	1.091
5.5	1.094
6.0	1.096
6.5	1.097
7.0	1.097
8.0	1.098
10.0	1.099

re/rw=3.5

Dimensionless time t	Pressure change p(t)
$5.0(10)^{-1}$	0.620
6.0 "	0.665
7.0 "	0.705
8.0 "	0.741
9.0 "	0.774
1.0	0.804
1.2	0.858
1.4	0.904
1.6	0.945
1.8	0.981
2.0	1.013
2.2	1.041
2.4	1.065
2.6	1.087
2.8	1.106
3.0	1.123
3.5	1.158
4.0	1.183
5.0	1.215
6.0	1.232
7.0	1.242
8.0	1.247
9.0	1.250
10.0	1.251
12.0	1.252
14.0	1.253
16.0	1.253

re/rw=4.0

Dimensionless time t	Pressure change p(t)
1.0	0.802
1.2	0.857
1.4	0.905
1.6	0.947
1.8	0.985
2.0	1.020
2.2	1.052
2.4	1.080
2.6	1.106
2.8	1.130
3.0	1.152
3.4	1.190
3.8	1.222
4.5	1.266
5.0	1.290
5.5	1.309
6.0	1.325
7.0	1.347
8.0	1.361
9.0	1.370
10.0	1.376
12.0	1.382
14.0	1.385
16.0	1.386
18.0	1.386

re/rw=5.0

Dimensionless time t	Pressure change p(t)
4.0	1.275
4.5	1.320
5.0	1.361
5.5	1.398
6.0	1.432
6.5	1.462
7.0	1.490
7.5	1.516
8.0	1.539
8.5	1.561
9.0	1.580
10.0	1.615
12.0	1.667
14.0	1.704
16.0	1.730
18.0	1.749
20.0	1.762
22.0	1.771
24.0	1.777
26.0	1.781
28.0	1.784
30.0	1.787
35.0	1.789
40.0	1.791
50.0	1.792

re/rw=8.0

Dimensionless time t	Pressure change p(t)
7.0	1.499
7.5	1.527
8.0	1.554
8.5	1.580
9.0	1.604
9.5	1.627
10.0	1.645
12.0	1.724
14.0	1.786
16.0	1.837
18.0	1.879
20.0	1.914
22.0	1.943
24.0	1.967
26.0	1.988
28.0	2.002
30.0	2.016
35.0	2.040
40.0	2.055
45.0	2.064
50.0	2.070
60.0	2.076
70.0	2.078
80.0	2.079

re/rw=10.0

Dimensionless time t	Pressure change p(t)
10.0	1.651
12.0	1.730
14.0	1.798
16.0	1.856
18.0	1.907
20.0	1.952
25.0	2.043
30.0	2.111
35.0	2.160
40.0	2.197
45.0	2.224
50.0	2.245
55.0	2.260
60.0	2.271
65.0	2.279
70.0	2.285
75.0	2.290
80.0	2.293
90.0	2.297
$10.0(10)^{1}$	2.300
11.0 "	2.301
12.0 "	2.302
13.0 "	2.302
14.0 "	2.302
16.0 "	2.303

re/rw=15.0

Dimensionless time t	Pressure change p(t)
20.0	1.960
22.0	2.003
24.0	2.043
26.0	2.080
28.0	2.114
30.0	2.146
35.0	2.218
40.0	2.279
45.0	2.332
50.0	2.379
60.0	2.455
70.0	2.513
80.0	2.558
90.0	2.592
$10.0(10)^{1}$	2.619
12.0 "	2.655
14.0 "	2.677
16.0 "	2.689
18.0 "	2.697
20.0 "	2.701
22.0 "	2.704
24.0 "	2.706
26.0 "	2.707
28.0 "	2.707
30.0 "	2.708

re/rw=20.0

Dimensionless time t	Pressure change p(t)
30.0	2.148
35.0	2.219
40.0	2.282
45.0	2.338
50.0	2.388
60.0	2.475
70.0	2.547
80.0	2.609
90.0	2.658
$10.0(10)^{1}$	2.707
10.5 "	2.728
11.0 "	2.747
11.5 "	2.764
12.0 "	2.781
12.5 "	2.796
13.0 "	2.810
13.5 "	2.823
14.0 "	2.835
14.5 "	2.846
15.0 "	2.857
16.0 "	2.876
18.0 "	2.906
20.0 "	2.929
24.0 "	2.958
28.0 "	2.975
30.0 "	2.980
40.0 "	2.992
50.0 "	2.995

re/rw=25.0

Dimensionless time t	Pressure change p(t)
50.0	2.389
55.00	2.434
60.0	2.476
65.0	2.514
70.0	2.550
75.0	2.583
80.0	2.614
85.0	2.643
90.0	2.671
95.0	2.697
$10.0(10)^{1}$	2.721
12.0 "	2.807
14.0 "	2.878
16.0 "	2.936
18.0 "	2.984
20.0 "	3.024
22.0 "	3.057
24.0 "	3.085
26.0 "	3.107
28.0 "	3.126
30.0 "	3.142
35.0 "	3.171
40.0 "	3.189
45.0 "	3.200
50.0 "	3.207
60.0 "	3.214
70.0 "	3.217
80.0 "	3.218
90.0 "	3.219

re/rw=30.0

Dimensionless time t	Pressure change p(t)
70.0	2.551
80.0	2.616
90.0	2.672
$10.0(10)^{1}$	2.723
12.0 "	2.812
14.0 "	2.886
16.0 "	2.950
16.5 "	2.965
17.0 "	2.979
17.5 "	2.992
18.0 "	3.006
20.0 "	3.054
25.0 "	3.150
30.0 "	3.219
35.0 "	3.269
40.0 "	3.306
45.0 "	3.332
50.0 "	3.351
60.0 "	3.376
70.0 "	3.387
80.0 "	3.394
90.0 "	3.397
$10.0(10)^{2}$	3.399
12.0 "	3.401
14.0 "	3.401

re/rw=40.0

Dimensionless time t	Pressure change p(t)
$12.0(10)^{1}$	2.813
14.0 "	2.888
16.0 "	2.953
18.0 "	3.011
20.0 "	3.063
22.0 "	3.109
24.0 "	3.153
26.0 "	3.191
28.0 "	3.226
30.0 "	3.259
35.0 "	3.331
40.0 "	3.391
45.0 "	3.440
50.0 "	3.482
55.0 "	3.516
60.0 "	3.545
65.0 "	3.568
70.0 "	3.588
80.0 "	3.619
90.0 "	3.640
$10.0(10)^{2}$	3.655
12.0 "	3.672
14.0 "	3.681
16.0 "	3.685
18.0 "	3.687
20.0 "	3.688
25.0 "	3.689

re/rw=50.0

Dimensionless time t	Pressure change p(t)
$20.0(10)^{1}$	3.064
22.0 "	3.111
24.0 "	3.154
26.0 "	3.193
28.0 "	3.229
30.0 "	3.263
35.0 "	3.339
40.0 "	3.406
45.0 "	3.461
50.0 "	3.512
55.0 "	3.556
60.0 "	3.595
65.0 "	3.630
70.0 "	3.661
75.0 "	3.688
80.0 "	3.713
85.0 "	3.735
90.0 "	3.754
95.0 "	3.771
$10.0(10)^{2}$	3.787
12.0 "	3.833
14.0 "	3.862
16.0 "	3.881
18.0 "	3.892
20.0 "	3.900
22.0 "	3.904
24.0 "	3.907
26.0 "	3.909
28.0 "	3.910

re/rw=60.0

Dimensionless time t	Pressure change p(t)
$3.0(10)^{2}$	3.257
4.0 "	3.401
5.0 "	3.512
6.0 "	3.602
7.0 "	3.676
8.0 "	3.739
9.0 "	3.792
10.0 "	3.832
12.0 "	3.908
14.0 "	3.959
16.0 "	3.996
18.0 "	4.023
20.0 "	4.043
25.0 "	4.071
30.0 "	4.084
35.0 "	4.090
40.0 "	4.092
45.0 "	4.093
50.0 "	4.094
55.0 "	4.094

re/rw=70.0

Dimensionless time t	Pressure change p(t)
$5.0(10)^{2}$	3.512
6.0 "	3.603
7.0 "	3.680
8.0 "	3.746
9.0 "	3.803
10.0 "	3.854
12.0 "	3.937
14.0 "	4.003
16.0 "	4.054
18.0 "	4.095
20.0 "	4.127
25.0 "	4.181
30.0 "	4.211
35.0 "	4.228
40.0 "	4.237
45.0 "	4.242
50.0 "	4.245
55.0 "	4.247
60.0 "	4.247
65.0 "	4.248
70.0 "	4.248
75.0 "	4.248
80.0 "	4.248

re/rw=80.0

Dimensionless time t	Pressure change p(t)
$6.0(10)^{2}$	3.603
7.0 "	3.650
8.0 "	3.747
9.0 "	3.805
10.0 "	3.857
12.0 "	3.946
14.0 "	4.019
15.0 "	4.051
16.0 "	4.080
18.0 "	4.130
20.0 "	4.171
25.0 "	4.248
30.0 "	4.297
35.0 "	4.328
40.0 "	4.347
45.0 "	4.360
50.0 "	4.368
60.0 "	4.376
70.0 "	4.380
80.0 "	4.381
90.0 "	4.382
$10.0(10)^{3}$	4.382
11.0 "	4.382

re/rw=90.0

Dimensionless time t	Pressure change p(t)
$8.0(10)^{2}$	3.747
9.0 "	3.806
$1.0(10)^{3}$	3.858
1.2 "	3.949
1.3 "	3.988
1.4 "	4.025
1.5 "	4.058
1.8 "	4.144
2.0 "	4.192
2.5 "	4.285
3.0 "	4.349
3.5 "	4.394
4.0 "	4.426
4.5 "	4.448
5.0 "	4.464
6.0 "	4.482
7.0 "	4.491
8.0 "	4.496
9.0 "	4.498
10.0 "	4.499
11.0 "	4.499
12.0 "	4.500
14.0 "	4.500

re/rw=100.0

Dimensionless time t	Pressure change p(t)
$1.0(10)^{3}$	3.859
1.2 "	3.949
1.4 "	4.026
1.6 "	4.092
1.8 "	4.150
2.0 "	4.200
2.5 "	4.303
3.0 "	4.379
3.5 "	4.434
4.0 "	4.478
4.5 "	4.510
5.0 "	4.534
5.5 "	4.552
6.0 "	4.565
6.5 "	4.579
7.0 "	4.583
7.5 "	4.588
8.0 "	4.593
9.0 "	4.598
10.0 "	4.601
12.5 "	4.604
15.0 "	4.605

re/rw=200.0

Dimensionless time t	Pressure change p(t)
$1.5(10)^{3}$	4.051
2.0 "	4.205
2.5 "	4.317
3.0 "	4.408
3.5 "	4.485
4.0 "	4.552
5.0 "	4.663
6.0 "	4.754
7.0 "	4.829
8.0 "	4.894
9.0 "	4.949
10.0 "	4.996
12.0 "	5.072
14.0 "	5.129
16.0 "	5.171
18.0 "	5.203
20.0 "	5.227
25.0 "	5.264
30.0 "	5.282
35.0 "	5.290
40.0 "	5.294

re/rw=300.0

Dimensionless time t	Pressure change p(t)
$6.0(10)^{3}$	4.754
8.0 "	4.898
10.0 "	5.010
12.0 "	5.101
14.0 "	5.177
16.0 "	5.242
18.0 "	5.299
20.0 "	5.348
24.0 "	5.429
28.0 "	5.491
30.0 "	5.517
40.0 "	5.606
50.0 "	5.652
60.0 "	5.676
70.0 "	5.690
80.0 "	5.696
90.0 "	5.700
$10.0(10)^{4}$	5.702
12.0 "	5.703
14.0 "	5.704
15.0 "	5.704

re/rw=400.0

Dimensionless time t	Pressure change p(t)
$1.5(10)^{4}$	5.212
2.0 "	5.356
3.0 "	5.555
4.0 "	5.659
5.0 "	5.781
6.0 "	5.845
7.0 "	5.889
8.0 "	5.920
9.0 "	5.942
10.0 "	5.957
11.0 "	5.967
12.0 "	5.975
12.5 "	5.977
13.0 "	5.980
14.0 "	5.983
16.0 "	5.988
18.0 "	5.990
20.0 "	5.991
24.0 "	5.991
26.0 "	5.991

re/rw=500.0

Dimensionless time t	Pressure change p(t)
$2.0(10)^{4}$	5.356
2.5 "	5.468
3.0 "	5.559
3.5 "	5.636
4.0 "	5.702
4.5 "	5.759
5.0 "	5.810
6.0 "	5.894
7.0 "	5.960
8.0 "	6.013
9.0 "	6.055
10.0 "	6.088
12.0 "	6.135
14.0 "	6.164
16.0 "	6.183
18.0 "	6.195
20.0 "	6.202
25.0 "	6.211
30.0 "	6.213
35.0 "	6.214
40.0 "	6.214

Continued.

TABLE 5. Finite radial system with fixed constant pressure at Exterior Boundary — Rate case. — (Continued)

re/rw=600.0		re/rw=700.0		re/rw=800.0		re/rw=900.0		re/rw=1000.0		re/rw=1200.0		re/rw=1400.0		re/rw=1600.0	
Dimensionless time t	Pressure change p(t)	Dimensionless time t	Pressure change p(t)	Dimensionless time t	Pressure change p(t)	Dimensionless time t	Pressure change p(t)	Dimensionless time t	Pressure change p(t)	Dimensionless time t	Pressure change p(t)	Dimensionless time t	Pressure change p(t)	Dimensionless time t	Pressure change p(t)
4.0(10)^4	5.703	5.0(10)^4	5.814	7.0(10)^4	5.983	8.0(10)^4	6.049	1.0(10)^5	6.161	2.0(10)^5	6.507	2.0(10)^5	6.507	2.5(10)^5	6.619
4.5 "	5.762	6.0 "	5.905	8.0 "	6.049	9.0 "	6.103	1.2 "	6.252	3.0 "	6.704	2.5 "	6.619	3.0 "	6.710
5.0 "	5.814	7.0 "	5.982	9.0 "	6.108	10.0 "	6.161	1.4 "	6.329	4.0 "	6.833	3.0 "	6.709	3.5 "	6.787
6.0 "	5.904	8.0 "	6.048	10.0 "	6.160	12.0 "	6.251	1.6 "	6.395	5.0 "	6.918	3.5 "	6.785	4.0 "	6.853
7.0 "	5.979	9.0 "	6.105	12.0 "	6.249	14.0 "	6.327	1.8 "	6.452	6.0 "	6.975	4.0 "	6.849	5.0 "	6.962
8.0 "	6.041	10.0 "	6.156	14.0 "	6.322	16.0 "	6.392	2.0 "	6.503	7.0 "	7.013	5.0 "	6.950	6.0 "	7.046
9.0 "	6.094	12.0 "	6.239	16.0 "	6.382	18.0 "	6.447	2.5 "	6.605	8.0 "	7.038	6.0 "	7.026	7.0 "	7.114
10.0 "	6.139	14.0 "	6.305	18.0 "	6.432	20.0 "	6.494	3.0 "	6.681	9.0 "	7.056	7.0 "	7.082	8.0 "	7.167
12.0 "	6.210	16.0 "	6.357	20.0 "	6.474	25.0 "	6.587	3.5 "	6.738	10.0 "	7.067	8.0 "	7.123	9.0 "	7.210
14.0 "	6.262	18.0 "	6.398	25.0 "	6.551	30.0 "	6.652	4.0 "	6.781	12.0 "	7.080	9.0 "	7.154	10.0 "	7.244
16.0 "	6.299	20.0 "	6.430	30.0 "	6.599	40.0 "	6.729	4.5 "	6.812	14.0 "	7.085	10.0 "	7.177	15.0 "	7.334
18.0 "	6.326	25.0 "	6.484	35.0 "	6.630	45.0 "	6.751	5.0 "	6.837	16.0 "	7.088	15.0 "	7.229	20.0 "	7.364
20.0 "	6.345	30.0 "	6.514	40.0 "	6.650	50.0 "	6.768	5.5 "	6.854	18.0 "	7.089	20.0 "	7.241	25.0 "	7.373
25.0 "	6.374	35.0 "	6.530	45.0 "	6.663	55.0 "	6.777	6.0 "	6.868	19.0 "	7.089	25.0 "	7.243	30.0 "	7.376
30.0 "	6.387	40.0 "	6.540	50.0 "	6.671	60.0 "	6.785	7.0 "	6.885	20.0 "	7.090	30.0 "	7.244	35.0 "	7.377
35.0 "	6.392	45.0 "	6.545	55.0 "	6.676	70.0 "	6.794	8.0 "	6.895	21.0 "	7.090	31.0 "	7.244	40.0 "	7.378
40.0 "	6.395	50.0 "	6.548	60.0 "	6.679	80.0 "	6.798	9.0 "	6.901	22.0 "	7.090	32.0 "	7.244	42.0 "	7.378
50.0 "	6.397	60.0 "	6.550	70.0 "	6.682	90.0 "	6.800	10.0 "	6.904	23.0 "	7.090	33.0 "	7.244	44.0 "	7.378
60.0 "	6.397	70.0 "	6.551	80.0 "	6.684	10.0(10)^4	6.801	12.0 "	6.907	24.0 "	7.090				
		80.0 "	6.551	100.0 "	6.684			14.0 "	6.907						
								16.0 "	6.908						

re/rw=1800.0		re/rw=2000.0		re/rw=2200.0		re/rw=2400.0		re/rw=2600.0		re/rw=2800.0		re/rw=3000.0	
Dimensionless time t	Pressure change p(t)	Dimensionless time t	Pressure change p(t)	Dimensionless time t	Pressure change p(t)	Dimensionless time t	Pressure change p(t)	Dimensionless time t	Pressure change p(t)	Dimensionless time t	Pressure change p(t)	Dimensionless time t	Pressure change p(t)
3.0(10)^5	6.710	4.0(10)^5	6.854	5.0(10)^5	6.966	6.0(10)^5	7.057	7.0(10)^5	7.134	8.0(10)^5	7.201	1.0(10)^6	7.312
4.0 "	6.854	5.0 "	6.966	5.5 "	7.012	7.0 "	7.134	8.0 "	7.201	9.0 "	7.260	1.2 "	7.403
5.0 "	6.965	6.0 "	7.056	6.0 "	7.057	8.0 "	7.200	9.0 "	7.259	10.0 "	7.312	1.4 "	7.480
6.0 "	7.054	7.0 "	7.132	6.5 "	7.097	9.0 "	7.259	10.0 "	7.312	12.0 "	7.403	1.6 "	7.545
7.0 "	7.120	8.0 "	7.196	7.0 "	7.133	10.0 "	7.310	12.0 "	7.401	16.0 "	7.542	1.8 "	7.602
8.0 "	7.188	9.0 "	7.251	7.5 "	7.167	12.0 "	7.398	14.0 "	7.475	20.0 "	7.644	2.0 "	7.651
9.0 "	7.238	10.0 "	7.298	8.0 "	7.199	16.0 "	7.526	16.0 "	7.536	24.0 "	7.719	2.4 "	7.732
10.0 "	7.280	12.0 "	7.374	8.5 "	7.229	20.0 "	7.611	18.0 "	7.583	28.0 "	7.775	2.8 "	7.794
15.0 "	7.407	14.0 "	7.431	9.0 "	7.256	24.0 "	7.668	20.0 "	7.631	30.0 "	7.797	3.0 "	7.820
20.0 "	7.459	16.0 "	7.474	10.0 "	7.307	28.0 "	7.706	24.0 "	7.699	35.0 "	7.840	3.5 "	7.871
30.0 "	7.489	18.0 "	7.506	12.0 "	7.390	30.0 "	7.720	28.0 "	7.746	40.0 "	7.870	4.0 "	7.908
40.0 "	7.495	20.0 "	7.530	16.0 "	7.507	35.0 "	7.745	30.0 "	7.765	50.0 "	7.905	4.5 "	7.935
50.0 "	7.495	25.0 "	7.566	20.0 "	7.579	40.0 "	7.760	35.0 "	7.799	60.0 "	7.922	5.0 "	7.955
51.0 "	7.495	30.0 "	7.584	25.0 "	7.631	50.0 "	7.775	40.0 "	7.821	70.0 "	7.930	6.0 "	7.979
52.0 "	7.495	35.0 "	7.593	30.0 "	7.661	60.0 "	7.780	50.0 "	7.845	80.0 "	7.934	7.0 "	7.992
53.0 "	7.495	40.0 "	7.597	35.0 "	7.677	70.0 "	7.782	60.0 "	7.856	90.0 "	7.936	8.0 "	7.999
54.0 "	7.495	50.0 "	7.600	40.0 "	7.686	80.0 "	7.783	70.0 "	7.860	10.0(10)^6	7.937	9.0 "	8.002
56.0 "	7.495	60.0 "	7.601	50.0 "	7.693	90.0 "	7.783	80.0 "	7.862	12.0 "	7.937	10.0 "	8.004
		64.0 "	7.601	60.0 "	7.695	95.0 "	7.783	90.0 "	7.863	13.0 "	7.937	12.0 "	8.006
				70.0 "	7.696			10.0(10)^6	7.863			15.0 "	8.006
				80.0 "	7.696								

Note: The numberical values in Tables 3, 4, and 5 and part of those in Table 2 were taken directly from the Hurst and van Everdingen report.[1] The values in Table 1 and those in Table 2 including the range t = 1 to t = 125,000 were supplied to the author by A. F. van Everdingen through the courtesy of the Shell Oil Company, and appear in publication for the first time.

Assumptions Underlying Hurst-Van Everdingen Equations

1. The effects of gravity on the fluid flow are neglected totally.
2. All flow through reservoir systems is assumed macroscopically laminar and thus governed by Darcy's law.
3. The sum expressed by Equation (24) is really the approximation

$$P_o - P(1, \theta_M) = \frac{\mu}{2\pi kh}\left\{Q(\theta_o)\,p(t_M) + \int_o^{\theta_M} \frac{d}{d\theta}\,[Q(\theta)]\,p(t_M - t)\,d\theta\right\}$$

$$\approx \frac{\mu}{2\pi kh}\left\{Q(\theta_o)\,p(t_M) + \sum_{i=1}^{n}\,[Q(\theta_i) - Q(\theta_{i-1})]\,p(t_M - t_i)\right\}$$

hence, increments of θ should be chosen as small as practicable.

4. Likewise, the sum expressed by Equation (31) is the approximation

$$F_c(\theta_M) = 2\pi\phi c_f r_w^2 h \int_o^{\theta_M} \frac{\partial \Delta P}{\partial \theta}\,q(t_M - t)\,d\theta$$

$$\approx 2\pi\phi c_f r_w^2 h \sum_{i=o}^{n}\,[P(\theta_i) - P(\theta_{i+1})]\,q(t_M - t_i)$$

hence, the increments of θ should here be also chosen as small as practicable.

5. Assumptions "3" and "4" apply to the corresponding expressions for linear systems.
6. For radial systems the relations $p(t) = 2\sqrt{t/\pi}$ and $pq(t) = 2\sqrt{t/\pi}$, for $t < 0.01$, are only close approximations of the rigorous equations.
7. The analytical results are based on ideal radial and linear symmetry.
8. Values for the pressure-change and fluid-influx terms are available only for specified boundary conditions.
9. The relation expressed by Equation (49) for obtaining the "annulus volume adjustment term," C, is an approximation based primarily on the assumption that the casing-head pressure is equivalent to a head of oil identical in height to the gas column in the annulus, throughout the bottom hole pressure decline. A value of C so obtained should suffice for most engineering purposes; however, if a more exact value is desired, then the actual casing-head pressure history of a well and the PVT relations of the fluids in the annulus must be used to evaluate the volume of fluid unloaded from the annulus per unit bottom-hole pressure drop, and, in general, the values of C determined with the aid of this ratio will vary with the bottom-hole pressure.
10. Only equivalent single-phase fluids that satisfy the thermodynamic relation

$$\rho = \rho_s\,[1 + c_f(P - P_s)]$$

can exist between the bounding surfaces of a system.

Acknowledgment

The author wishes to thank the management of the Magnolia Petroleum Company for permission to present this paper for publication. The author acknowledges the help of Charles R. Rahn, who prepared the graphs; of William L. Wahl, who checked the numerical accuracy of the calculations; and of Julius Aronofsky, Sam Faris, Paul Reichertz, and Terry Pollard of Magnolia's Field Research Laboratories, who reviewed the original manuscript. Grateful acknowledgment is also made to A. F. van Everdnigen of the Shell Oil Company, who provided the author with tabular information, and to Dr. Morris Muskat of the Gulf Oil Corporation, who reviewed the edited manuscript and made some valuable criticisms. ★ ★

change with the symbol, $p(t)$ is $p_D(t_D)$ in present day nomenclature, for it is also dimensionless.

We would like to look at the behavior of the solution in some detail, including a comparison with the line source solution often used in well testing. A detailed look at this behavior is shown in Fig. 1 from Muieller and Witherspoon (1965). In this figure, dimensionless pressure is graphed against the dimensionless time/radius ratio, t_D / r_D^2. This time function looks at pressure history at the inner boundary $(r_D = 1)$ as well as pressure histories at other radial locations. The $r_D = 1$ curve is the same as Chatas' Table 1.

This set of curves contains much useful information. Note that at the inner boundary, at early times, Chatas' solution and the line source solution differ quite a bit, but they approach each other rapidly, so that at a $t_D / r_D^2 \approx 20$ they are nearly identical. Also notice, that as we move out further into the aquifer $(r_D > 1.0)$, the solutions more closely approach the simple line source solution, so that at $r_D \geq 20$ they are nearly identical.

In well testing this condition is often reached rapidly in time, so analysis of the line source behavior is often useful. This is generally not true in aquifer flow problems, for the inner boundary condition is an oil reservoir, not a well. The r_w^2 term in the dimensionless time function forces real times to be very great before the curves coincide.

A careful look at Chatas' solution at $r_D = 1$, shows that the p_D versus t_D graph has a slope approaching 1/2 at very small t_D. This result is what we should expect. The reason is that, at very early time, the pressure has only changed significantly at points very close to the internal radial boundary. Thus, for practical purposes, we can treat this early time data as though the flow were linear near the periphery of the circle. As we'll discuss later, the equation for early time for all linear problems is,

$$p_D = \frac{2}{\sqrt{\pi}} \sqrt{t_D} \tag{12}$$

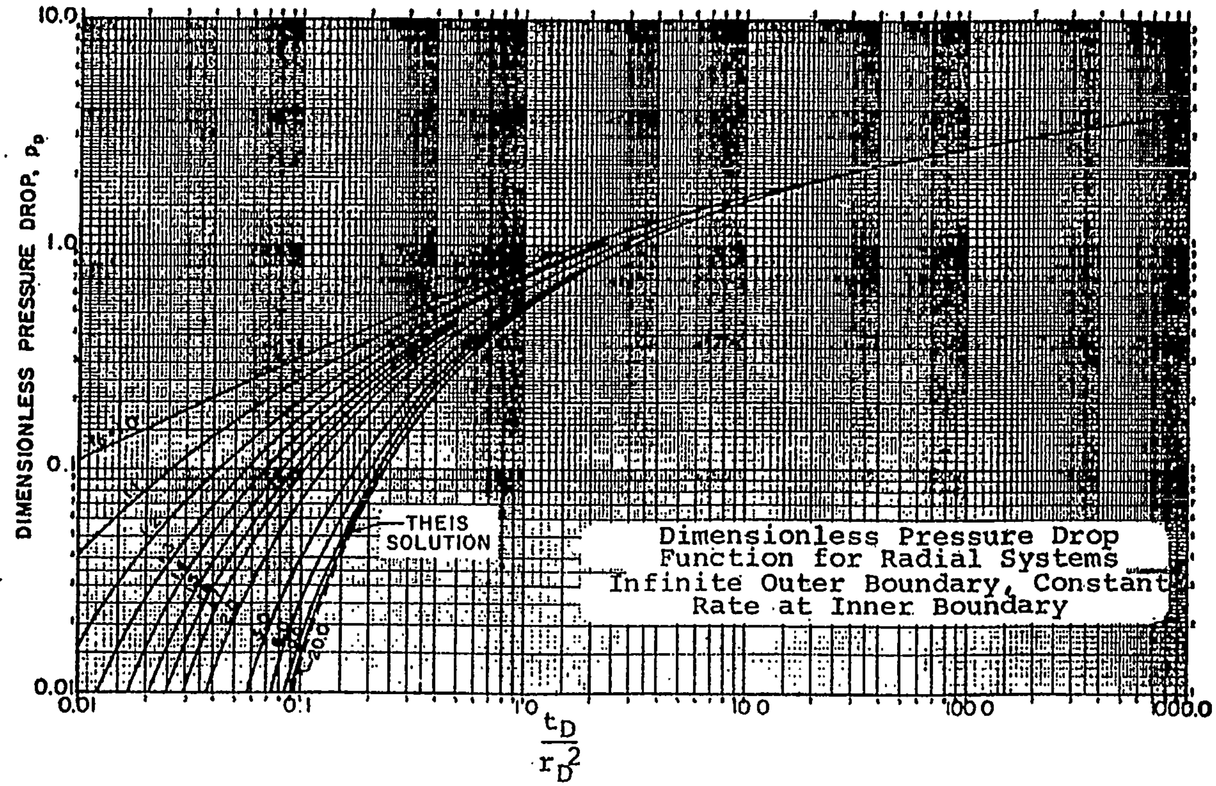

Figure 1. Dimensionless pressure drop function for radial systems: Infinite outer boundary, constant rate at inner boundary (after Mueller and Witherspoon).

From this equation, at $t_D = 0.1$, p_D should equal 0.3568. It actually is 0.3144; that is, it is about 12 % lower than predicted by Eq. 12. At $t_D = 0.01$, the earliest time in Fig. 1, Eq. 12 predicts $p_D = 0.1128$ compared to 0.1081 in Chatas' Table 1. The error is about 4 %.

Now let us turn our attention to the longer time values of p_D. It is well known, in well testing lore, that at long time in an infinite-acting system, the following simple semi-logarithmic equation is valid.

$$p_D = \frac{1}{2}(\ln t_D + 0.80907) \tag{13}$$

Since the mathematical equations for aquifer flow are identical in form, Eq.13 should also hold true for the data in Chatas' Table 1. We will test this assumption for various values of t_D, as seen in the table below. From the results in this table it is clear that, for practical purposes, the two equations are the same after a dimensionless time ranging from about 20 to 50, depending on how accurate you expect your pressure difference data to be. It is also clear, from Fig. 1, that from this time onward, the line source solution and the finite radius solution are also nearly identical.

Comparisons of Actual p_D with Eq. 13

t_D	p_D (Chatas' Table 1)	p_D Eq. 13	% Error
10	1.6509	1.5558	-5.8
15	1.8294	1.7586	-3.9
20	1.9601	1.9024	-2.9
30	2.1470	2.1051	-2.0
50	2.3884	2.3605	-1.2
70	2.5501	2.5288	-0.8
100	2.7233	2.7071	-0.6

Since the early time data approaches Eq. 12, and the late time data approaches Eq. 13, it seems likely that we can use this information to develop simple closed form approximate equations which will fit the data over the entire time range. I have tested this idea, and it works. The short time data were fit to the following equation,

$$p_D = 1.1237\ (t_D)^{1/2} - 0.4326\ t_D + 0.106\ (t_D)^{3/2} \qquad (14)$$

A comparison of early time results from this equation with the tabulated results in Chatas' Table 1 is shown in the table below for t_D's ranging from 0.0005 to 2.00.

Early Time Comparisons of Eq. 14 and Chatas' Table 1

t_D	p_D (Chatas)	p_D Eq. 14	% Error
0.0005	0.0250	0.02491	-0.36
0.001	0.0352	0.03508	-0.34
0.002	0.0495	0.04935	-0.30
0.004	0.0694	0.06932	-0.12
0.007	0.0911	0.09108	-0.02
0.010	0.1081	0.10815	0.05
0.02	0.1503	0.15054	0.16
0.04	0.2077	0.20829	0.28
0.07	0.2680	0.26901	0.38
0.10	0.3144	0.31589	0.47
0.20	0.4241	0.42548	0.33
0.40	0.5645	0.56452	0.00
0.70	0.7024	0.69946	-0.42
1.00	0.8019	0.79710	-0.60
2.00	1.0195	1.02375	0.42

Note that all the values are quite close to Chatas' table over this time range. The greatest difference is 0.60%, which is far more accurate than we would expect real pressure data to be. Note, also, that the first constant in the equation is 1.1237 rather than $2\sqrt{\pi}$ which is 1.1284. This slight difference comes from the least squares fitting routine I used, and is not enough difference to be worrisome. Notice also, that the errors change rapidly from -0.60 % at t_D= 1.00, to + 0.42 % at t_D= 2.00. So the user should not extend this equation beyond this limit. This will not be a problem, for the long time match, that I'll show next, extends over this time range.

For the long time match, I used Eq. 13 as a starting point and added an empirical time function which declines as time increases. The equation I ended up with was as follows,

$$p_D = \frac{1}{2}\left[\ln t_D + 0.80907 + \frac{1.024}{(t_D + 0.40)^{0.729}}\right] \tag{15}$$

Equation 15 was found to fit Chatas' $p_D(t_D)$ data quite well for times, $0.70 \le t_D$. The table on page 19 shows the results in detail.

Notice that these two tables overlap in the time range $0.70 \le t_D \le 2.00$. Also notice that the long time data fit Chatas' Table 1 with good accuracy, with a maximum error of 0.40%. The amount of error decreases at longer times, as we would expect, except at $t_D = 1000$ where the error is 0.09%. From a careful look at Chatas' results it is clear that this value is slightly in error in his table.

Since the infinite aquifer solution becomes a semi-log straight line after a period of time, it can be graphed simply. Also this same graph can be used to compare this behavior with that of other outer boundary conditions. Such a graph is shown in Fig. 2, page 18, from Aziz and Flock (1963). This graph is really remarkable, for it shows that the lines for a constant pressure outer boundary look much like each other (becoming horizontal), and the lines for the no flow outer boundary also look similar in the way they rise. We'll discuss these solutions next.

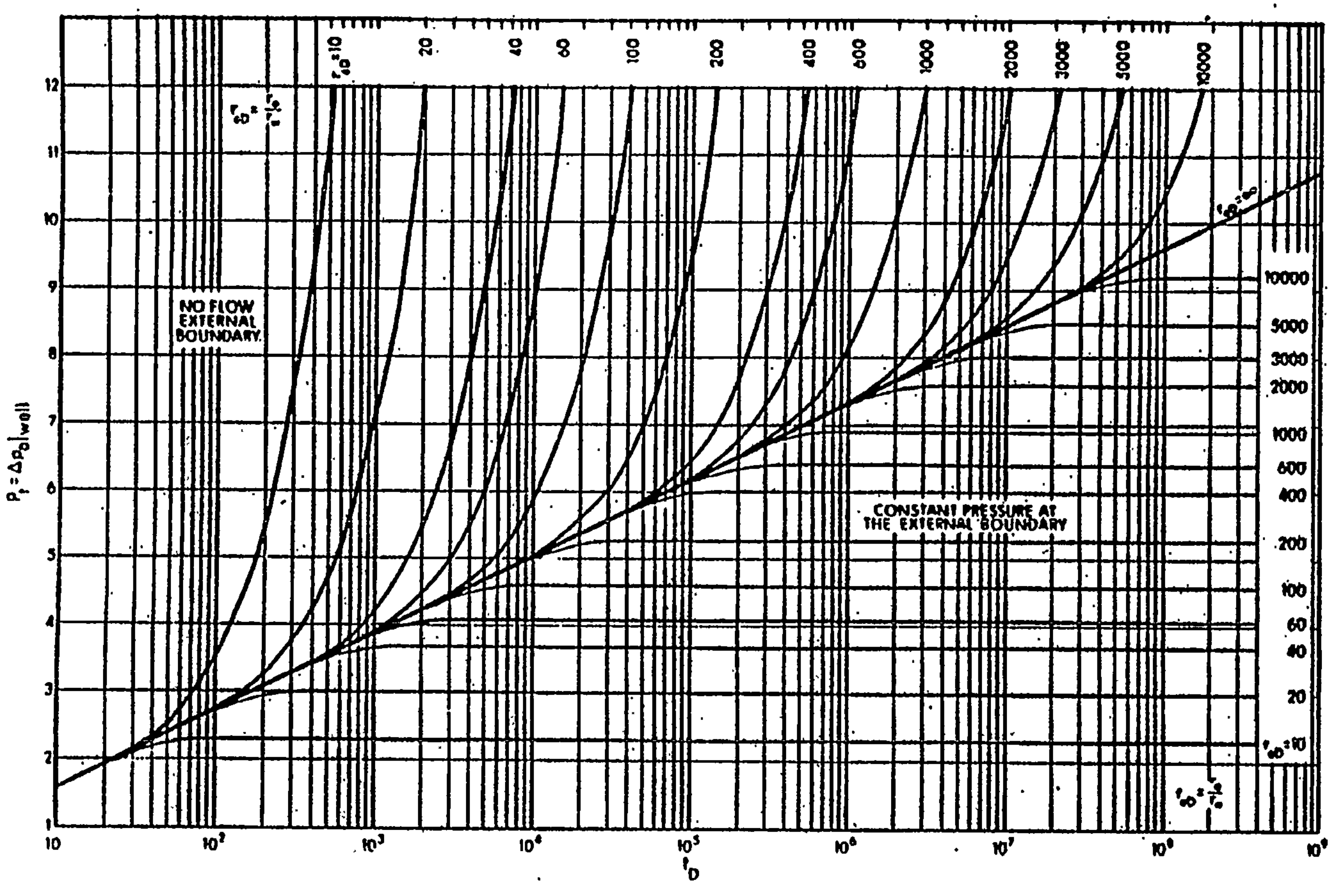

Figure 2. Values of $p_t(=\Delta p_D|_{well})$ for infinite reservoirs, for finite circular reservoirs with no flow at the external boundary and for finite circular reservoirs with constant pressure at the external boundary. From Aziz and Flock (1963).

Late Time Comparisons of Eq. 15 and Chatas' Table 1

t_D	p_D (Chatas)	p_D Eq. 15	% Error
0.70	0.7024	0.7038	0.20
1.00	0.8019	0.8051	0.40
2.0	1.0195	1.0216	0.21
4.0	1.2750	1.2716	-0.27
7.0	1.4997	1.4963	-0.23
10.0	1.6509	1.6487	-0.13
20.0	1.9601	1.9592	-0.05
40	2.2824	2.2835	0.05
70	2.5501	2.5518	0.07
100	2.7233	2.7249	0.06
200	3.0636	3.0644	0.03
400	3.4057	3.4068	0.03
700	3.6842	3.6844	0.01
1000	3.8584	3.8617	0.09

Constant Pressure Outer Boundary

Consider the cases where the pressure is fixed at the outer boundary, the ones that become horizontal and constant in Fig. 2, after a period of time. With a little thought, we should realize that these systems approach the steady state condition after a period of time, for the flow rate is constant, and the outer boundary pressure is fixed. Further, this constant value is based on Darcy's Law, and the equation is quite simple, based on the definitions of the variables.

$$p_D = \ln(r_D) \qquad (16)$$

We can test this conclusion for a couple of cases in Chatas' Table 5, which defines the pressure behavior of this finite system. Note that at late time for $r_D = 10.0$ the pressure value is 2.303, the natural logarithm of 10, and at $r_D = 100$, it is 4.605, as we predict.

We can think further about these results to generalize their behavior, for we know how they work at both early and late times from Eqs. 13 and 16. Using these equations as a guide, we would expect that an equation of the form,

$$p_D - \ln(r_D) = \frac{1}{2}\left[\ln\left(t_D / r_D^2\right) + 0.80907\right] \tag{17}$$

will have the same shape as Eq. 13, and all results would fall exactly on top of each other at early time, for Eq. 13 has really not been changed. At late time, however, the pressures are independent of time, so the left-hand side of Eq. 17 should be identically equal to zero for all radii. We'll check this idea out for certain cases in Chatas' Table 5, as listed in the tables below.

Equation 17 Values for $r_D = 2.0$, 10, 100 and 1,000

$r_D = 2.0$				$r_D = 10$			
p_D	$p_D - \ln(r_D)$	t_D	t_D / r_D^2	p_D	$p_D - \ln(r_D)$	t_D	t_D / r_D^2
0.424	-0.269	0.200	0.0500	1.651	-0.652	10.0	0.1000
0.498	-0.195	0.300	0.0750	1.952	-0.351	20.0	0.2000
0.591	-0.102	0.500	0.4000	2.197	-0.106	40.0	0.4000
0.647	-0.046	0.750	0.1875	2.271	-0.032	60.0	0.6000
0.673	-0.020	1.000	0.2500	2.300	-0.003	100.0	1.0000
0.688	-0.005	1.400	0.3500	2.303	-0.000	160.0	1.6000
0.693	-0.000	3.000	0.7500				
$r_D = 100$				$r_D = 1{,}000$			
p_D	$p_D - \ln(r_D)$	t_D	t_D / r_D^2	p_D	$p_D - \ln(r_D)$	t_D	t_D / r_D^2
3.859	-0.746	1000	0.1000	6.161	-0.747	1×10^5	0.1000
4.150	-0.455	1800	0.1800	6.605	-0.303	2.5×10^5	0.2500
4.434	-0.171	3500	0.3500	6.813	-0.095	4.5×10^5	0.4500
4.552	-0.053	5500	0.5500	6.885	-0.023	7.0×10^5	0.7000
4.598	0.007	9000	0.9000	6.904	-0.004	10.0×10^5	1.0000
4.605	-0.000	15000	1.5000	6.909	-0.000	16.0×10^5	1.6000

The results of these calculations are graphed on Fig. 3, page 22, using $p_D - \ln(r_D)$ on the arithmetic coordinate and t_D/r_D^2 on the logarithmic coordinate, as suggested by Eq. 17. It is clear from this figure, that all the tabulated values do not fit with each other; but it is important to see that they do fit for $r_D = 100$ and 1000. The reason, of course, is that the form of Eq. 17 came from Eq. 13, which we know from Fig. 1 isn't correct until after a period of time. This, in turn, means that the system must be large enough that the outer boundary is not felt before Eq. 13 becomes valid.

Notice, also, that the $r_D = 10$ data fit fairly closely to the data at larger radii. This is because at $r_D = 10$ the assumptions inherent in Eq. 17 are not unreasonable. Again, we could have predicted this from looking at the results in Fig. 1 at $r_D = 10.0$.

An additional point should be made about these results. It is obvious from Fig. 3 that all the columns of Chatas' Table 5 were not necessary. The results at $r_D = 100$ can be transposed to any other higher value of r_D using Eq. 17. This is a useful concept that can be of great help in understanding how aquifer influx behaves (or any transient flow) at large r_D.

To translate from one value of r_D to another, we use Eq. 17 to conclude that at another radius, we should look at pressure results at differing times, as follows,

$$t_{D2} = t_{D1}(r_{D2}/r_{D1})^2 = t_{D1}(r_2/r_1)^2 \tag{18}$$

Also, from Eq. 17, the pressure behavior for the second case (at $r_D = r_{D2}$) is related at these times to that of the first case $(r_D = r_{D1})$ by,

$$p_{D2} = p_{D1} + \ln(r_{D2}/r_{D1}) \tag{19}$$

To test this idea out, I've listed values of p_D at various values of t_D from Chatas' Table 5 at $r_D = 100$ and 1000, as shown in the table on page 23. Some comments about this table seem in order. The values of t_{D1} and p_{D1} in the table come directly from Chatas' Table 5 at $r_D = 100$. Equation 18 tells us that, if $r_{D2} = 1000$, we should evaluate p_D at dimensionless times 100 times as great. These are the times used in the third column, while the fourth column shows the pressure differences listed in

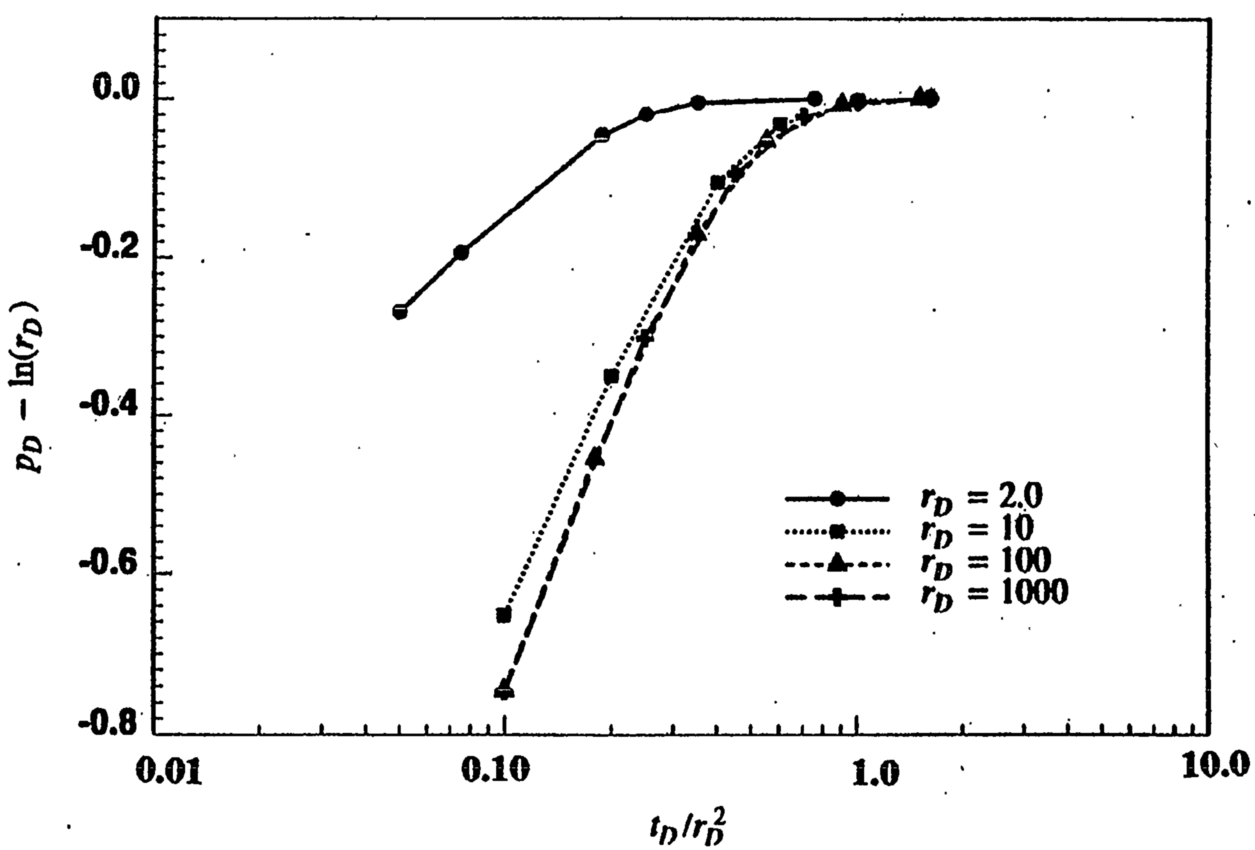

Figure 3. Comparisons of tabulated data using Eq. 17.

Chatas' Table 5 at $r_D = 1000$. The fifth column comes from Eq. 19, which states that these pressure terms should be the same as in the second column with a simple adjustment by $\ln(r_2 / r_1)$. Note from comparing the last two pressure columns that this statement is exactly true, so it is clear that Eqs. 18 and 19 can be used to generate any set of pressure calculations one wishes to use for any large value of r_D.

Comparisons of p_D Values at $r_D = 100$ and 1,000

$r_{D1} = 100$		$r_{D2} = 1000$		$\ln r_2 / r_1 = 2.303$
t_{D1}	p_{D1}	$t_{D2} = t_{D1}(r_2 / r_1)^2$	p_{D2}	$p_{D1} + 2.303$
1.0×10^3	3.589	1.0×10^5	6.161	6.162
2.0	4.200	2.0	6.503	6.503
4.0	4.478	4.0	6.781	6.781
6.0	4.565	6.0	6.868	6.868
10.0	4.601	10.0	6.904	6.904

As discussed later in this report, certain outer boundary conditions cause exponential decline when the data are graphed properly. This idea is discussed in some detail for the radial system with a closed outer boundary and a constant pressure inner boundary in the next section of these notes. But it is also true that finite aquifers, with constant pressure at the outer boundary, and produced at a constant rate, will exhibit exponential decline when graphed properly.

To show this concept, I've looked at one case in detail, at $r_D = 10.0$. The exponential decline equation tells us that, if we were to graph the log of the pressure difference against time on arithmetic coordinates, we should get a straight line. For this purpose, the pressure term graphed should be $p_D(\infty) - p_D(t_D)$; and for $r_D = 10$, The values of $p_D(\infty)-p_D(t_D)\,[2.303-p_D(t_D)]$ are graphed on semi-log paper against time in Fig. 4 on the next page. Clearly a perfect straight line is found. The slight scatter of a few points off that straight line are an indication of the slight errors in Chatas' table. Note that the first point on this graph is at $t_D=10$, and the value of $p_D(t_D)\,[1.651]$ is the same as in Chatas' Table 1 for the infinite system. Thus, this, and

Exponential Decline Parameters for Radial System at Constant Rate
With a Constant Pressure Outer Boundary, $r_D=10$, $p_D(\infty)=\ln r_D=2.303$

t_D	$p_D(t_D)$	$2.303-p_D(t_D)$
10	1.651	0.652
12	1.730	0.583
14	1.798	0.505
16	1.856	0.447
18	1.907	0.396
20	1.952	0.351
25	2.043	0.260
30	2.111	0.192
35	2.160	0.143
40	2.197	0.106
45	2.224	0.079
50	2.245	0.058
55	2.260	0.043
60	2.271	0.032
65	2.279	0.024
70	2.285	0.018
75	2.290	0.013
80	2.293	0.010

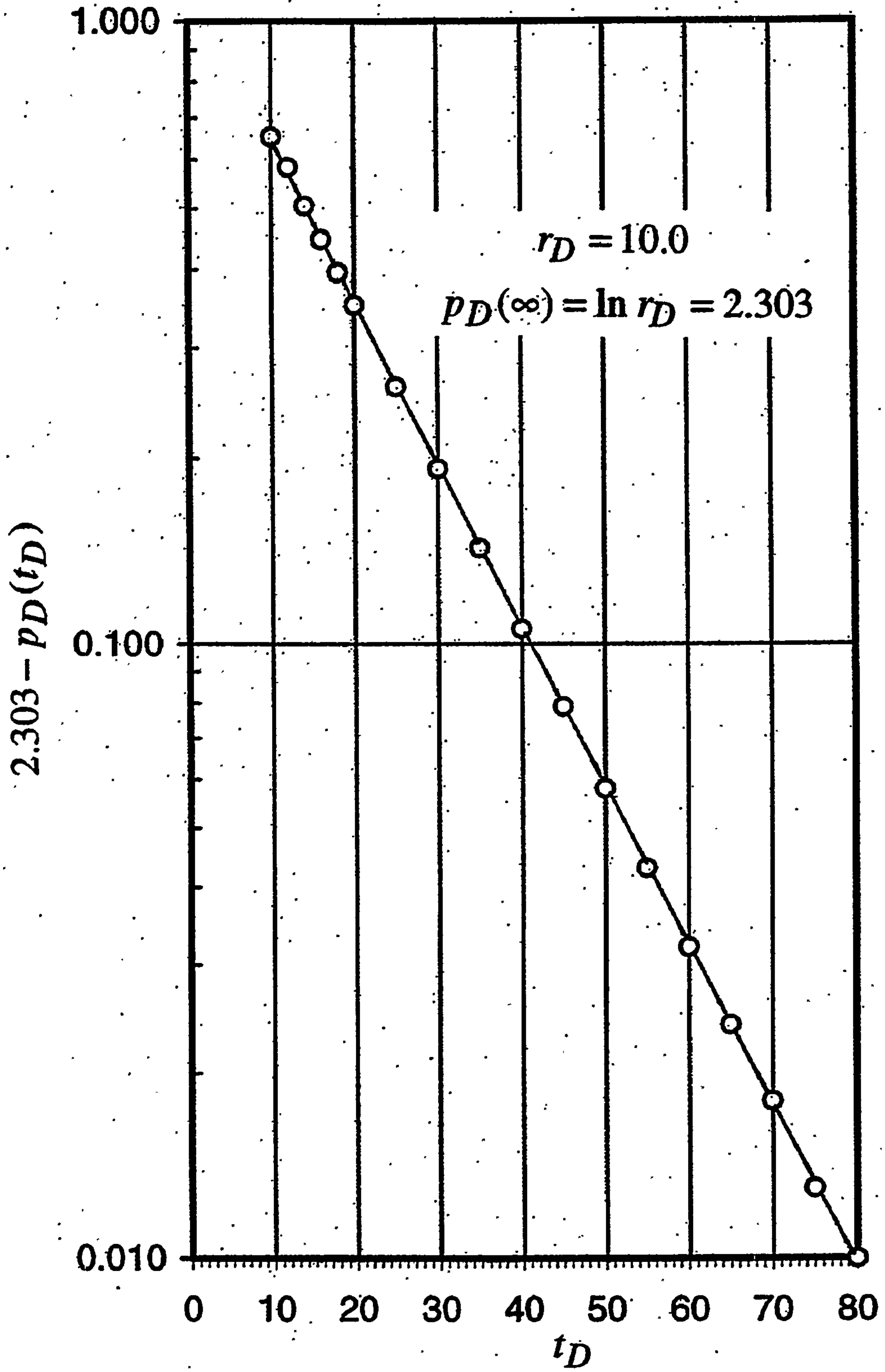

Figure 4. Exponential decline for constant rate with a constant pressure outer boundary.

all other finite radial systems, can be treated as though it were an infinite system for some time, and then the exponential decline equation can be used thereafter.

Clearly, systems at other radii will behave in this same way. Thus it would be possible to derive closed form solutions for the times to switch from infinite acting to exponential behavior, and to define the slopes and interrupts of these exponential decline equations, just as will be done later for the constant pressure cases. I've not done that here, for the constant pressure case is the one most commonly used in water influx calculations. However, if the reader needs to use this idea for constant rate calculations, it would not be difficult to accomplish.

These exercises also make it clear why the curves which become horizontal in Fig. 2 look so much like each other. We will find that other boundary conditions can also be put into useful generalized equation forms which provide insight on the nature of the resulting solutions and graphs.

Closed Outer Boundary

The lines that rise above the semi-log straight line in Fig. 2 are for the closed outer boundary. They curve on this graph, but if they are plotted on arithmetic paper, we find that they are straight lines. The reason for this is simple. At late times, with a closed outer boundary, the entire system approaches pseudo-steady state flow. We'll address this concept next.

In earlier notes (Brigham, 1988), I wrote about pseudo-steady state flow, and pointed out that, if we are producing at a constant rate, after a period of time the entire system is depleting at an equal rate. The resulting equations look a good deal like the steady state equations, and this is the reason it is called "pseudo-steady state."

One of the equations in these earlier notes related the difference between the average pressure and the inner boundary pressure to the reservoir parameters, as follows,

$$\frac{2\pi k h}{q_w \mu}(\overline{p} - p_w) = \frac{r_e^4 \ln(r_e / r_w)}{\left(r_e^2 - r_w^2\right)^2} - \left[\frac{1}{r_e^2 - r_w^2}\right]\left[\frac{3r_e^2}{4} - \frac{r_w^2}{4}\right] \tag{20}$$

To compare this equation to the aquifer flow equation used by Chatas, we need $p_i - p_w$ rather $\overline{p} - p_w$. To accomplish this we need to derive an equation for $p_i - \overline{p}$. But this can be done easily with a simple material balance, as follows,

$$p_i - \overline{p} = \frac{q_w t}{\pi c_t \phi h \left(r_e^2 - r_w^2\right)} \tag{21a}$$

which, when we insert the definition for t_D , simplifies to,

$$\frac{2\pi k h (p_i - \overline{p})}{q \mu} = \frac{2t_D}{(r_e / r_w)^2 - 1} \tag{21b}$$

Now we can combine Eqs. 20 and 21b to get a general equation relating Chatas' pressure drop with pseudo-steady state conditions,

$$\frac{2\pi k h (p_i - p_w)}{q \mu} = \frac{(r_e / r_w)^4 \ln (r_e / r_w)}{[(r_e / r_w)^2 - 1]^2} - \frac{3(r_e / r_w)^2 - 1}{4[(r_e / r_w)^2 - 1]} + \frac{2t_D}{(r_e / r_w)^2 - 1} \tag{22}$$

What we would like to do is to compare Chatas' pressures in Table 4, for the closed outer boundary, with the results one would calculate using various assumptions about the flow equations. At early times, one would expect that the outer boundary would not affect the pressure behavior, while at later times we would expect that the pseudo-steady state assumption would be valid. To test this idea, I've listed pressure data from Chatas' Table 1, $(p_D)_\infty$, and from his Table 4, $(p_D)_c$, and from calculations using Eq. 22, $(p_D)_{pss}$, at values of $r_D = 2$, 5 and 10 in the first table on page 29.

There are also data available for closed systems with larger radii, as shown on the attached table (page 28) by Katz *et al.* (1968). In that table, the terms labeled, R, we have called r_D . The headings, $r = 1$ are at r_w , and the term, θ, we call p_D . I list the $r_D = 100$ $(R = 100)$ data in the same way in a table at the bottom of page 29. To do this at longer times, it was also necessary to calculate $(p_D)_\infty$ using Eq. 13, for these data are not listed in Chatas' Table 1.

Table of Dimensionless Pressure Drop Distribution, $P_D(r_D, t_D)$, Finite Radial Aquifer with Closed Exterior Boundary, Constant Terminal Rate. From Katz, et al. (1968).

R = 6.0

θ	r = 1	r = 2	r = 5	r = 8
1.0	.8021	.2204	.0008	.0000
2.5	1.100	.4632	.0229	.0007
5	1.362	.7011	.0967	.0168
10	1.654	.9783	.2590	.1171
25	2.180	1.500	.7371	.5698
50	2.975	2.295	1.531	1.363
100	4.653	3.882	3.118	2.950

R = 10.0

θ	r = 1	r = 2	r = 4	r = 7	r = 10
1	.8021	.2204	.0073	.0000	.0000
2.5	1.100	.4632	.0703	.0015	.0000
5	1.362	.7010	.1942	.0195	.0021
10	1.651	.9752	.3894	.0928	.0343
25	2.085	1.401	.7660	.3781	.2797
50	2.604	1.919	1.280	.8813	.7787
100	3.614	2.929	2.290	1.891	1.789
250	6.645	5.960	5.321	4.922	4.819
500	11.695	11.010	10.371	9.972	9.869

R = 12.0

θ	r = 1	r = 3	r = 6	r = 12
5	1.362	.3737	..0448	..0002
10	1.651	.6133	.1501	.0087
25	2.066	.9948	.4182	.1356
50	2.462	1.384	.7826	.4648
100	3.165	2.087	1.483	1.163
250	5.263	4.184	3.581	3.261
500	8.760	7.681	7.077	6.757
1000	15.752	14.674	14.070	13.750

R = 14.0

θ	r = 1	r = 3	r = 7	r = 14
5	1.362	.3736	.0195	.0000
10	1.651	.6133	.0897	.0019
25	2.062	.9906	.3048	.0633
50	2.411	1.329	.5889	.2805
100	2.939	1.855	1.106	.7868
250	4.478	3.394	2.645	2.325
500	7.042	5.958	5.209	4.889
1000	12.170	11.337	10.337	10.017

R = 16

θ	r = 1	r = 4	r = 8	r = 16
5	1.362	.1942	.0079	.0000
10	1.651	.3891	.0521	.0004
25	2.062	.7310	.2235	.0281
50	2.394	1.039	.4585	.1681
100	2.825	1.463	.8620	.5442
250	4.003	2.641	2.039	1.720
500	5.964	4.602	4.000	3.681
1000	0.886	8.523	7.921	7.602

R = 18.0

θ	r = 1	r = 4	r = 9	r = 18
5	1.362	.1942	.0029	.0000
10	1.651	.3891	.0292	.0001
25	2.062	.7310	.1633	.0118
50	2.390	1.033	.3638	.0991
100	2.768	1.402	.6935	.3798
250	3.705	2.337	1.625	1.305
500	5.253	3.885	3.173	2.853
1000	8.349	6.981	6.289	5.949

R = 20

θ	r = 1	r = 4	r = 10	r = 20
10	1.651	.3890	.0158	.0000
25	2.062	.7309	.1182	.0047
50	2.389	1.031	.2911	.0572
100	2.742	1.373	.5710	.2654
250	3.513	2.142	1.328	1.009
500	4.766	3.395	2.581	2.263
1000	7.272	5.901	5.088	4.769
2500	14.791	13.420	12.607	12.288

R = 50

θ	r = 1	r = 6	r = 20	r = 50
25	2.062	.4063	..0022	.0000
50	2.388	.6691	.0260	.0000
100	2.723	.9687	.1124	.0003
500	3.522	1.738	.6263	.1692
1000	3.963	2.178	1.047	.5526
2500	5.166	3.380	2.249	1.752
5000	7.167	5.381	4.249	3.753

R = 100

θ	r = 1	r = 3	r = 6	r = 10	r = 20	r = 50	r = 100
100	2.723	1.632	.9689	.5294	.1126	.0002	.0000
250	3.173	2.077	1.396	.9157	.3539	.0128	.0000
500	3.516	2.419	1.732	1.237	.6133	.0738	.0012
1000	3.861	2.763	2.073	1.570	.9128	.2173	.0271
2500	4.335	3.237	2.545	2.038	1.362	.5628	.2590
5000	4.856	3.757	3.065	2.558	1.880	1:069	.7507
10000	5.856	4.758	4.066	3.558	2.880	2.069	1.751
25000	8.857	7.758	7.066	6.559	5.880	5.069	4.751

Comparisons of Calculated p_D's at Various Values of r_D and t_D for Closed Systems

$r_D = 2$

t_D	$(p_D)_\infty$	$(p_D)_c$	$(p_D)_{pss}$
0.20	0.4241	0.427	0.4489
0.30	0.5024	0.507	0.5156
0.40	0.5645	0.579	0.5823
0.50	0.6167	0.648	0.6489

$r_D = 5$

t_D	$(p_D)_\infty$	$(p_D)_c$	$(p_D)_{pss}$
3.0	1.1665	1.167	1.2255
4.0	1.2750	1.281	1.3088
5.0	1.3625	1.378	1.3922
6.0	1.4362	1.469	1.4755
7.0	1.4997	1.556	1.5588
10.0	1.6509	1.808	1.8088

$r_D = 10$

t_D	$(p_D)_\infty$	$(p_D)_c$	$(p_D)_{pss}$
15	1.8294	1.832	1.8973
20	1.9601	1.968	1.9983
30	2.1470	2.194	2.2003
40	2.2824	2.401	2.4024
50	2.3884	2.604	2.6044

Comparisons of p_D's at $r_D = 100$,
Closed Outer Boundary (Katz *et al.*, 1968)

t_D	$(p_D)_\infty$	$(p_D)_c$	$(p_D)_{pss}$
100	2.7233	2.723	3.8760
250	3.1726	3.173	3.9060
500	3.5164	3.516	3.9560
1,000	3.8584	3.861	4.0560
2,500	4.3166	4.335	4.3561
5,000	4.6631	4.856	4.8561
10,000	5.0097	5.856	5.8562
25,000	5.4679	8.857	8.8569

If we look at the results from all four of these tables in detail, certain trends and comparisons become obvious. First it is clear that the infinite system tables show the smallest pressure drops, as we should expect. But of great importance, is that, at early times, the actual pressure behavior of the finite systems closely follows that of the infinite system.

The pseudo-steady state equations predict the greatest pressure drops. Again this is as we would expect. But again, we reach the important conclusion that the later time behavior of all the real systems closely follow the pseudo-steady state equations, as we had anticipated.

A most important conclusion can be reached by evaluating the tabulated data in detail. We see that one or the other of these simpler equations will predict the values in the tables with an error of only about 1% over the entire range of data! Real pressure drop data are never this accurate. So, in brief, the tables for finite systems are not needed at all! We can use the infinite system equations at early times and then switch to the pseudo-steady state equation to calculate later pressure drop history.

To carry the idea out in detail, I have performed these same calculations for a host of r_D's ranging from 1.5 to 100, and have listed the values for the t_D's at the crossover times. These results are listed in the table on page 32.

Other columns are also listed in this table, and the reasons for them will be discussed. The square root of t_D is listed because I wished to graph these data on log-log paper, and this was a convenient way to reduce the range of data to fit on 3×3 cycle log-log paper. These data are graphed as circles in Fig. 5, page 31. Notice that the data curve at smaller values of t_D and r_D, but they are nearly a straight line at large values of these parameters.

It seemed likely that it would be possible to straighten this line by making adjustments for r_D, in either the t_D term or in the r_D coordinator itself. Several ideas were tried, and the most successful one was to simply graph $r_D - 1$ rather than r_D. The resulting data are shown as diamonds on Fig. 5. They clearly fall on a straight line,

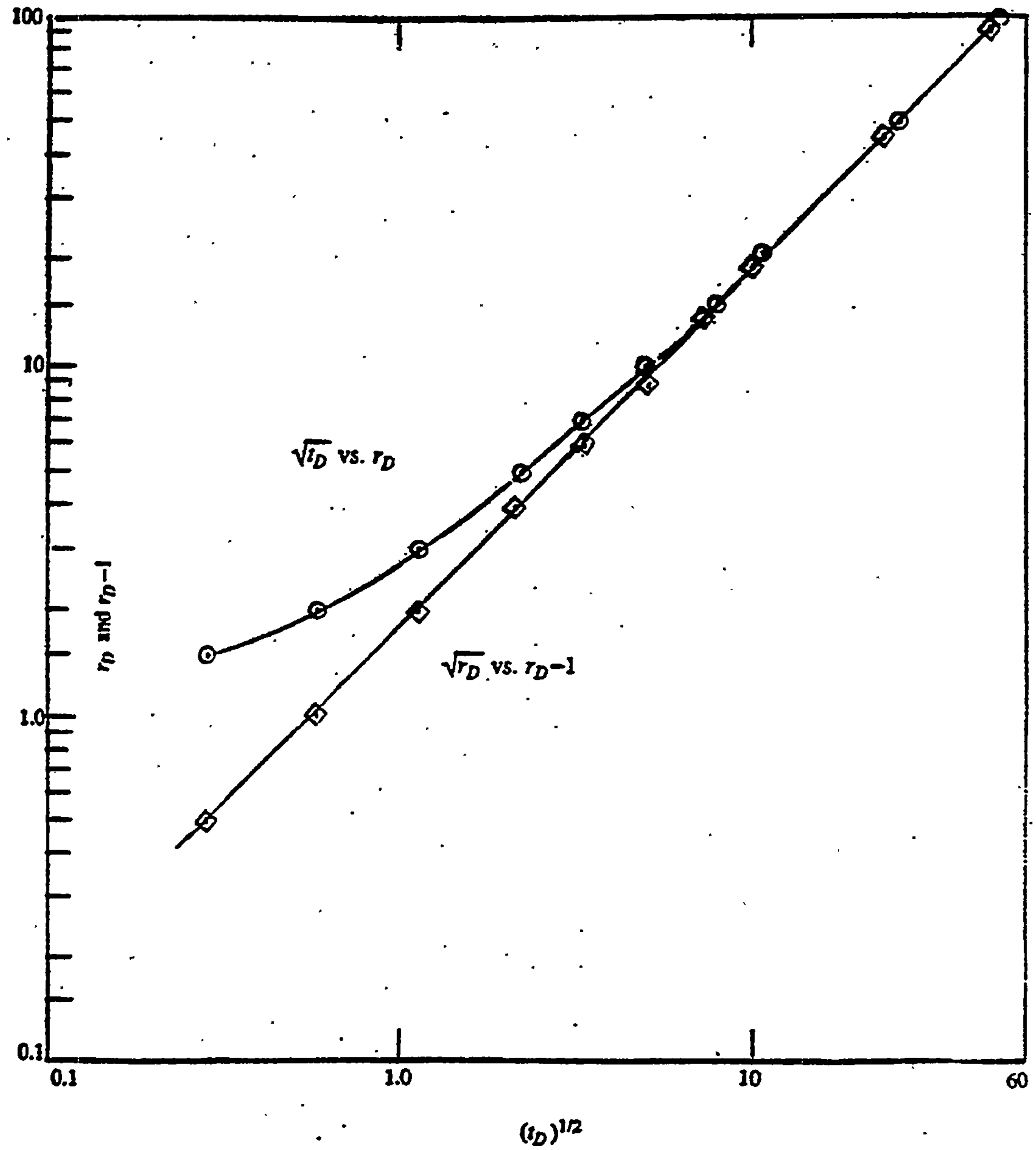

Figure 5. Time for crossover from infinite acting to pseudo-steady state.
Constant rate-closed outer boundary

whose slope is almost equal to 1.00. This straight line was fit to an equation, as follows,

$$t_D = 0.328\,(r_D - 1)^{1.945} \tag{23}$$

Note that the exponent on $r_D - 1$ is 1.945 rather than 2.000, which it would have been if the slope had been 1.00 in Fig. 5. Equation 23 was used to calculate t_D's and these are listed in the last column of the table below. These values can be compared with the data in the second column. Clearly, the fit is excellent. A fit of $\pm 10\%$ on t_D would have been quite satisfactory, and this fit is considerably better than that.

Times for Switching From Infinite Acting
Behavior to Pseudosteady State Behavior

r_D	Crossover t_D	$\sqrt{t_D}$	$r_D - 1$	Calculated t_D
1.5	0.08	0.283	0.5	0.0852
2.0	0.35	0.592	1.0	0.328
3.0	1.3	1.14	2.0	1.26
5.0	4.5	2.12	4.0	4.86
7.0	11	3.32	6.0	10.7
10	25	5.00	9	23.5
14	50	7.07	13	48.1
20	100	10.0	19	101
50	675	26	49	636
100	2500	50	99	2497

In summary, to make calculations for a closed system at constant rate; at early times the equation for an infinite system can be used, and at late times, Eq. 22 can be used. Equation 23 defines the time, t_D , to switch from early to late time calculations.

One last useful idea for this system is the concept of a drainage radius, r_d. If we were to flow at a constant rate in an infinite system, we find that the pressure/distance curve looks much like Fig. 6. A graph of the Katz, *et al.* data, for $r_D = 100$, at $t_D = 100$ and also at $t_D = 250$, would show this sort of behavior. The value of p_D varies linearly with the logarithm of r_D for some distance, and then curves gradually toward $p_D = 0$ at larger values of r_D. At later times, t_{D2}, the straight line extends further into the system, but the gradual curve toward $p_D = 0$ at larger r_D, is similar.

The important point is that the slopes of the straight line portions of these curves, at small r_D's, are the same; and these slopes can be extended as straight lines toward $p_D = 0$, as indicated by the dashed lines in Fig. 6. These straight line intercepts have commonly been called the drainage ratios, r_d. This is somewhat unfortunate nomenclature, for it gives the erronious impression that the aquifer is only being drained out to that distance; while we know that drainage actually extends out to infinity, or to the outer boundary of the aquifer.

If the aquifer radius is quite large, we can use this idea of drainage radius in a useful way to calculate pressure histories. The slopes of the straight lines in Fig. 6 are proportional to q_w, and one can write an equation for them using Darcy's Law.

$$q_w = \frac{2\pi k h (p_i - p_w)}{\mu \ln (r_d / r_w)} \tag{24a}$$

or,

$$p_D = \ln (r_d / r_w) \tag{24b}$$

and, invoking Eq. 13, the log approximation, which is valid for the infinite system after a period of time, we can set the two equations equal, as follows,

$$\ln (r_d / r_w) = p_D = 1/2 (\ln t_D + 0.80907) \tag{25a}$$

which simplifies to,

$$(r_d / r_w) = (2.2458\, t_D)^{1/2} \tag{25b}$$

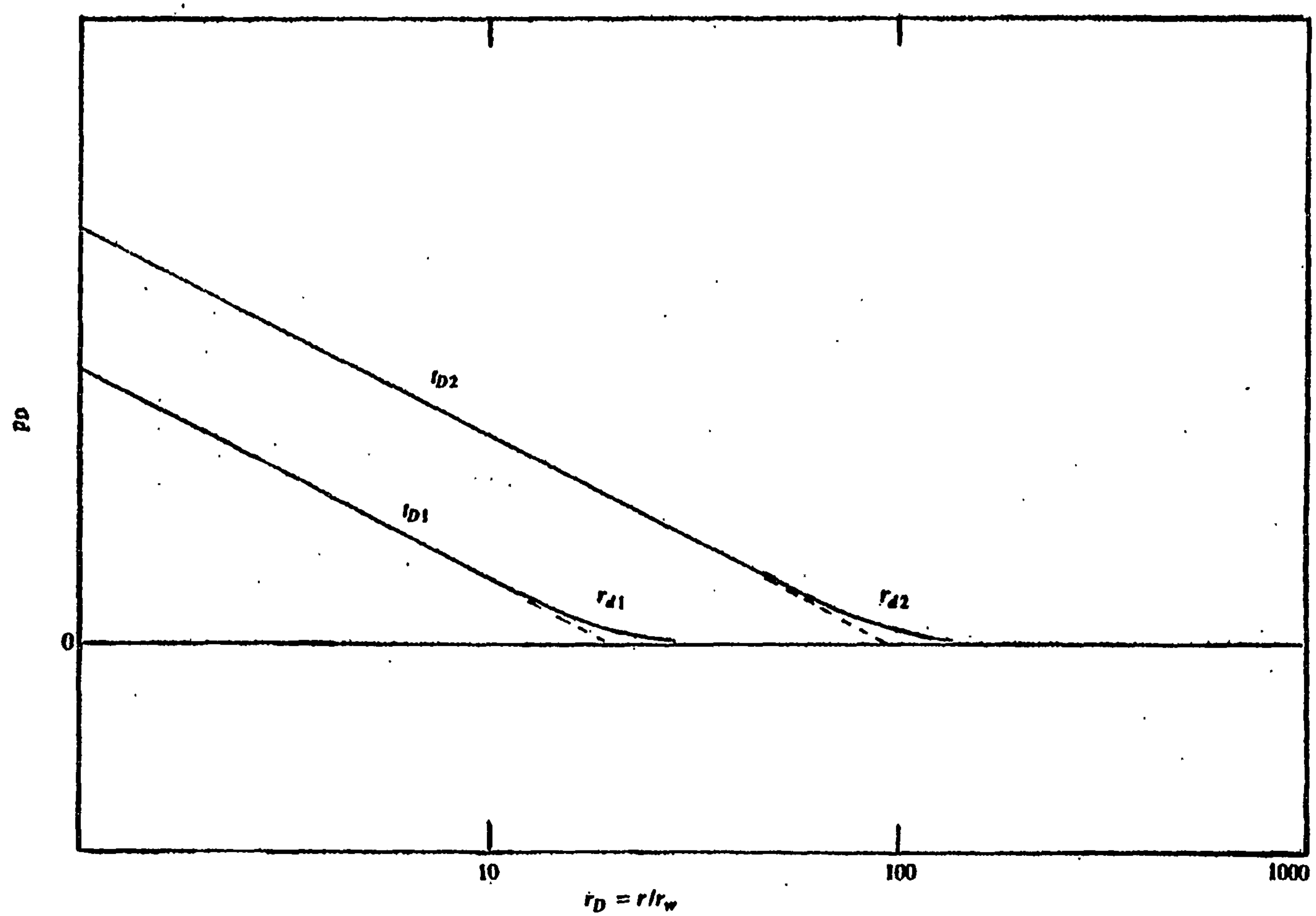

Figure 6. Example pressure profiles at constant rate.

In a finite aquifer, at late times, we already know that the system reaches pseudo-steady state, as defined by Eq. 20. If the aquifer is large, the ratio, $(r_e / r_w)^2$, is far greater than 1.0, and Eq. 20 then simplifies to,

$$\frac{2\pi kh(\overline{p}-p_w)}{q_w\mu} = \ln(0.472\, r_e / r_w) \tag{26a}$$

$$= \ln(r_d / r_w)$$

or

$$r_d = 0.472\, r_e \tag{26b}$$

So Eq. 25 defines r_d for a large infinite acting system, while Eq. 26b defines r_d for a large finite system. We would like to combine these equations and relate them to the data in the Katz *et al.* table. In that table, the pressure drop was expressed in terms of $p_i - p_w$ rather than $\overline{p} - p_w$ as it is in Eq. 26. To change the pressure difference used, we can invoke Eq. 21b, as we did before,

$$\frac{2\pi kh}{q\mu}(p_i - \overline{p}) = \frac{2t_D}{(r_e / r_w)^2 - 1} \tag{21b}$$

which for large values of $(r_e / r_w)^2$, simplifies to,

$$\frac{2\pi kh}{q\mu}(p_i - \overline{p}) = 2t_D (r_w / r_e)^2 \tag{21c}$$

Adding Eqs. 21c and 24b, and rearranging, we get,

$$\ln(r_d / r_w) = p_D(1, t_D) - 2t_D (r_w / r_e)^2 \tag{27}$$

Now we are in a position to look at the behavior of these closed systems, using the radius of drainage concept, to see if they can be related to each other in a general way. Clearly, at early times, Eq. 25b will be valid. In the table, at the top of page 37, I evaluate this equation at various times, in terms of r_d / r_e rather than r_d / r_w. These data are graphed as diamonds on Fig. 7, on page 36.

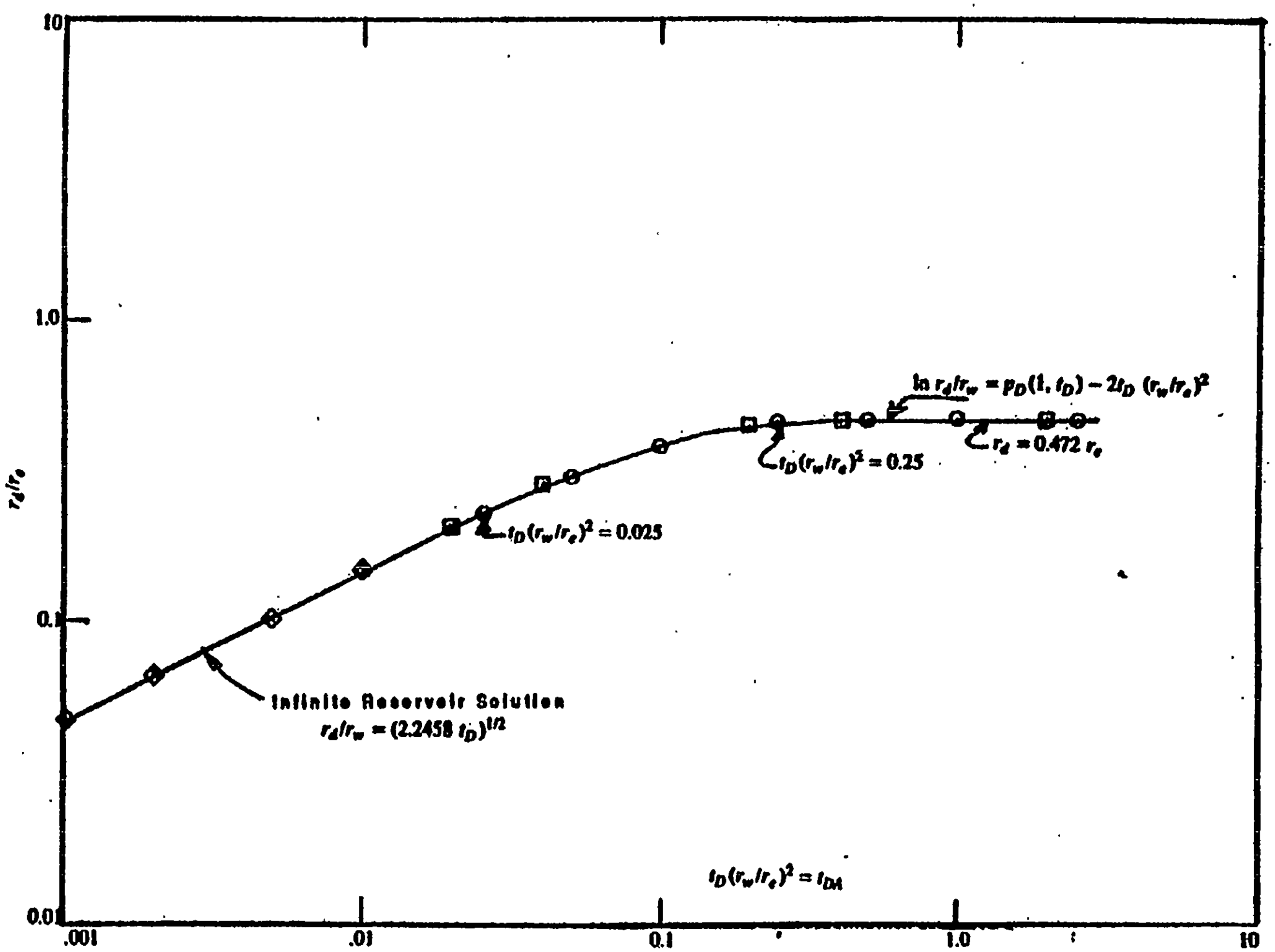

Figure 7. Generalized radius of drainage curve.

Infinite Acting Radius of Drainage, r_d

$t_D (r_w / r_e)^2$	$\sqrt{2.2458 t_D (r_w / r_e)^2} = r_d / r_e$
0.001	0.0474
0.002	0.0670
0.005	0.106
0.010	0.150
0.020	0.212

For comparison, we'll also look at the results in Katz's table at $(r_e / r_w) = 50$ and 100, calculate their drainage radii as functions of time, and graph the results using (r_d / r_e). The results from Katz's table (from Eq. 27) are shown in the table below.

Radii of Drainage for Finite Closed Systems

$(r_e / r_w) = 50$				$(r_e / r_w) = 100$			
t_D	$t_D (r_w / r_e)^2$	$p_D(1, t_D)$	r_d / r_e	t_D	$t_D (r_w / r_e)^2$	$p_D(1, t_D)$	r_d / r_e
25	0.01	2.062	0.154	100	0.010	2.723	0.149
50	0.02	2.388	0.209	250	0.025	3.173	0.227
100	0.04	2.723	0.231	500	0.050	3.516	0.304
500	0.20	3.522	0.454	1,000	0.100	3.861	0.389
1,000	0.40	3.963	0.473	2,500	0.250	4.335	0.463
2,500	1.00	5.166	0.474	5,000	0.500	4.856	0.473
5,000	2.00	7.167	0.475	10,000	1.000	5.856	0.473
				15,000	2.500	8.857	0.473

The data for $(r_e / r_w) = 50$ are graphed as squares on Fig. 7, and the data for $(r_e / r_w) = 100$ are graphed as circles. Notice in this figure that all the data fit closely with each other. The early data for the infinite system (the diamonds) join smoothly with the systems of finite radius. Also, the data for $(r_e / r_w) = 50$ and $(r_e / r_w) = 100$ fit well with each other at later times. As a good approximation at $t_D(r_w / r_e)^2 \leq 0.025$, all the systems are infinite acting; and at $t_D(r_w / r_e)^2 \geq 0.25$, the systems act as the pseudo-steady state equation predicts.

All this is interesting and informative, but, to be honest, it is not very useful for aquifer problems. It is seldom of importance to consider aquifers whose r_e / r_w are greater than 50. As you might expect, it is of use for reservoir problems where r_e / r_w are nearly always greater than 50. Since these ideas have not been discussed in my earlier notes on the diffusivity equation, I decided to include them here.

I should add that a quite nice practical use of those ideas was made several decades ago when Al Hussainy *et al.* (1966) developed their concept of the real gas potential to predict flow and depletion behavior of gas reservoirs. In developing their concepts, they used this same radius of drainage idea to simplify the equations of transient flow of gases.

Constant Pressure Inner Boundary

For the constant rate cases, Chatas looked at three outer boundaries: infinite, closed and constant pressure. We might expect that, for the constant pressure cases, he would have looked at the same outer boundaries. In Chatas' Table 2, he lists the infinite system, and in Table 3 he lists closed outer boundaries. He did not look at the constant pressure case. Christine Ehlig-Economides (1979) did look at this condition; but the smallest outer radius she looked at was $r_D = 20$. So the results are not very useful for aquifer flow problems. It is not too important to consider this case, so we'll ignore it, and begin by looking at the infinite system in Chatas' Table 2.

Infinite Aquifer

Note the headings in Chatas' Table 2 for the infinite aquifer. Dimensionless time is labeled, t, while we commonly use t_D in present day nomenclature. The fluid influx term is labeled $q(t)$. This is cumulative influx, and the present nomenclature we use for this is $Q_D(t_D)$. Dimensionless influx rate, the time derivative of the cumulative influx, is not listed in this table, but we will discuss this later, and its symbol is $q_D(t_D)$ in present day nomenclature. Note that the values of $Q_D(t_D)$ grow constantly with time and become quite large, as we should expect, upon reflection.

It should be of interest to look at the rates of influx as a function of time, for we know from well testing theory, that after a period of time, we would expect the log approximation, Eq. 13, to be valid. To test this idea out, I have listed many values of p_D for the infinite system from Chatas' Table 1, values of $1/q_D$ from Ehlig Economides, from the attached table on the next page, and compared them with the log approximation (Eq. 13) in Fig. 8 on page 41. The data for this figure are tabulated on page 42.

A look at Fig. 8 shows that, for the constant rate case, p_D approaches the log approximation solution quite closely at times, (t_D) , ranging from about 20 to about 100, depending on the accuracy we choose to invoke. The constant pressure data $(1/q_D)$ also approach the log approximation, but at a much slower rate. Even at $t_D = 1{,}000$, the error is still over 3%. So, in brief, this concept is not at all useful as a way of simplifying aquifer influx calculations. The only insight this exercise provided us was the knowledge that the results behave in a logical manner in a way we would expect them to. It turns out, however, that some of the concepts in these notes and graphs can be used to work out approximate equations for the infinite aquifer with a constant pressure inner boundary. These ideas will be discussed next.

For the constant rate inner boundary, we noted in the narrative following Eq. 12 that the very early time data closely followed the $(t_D)^{1/2}$ equation. This is also true for the constant pressure case. It seemed likely that this idea could be extended empirically by adding a term using t_D to some other power. It turned out this idea worked well up to a time, $t_D = 10$. The following equation was found to fit the tabulated data,

$$Q_D(t_D) = 1.058\, t_D^{1/2} + 0.510\, t_D^{0.90} \tag{28}$$

Flow Behavior for Constant Pressure Inner Boundary and Infinite Outer Boundary, Skin = 0; Elig-Economides (1979)

t_D	Q_D	q_D	t_D	Q_D	q_D
1.00D-01	4.0433D-01	2.2489D 00	1.00D 04	2.1986D 03	1.9594D-01
2.00D-01	5.9803D-01	1.7153D 00	2.00D 04	4.0887D 03	1.8471D-01
3.00D-01	7.5642D-01	1.4764D 00	3.00D 04	5.8910D 03	1.7722D-01
4.00D-01	8.9626D-01	1.3326D 00	4.00D 04	7.6405D 03	1.7209D-01
5.00D-01	1.0244D 00	1.2336D 00	5.00D 04	9.3527D 03	1.6966D-01
6.00D-01	1.1439D 00	1.1601D 00	6.00D 04	1.1036D 04	1.6712D-01
7.00D-01	1.2569D 00	1.1025D 00	7.00D 04	1.2697D 04	1.6502D-01
8.00D-01	1.3640D 00	1.0553D 00	8.00D 04	1.4330D 04	1.6325D-01
9.00D-01	1.4684D 00	1.0167D 00	9.00D 04	1.5963D 04	1.6172D-01
1.00D 00	1.5684D 00	9.8384D-01	1.00D 05	1.7573D 04	1.6037D-01
2.00D 00	2.4458D 00	8.0063D-01	2.00D 05	3.3140D 04	1.5203D-01
3.00D 00	3.1795D 00	7.1624D-01	3.00D 05	4.8102D 04	1.4753D-01
4.00D 00	3.8585D 00	6.6443D-01	4.00D 05	6.2697D 04	1.4450D-01
5.00D 00	4.5339D 00	6.2821D-01	5.00D 05	7.7030D 04	1.4223D-01
6.00D 00	5.1480D 00	6.0071D-01	6.00D 05	9.1161D 04	1.4013D-01
7.00D 00	5.7377D 00	5.7930D-01	7.00D 05	1.0513D 05	1.3894D-01
8.00D 00	6.3077D 00	5.6160D-01	8.00D 05	1.1896D 05	1.3767D-01
9.00D 00	6.8619D 00	5.4671D-01	9.00D 05	1.3267D 05	1.3650D-01
1.00D 01	7.4021D 00	5.3394D-01	1.00D 06	1.4628D 05	1.3561D-01
2.00D 01	1.2221D 01	4.6116D-01	2.00D 06	2.7850D 05	1.2957D-01
3.00D 01	1.6742D 01	4.2612D-01	3.00D 06	4.0637D 05	1.2678D-01
4.00D 01	2.0506D 01	4.0399D-01	4.00D 06	5.3144D 05	1.2405D-01
5.00D 01	2.4043D 01	3.8820D-01	5.00D 06	6.5462D 05	1.2237D-01
6.00D 01	2.8662D 01	3.7697D-01	6.00D 06	7.7631D 05	1.2103D-01
7.00D 01	3.2372D 01	3.6638D-01	7.00D 06	8.9678D 05	1.1992D-01
8.00D 01	3.5796D 01	3.5833D-01	8.00D 06	1.0162D 06	1.1897D-01
9.00D 01	3.9544D 01	3.5149D-01	9.00D 06	1.1348D 06	1.1815D-01
1.00D 02	4.3029D 01	3.4557D-01	1.00D 07	1.2526D 06	1.1742D-01
2.00D 02	7.5592D 01	3.1081D-01	2.00D 07	2.4012D 06	1.1286D-01
3.00D 02	1.0573D 02	2.9335D-01	3.00D 07	3.5164D 06	1.1035D-01
4.00D 02	1.3447D 02	2.8204D-01	4.00D 07	4.6110D 06	1.0863D-01
5.00D 02	1.6224D 02	2.7382D-01	5.00D 07	5.6908D 06	1.0734D-01
6.00D 02	1.8930D 02	2.6744D-01	6.00D 07	6.7590D 06	1.0621D-01
7.00D 02	2.1578D 02	2.6226D-01	7.00D 07	7.8179D 06	1.0540D-01
8.00D 02	2.4178D 02	2.5792D-01	8.00D 07	8.8686D 06	1.0471D-01
9.00D 02	2.6734D 02	2.5421D-01	9.00D 07	9.9126D 06	1.0458D-01
1.00D 03	2.9264D 02	2.5097D-01	1.00D 08	1.0951D 07	1.0351D-01
2.00D 03	5.3354D 02	2.3151D-01	2.00D 08	2.1102D 07	9.9943D-02
3.00D 03	7.5842D 02	2.2142D-01	3.00D 08	3.0992D 07	9.7967D-02
4.00D 03	9.7451D 02	2.1477D-01	4.00D 08	4.0718D 07	9.6412D-02
5.00D 03	1.1085D 03	2.0986D-01	5.00D 08	5.0327D 07	9.5586D-02
6.00D 03	1.3967D 03	2.0602D-01	6.00D 08	5.9843D 07	9.4764D-02
7.00D 03	1.6011D 03	2.0787D-01	7.00D 08	6.9287D 07	9.4089D-02
8.00D 03	1.8026D 03	2.0022D-01	8.00D 08	7.8666D 07	9.3495D-02
9.00D 03	2.0017D 03	1.9794D-01	9.00D 08	8.7991D 07	9.2903D-02

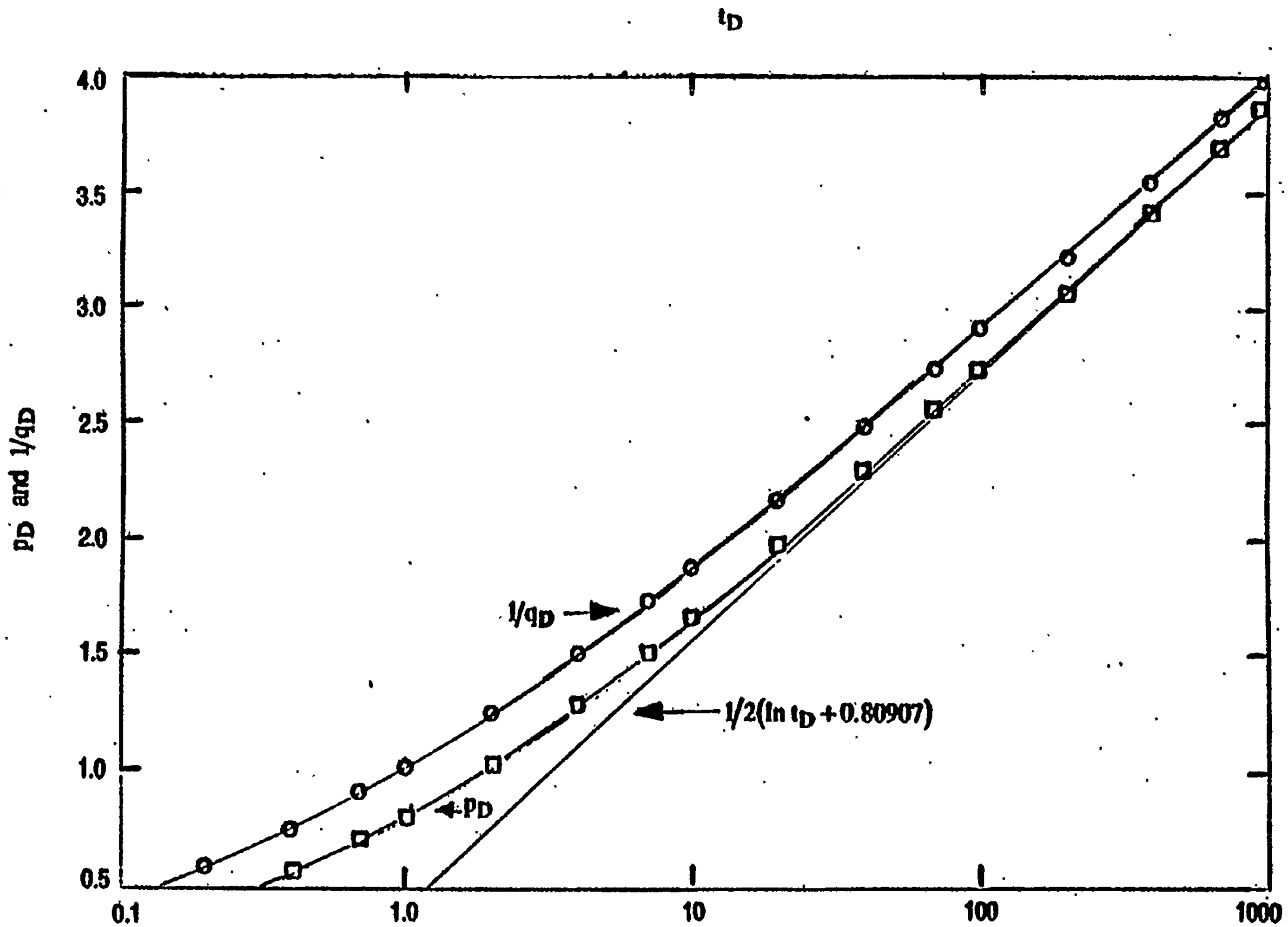

Figure 8. Comparisons of p_D and $1/q_D$ with logarithmic approximation.

Comparison of p_D and $1/q_D$ (Infinite Systems)

Time	Constant Pressure Inner Boundary		Constant Rate Inner Boundary
t_D	q_D	$1/q_D$	p_D
0.10	2.2489	0.445	0.314
0.20	1.7153	0.583	0.424
0.40	1.3326	0.750	0.565
0.70	1.1025	0.907	0.702
1.0	0.9838	1.016	0.802
2.0	0.8006	1.249	1.020
4.0	0.6644	1.505	1.275
7.0	0.5793	1.726	1.500
10	0.5339	1.873	1.651
20	0.4612	2.168	1.960
40	0.4040	2.475	2.282
70	0.3664	2.729	2.550
100	0.3456	2.894	2.723
200	0.3108	3.217	3.064
400	0.2820	3.546	3.406
700	0.2623	3.813	3.684
1000	0.2510	3.986	3.858

A comparison of this equation with Chatas' Table 2 is shown on the following page. Actually, for this comparison, we did not use Chatas' tabulated results, for we found that there are some minor errors in his table. The more recent work by Ehlig-Economides (1979) was used to fit and evaluate Eq. 28, and also in the longer time matches that will be discussed soon. A copy of her thesis table is on page 40. It does not extend to as short a time as Chatas' table, so the first two time values in the following table are from his work, while the remainder are from Ehlig-Economides.

Early Water Influx Calculations

Q_D for $0.01 \le t_D \le 10.00$

$Q_D(t_D) = 1.058\, t_D^{1/2} + 0.510\, t_D^{0.90}$; Eq. 28

t_D	$Q_D(t_D)$ Eq. 28	$Q_D(t_D)$ Ehlig-Economides	% Error
0.01	0.1139	0.112	+1.7
0.05	0.2710	0.278	-2.5
0.10	0.3987	0.404	-1.3
0.20	0.4929	0.598	-0.9
0.50	1.0211	1.024	-0.3
1.00	1.5680	1.568	0.0
2.00	2.4479	2.446	+0.1
5.00	4.5367	4.534	+0.1
10.00	7.3968	7.402	-0.1

Notice that the fit is quite accurate over this range. The values at $t_D = 0.01$ and 0.05 show rather large errors of up to 2.5 %, but these are usually not too important in practical use. Further, there is likely some inherent error in Chatas' table for these low values of t_D for they do not quite behave logically, based on the trend one would expect. This could have easily arisen, for very many terms of the infinite series are needed to calculate the early time solutions. But, in any case, for practical application, Eq. 28 is quite adequate up to $t_D = 10.00$.

At late time, the curves in Fig. 8 give us some insight on how to develop an approximate equation using a semi-logarithmic approach. It seems likely that an equation of the form,

$$\frac{t_D}{Q_D(t_D)} = a + b \ln(t_D) \qquad (29)$$

might be a useful way to handle the long time behavior. It is! However, we would like to extend this equation to a shorter time range if possible. A useful way to accomplish this goal is to add an emperical constant to the t_D on the left-hand side of Eq. 29. The final resulting equation I found was,

$$Q_D(t_D) = \frac{t_D - 1.4}{0.0407 + 0.4887\ \ln(t_D)} \tag{30}$$

This equation fit Ehlig-Economides' tabulated data from $t_D = 10.0$ to $t_D = 100{,}000$, as shown in the table below.

Late Time Water Influx Calculations

$Q_D(t_D)$ for $10 \le t_D \le 100{,}000$

$Q_D(t_D) = (t_D - 1.4)/[0.0407 + 0.4887\ \ln t_D]$ = Eq. 30

t_D	$t_D - 1.4$	$\ln t_D$	$Q_D(t_D)$ Eq. 30	$Q_D(t_D)$ Ehlig-Economides	% Error
10	8.6	2.30259	7.376	7.402	-0.4
20	18.6	2.99573	12.361	12.321	+0.3
50	48.6	3.91202	24.891	24.845	+0.2
100	98.6	4.60517	43.034	43.029	+0.0
200	198.6	5.29832	75.513	75.595	-0.1
500	498.6	6.21467	162.00	162.24	-0.1
1×10^3	998.6	6.90776	292.29	292.64	-0.1
2×10^3	1,998.6	7.60090	532.21	532.54	-0.1
5×10^3	4,998.6	8.51719	1,189.27	1,188.8	+0.0
1×10^4	9,998.6	9.21034	2,201.5	2,198.6	+0.1
2×10^4	2×10^4	9.90349	4,097.6	4,088.7	+0.2
5×10^4	5×10^4	10.81978	9,383.6	9,352.7	+0.3
1×10^5	1×10^5	11.51293	17,646	17,573	+0.4

Clearly, these two equations do a remarkably accurate job of predicting water influx for a radial infinite aquifer. The time limit of $t_D = 10^5$, is far larger than would normally be needed for water influx calculations.

The reader might be interested in the exact time range to use to switch from Eq. 28 to Eq. 30. I've evaluated these equations in the range near $t_D = 10$, and found that they were identical at $t_D = 11.4$. So this should theoretically be the crossover time. However, a time of $t_D = 10$ would be quite adequate for good accuracy.

Closed Outer Boundary

In thinking about a closed outer boundary, with a constant pressure inner boundary, we should realize that, after a period of time, water influx will stop. This will occur when the entire aquifer has been depleted to the pressure level set at the inner boundary.

We can calculate the values of maximum cumulative influx we can expect for a given system using simple material balance principles, as follows:

$$\Delta \overline{p} = \frac{Q(t)}{\pi\, c_t \phi h \left(r_e^2 - r_w^2\right)} \tag{31}$$

The variables in this equation can be put into dimensionless form. For pressure, the result is,

$$\overline{p}_D = \frac{\overline{p} - p_i}{p_w - p_i} = \frac{\Delta \overline{p}}{p_w - p_i} \tag{32a}$$

At the time when the average pressure equals the inner boundary pressure, p_w , Eq. 32a simplifies to,

$$\overline{p}_D(\infty) = \frac{\overline{p} - p_i}{p_w - p_i} = \frac{\Delta \overline{p}}{p_w - p_i} \equiv 1 \tag{32b}$$

The cumulative influx term, $Q(t)$, in dimensionless form, is,

$$Q_D(t_D) = \frac{Q(t)}{2\pi \phi c_t h r_w^2 (p_i - p_w)} \tag{33}$$

When Eqs. 32b and 33 are substituted into Eq. 31, the result is,

$$Q_D(\infty) = \frac{(r_e / r_w)^2 - 1}{2} = \frac{r_D^2 - 1}{2} \tag{34}$$

We can test the validity of this equation by looking at the long term results in Chatas' Table 3. At $r_D = 2.0$ the long time result is 1.500, just as Eq. 34 predicts; at $r_D = 10.0$, it is 49.36 in the table compared to 49.50 from Eq. 34. Clearly the time data were not as complete in this table as they should have been. Other radii show similar long time results.

The early time data in these tables also behave logically. We would expect that, at early time, the effect of the outer boundary would not be felt. So the finite systems should act the same way as an infinite system. At $r_D = 2.0$ and $t_D = 0.10$, the tabulated value for Q_D is 0.404 in Chatas' Table 3, exactly the same as it is in Table 2 for the infinite system. At $r_D = 10.0$ and $t_D = 10$, the value for Q_D in Table 3 is 12.32, again exactly the same as in Table 2. This is the reason that Chatas started his listings in Table 3 after a period of time, for he recognized that the early time data would be the same as in Table 2.

Ehlig-Economides, in her Ph.D. dissertation, looked at the behavior of reservoir flow for a constant inner boundary pressure. One important conclusion she reached was that all the finite systems exhibit exponential decline behavior once the outer boundary is felt. Of course this behavior should also be found in finite aquifers.

It is interesting that neither van Everdingen and Hurst (1949) nor Chatas recognized this fact. It's likely that the reason she noticed it, and they did not, is because she also calculated rate data in her work, while they only looked at cumulative influx data. It turns out, however, that if rate data show an exponential decline, so will cumulative influx data, if they are graphed properly. I'll discuss the ideas behind exponential decline to show how these equations are developed, and then show how these ideas can be used to tranform Chatas' tabulated results into simple equation forms.

For any system, we know that the flow rate is proportional to the pressure gradient. For any finite system, after a time, the flow rate at the inner boundary is also proportional to the difference between the average pressure and the inner boundary pressure, as follows.

$$q(t) = \frac{C_1\left[\overline{p}(t) - p_w\right]}{(p_i - p_w)} \equiv \frac{dQ(t)}{dt} \tag{35}$$

It was this concept that led to Eq. 20 of these notes. Also, we should realize from general material balance concepts, that we can define cumulative influx as follows,

$$Q(t) = \frac{C_2\left[p_i - \overline{p}(t)\right]}{(p_i - p_w)} \tag{36}$$

We can now combine Eqs. 35 and 36 to get,

$$Q(t) = C_2\left[1 - \frac{1}{C_1}\frac{dQ(t)}{dt}\right] \tag{37a}$$

which can be rearranged to,

$$\int_0^t dt = -\frac{C_2}{C_1}\int_0^{Q(t)} \frac{dQ}{Q - C_2} \tag{37b}$$

which, when integrated, becomes,

$$t = \frac{C_2}{C_1}\ln\left[\frac{C_2}{C_2 - Q(t)}\right] \tag{38a}$$

This is the form of the resulting exponential decline equation when it is expressed in terms of the cumulative production. The argument of the log term in Eq. 38a can be expressed as a rate function rather than a cumulative production, using Eq. 37a, as follows,

$$\frac{C_2 - Q(t)}{C_2} \equiv 1 - \frac{Q(t)}{C_2} = \frac{q(t)}{C_1} \tag{39}$$

As a result, Eq. 38a becomes,

$$t = \frac{C_2}{C_1}\ln\left[\frac{C_1}{q(t)}\right] \tag{38b}$$

which is the form of the exponential decline equation most commonly seen in various references. We, however, will concentrate on Eq. 38a, for our tabulated influx data are in terms of cumulative influxes.

Next we need to evaluate the constants, C_1 and C_2 in Eq. 38a. At time, $t=0$, $Q(t)=0$, and either from Eq. 37a or Eq. 39, we can define C_1 ,

$$q(t)=q(0)=C_1 \tag{40}$$

At the other end of the time spectrum, when $t=\infty$, the log term in Eq. 38a must be infinite, so we can conclude,

$$Q(t)=Q(\infty)=C_2 \tag{41}$$

As a result, Eq. 38a becomes,

$$t=\frac{Q(\infty)}{q(0)}\ln\left[\frac{Q(\infty)}{Q(\infty)-Q(t)}\right] \tag{38c}$$

Equation 38c is only valid from the time when exponential decline begins. However we can extrapolate the equation back to $t=0$, and it will change to the following approximate form, which is not quite correct, but very nearly so.

$$t=\frac{Q(\infty)-Q(0)}{q(0)}\ln\left[\frac{Q(\infty)-Q(0)}{Q(\infty)-Q(t)}\right] \tag{38d}$$

We also would prefer to write this equation in dimensionless terms, for the tabulated data are dimensionless. Since all the terms outside the logarithm combine to be dimensionless, and the ratio inside the log term is also dimensionless, the resulting equation can be written immediately,

$$t_D=\frac{Q_D(\infty)-Q_D(0)}{q_D(0)}\ln\left[\frac{Q_D(\infty)-Q_D(0)}{Q_D(\infty)-Q_D(t_D)}\right] \tag{38e}$$

It only remains to evaluate these terms from first principles and from the data in Chatas' tables.

The evaluation problem is a bit more difficult than it first appears to be. The reason can be seen by comparing the pressure fields that are developed for the constant rate depletion system with those seen for the constant pressure system. These are shown schematically in Figs. 9 and 10. First look at the constant rate case, Fig. 9. Note that the pressure fields will look exactly like each other, merely dropping with time. It was this concept that allowed us to derive the pseudo-steady state equation, Eq. 20.

For the constant pressure depletion, Fig. 10, the shapes of the curves are all similar, but their slopes decrease as the system depletes. This, of course, is reflected in the decreasing rates as they deplete. As far as I know, no simple analytic solutions have been derived for this type of depletion. I have been working on some ideas to define these equations analytically, but have not yet come up with any simple equation forms that correctly honor the boundary conditions and the necessary material balance principles in the way that the pseudo-steady state equation does for the constant rate case.

I have however, come up with an approximate way to express the behavior of Fig. 10. The idea is as follows. At any time, t_D, I assume that the pseudo-steady state equation is valid for the particular pressure range and rate that would be associated with that time. In essence, when doing this, I'm assuming that the pressure field in Fig. 10 declines everywhere at the same rate as it would in the pseudo-steady state formulation, as illustrated in Fig. 9. When first glancing at those figures, this appears to be a grossly erronious assumption, but it is not nearly as bad as it appears. The reason is that the radii on these figures are on logarithmic coordinates; and in reality, most of the volume being depleted is at the larger values of r_D, where the shapes don't change dramatically. Using this idea, the predicted depletion rate will be greater than is actually taking place, but not much greater.

All these ideas require a number of graphical procedures and calculations, plus some correlation work to correct for flow equation errors discussed above. The procedure I used was as follows. First I graphed $[Q_D(\infty) - Q_D(t_D)]$ from Chatas' Table 3 against t_D on semilog paper, as suggested by Eq. 38e. The straight line portions of these graphs were extrapolated to $t_D = 0$. These are the correct values of $[Q_D(\infty) - Q_D(0)]$ to use in Eq. 38e. After all of Chatas' tables had been evaluated using this procedure, an empirical equation was derived to account for these errors. It was only a function of r_e / r_w, as we would expect.

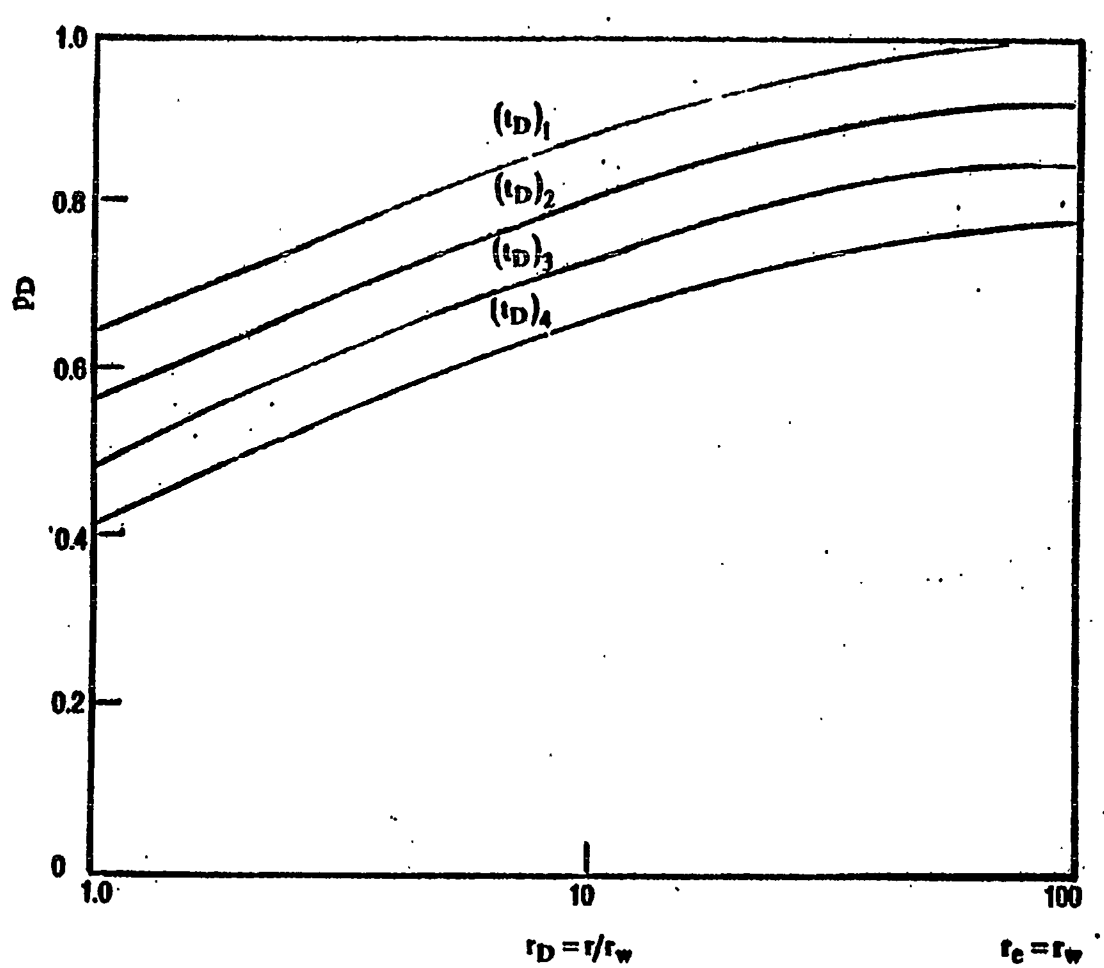

Figure 9. Pseudo-steady state (constant rate).

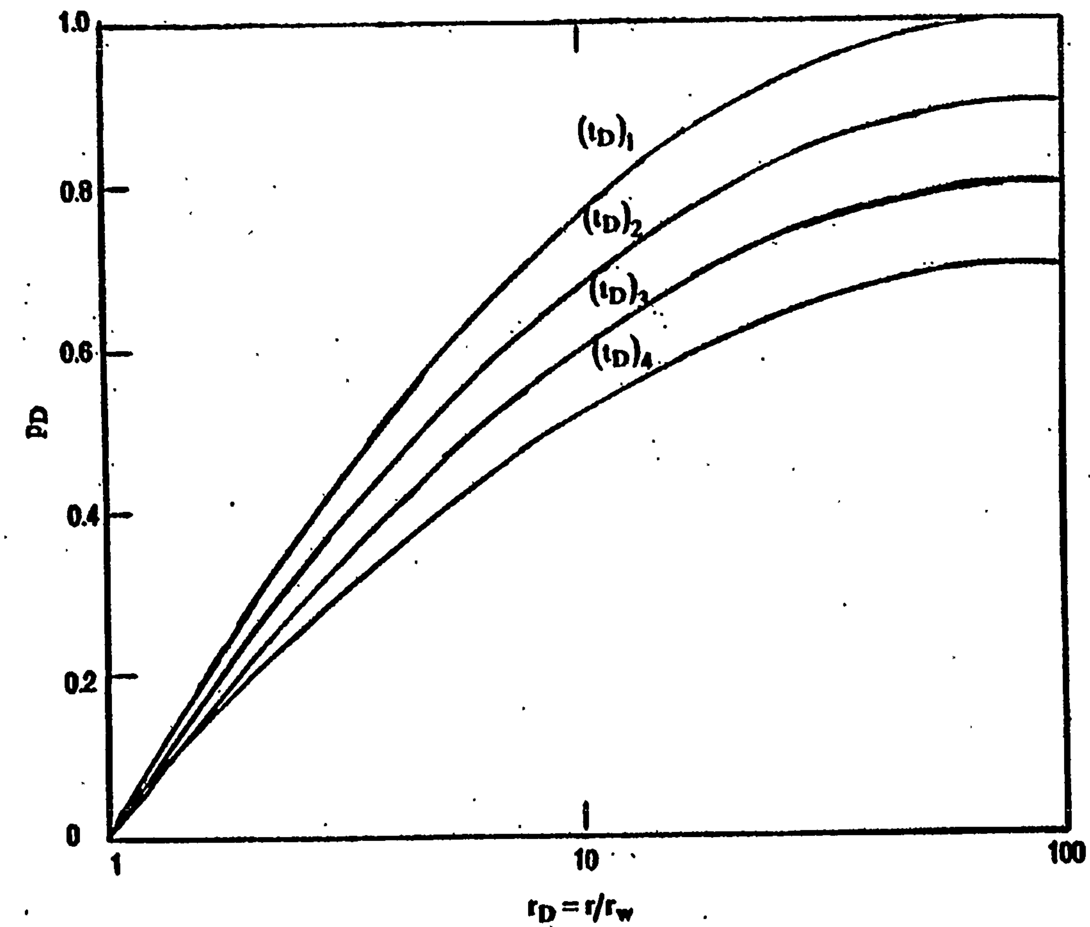

Figure 10. Constant pressure depletion.

Finally, I evaluated the slopes of the semilog straight lines, and compared them to the slopes one would calculate using the pseudo-steady state assumptions for the terms in front of the logarithm in Eq. 38e. Of course, there was a slight error, which I correlated against r_e / r_w .

Since all this procedure may be a bit hard to follow, I'll show a detailed set of example calculations, for $r_D = 4.0$, to show how this procedure was worked out. For $r_D = 4.0$, from Eq. 34, we can calculate $Q_D(\infty)$, as follows.

$$Q_D(\infty) = [(r_e / r_w)^2 - 1] / 2$$
$$= [(4.0)^2 - 1] / 2 = 7.500 \qquad (42)$$

The appropriate data from Chatas' Table 3 are listed in the table on the next page. From the graph of the data, Fig. 11, page 54, it is clear they fit a semilog straight line for times, $t_D \geq 2.00$. To evaluate the slope, I used values from the table at $t_D = 2.0$ and $t_D = 26.0$.

$$t_D = 2.00 \quad , \quad Q_D(t_D) = 2.442 \quad ; \quad Q_D(\infty) - Q_D(t_D) = 5.058$$
$$t_D = 26.0 \quad , \quad Q_D(t_D) = 7.377 \quad ; \quad Q_D(\infty) - Q_D(t_D) = 0.123$$

We evaluate the slope as follows,

$$\frac{\Delta t_D}{\ln[\Delta Q_D(2.00)] - \ln[\Delta Q_D(26.0)]} = \frac{26.0 - 2.00}{\ln(5.058) - \ln(0.123)}$$
$$= 6.4576 \qquad (43)$$

Using the slope from Eq. 43, and the value of $Q_D(\infty) - Q_D(2.00)$ equal to 5.058, the value of $Q_D(\infty) - Q_D(0)$ can be easily calculated,

$$\ln[Q_D(\infty) - Q_D(0)] = \frac{2.00}{6.4576} + \ln(5.058)$$
$$Q_D(\infty) - Q_D(0) = 6.8942 \qquad (44)$$

Exponential Decline Data for $r_e / r_w = 4.0$

$$Q_D(\infty) = [(r_e / r_w)^2 - 1] / 2 = 15/2 = 7.5$$

t_D	$Q_D(t_D)$	7.5-$Q_D(t_D)$
2.0	2.442	5.058
2.2	2.598	4.902
2.4	2.748	4.752
2.6	2.893	4.607
2.8	3.034	4.466
3.0	3.170	4.330
3.25	3.334	4.166
3.5	3.493	4.007
3.75	3.645	3.855
4.0	3.792	3.708
4.5	4.068	2.432
5.0	4.323	3.177
5.5	4.560	2.940
6.0	4.779	2.721
7.0	5.169	2.331
8.0	5.504	1.996
9.0	5.790	1.710
10.0	6.035	1.465
12.0	6.425	1.075
14.0	6.712	0.788
16.0	6.922	0.578
18.0	7.076	0.426
20.0	7.189	0.311
24.0	7.332	0.168
26.0	7.377	0.123

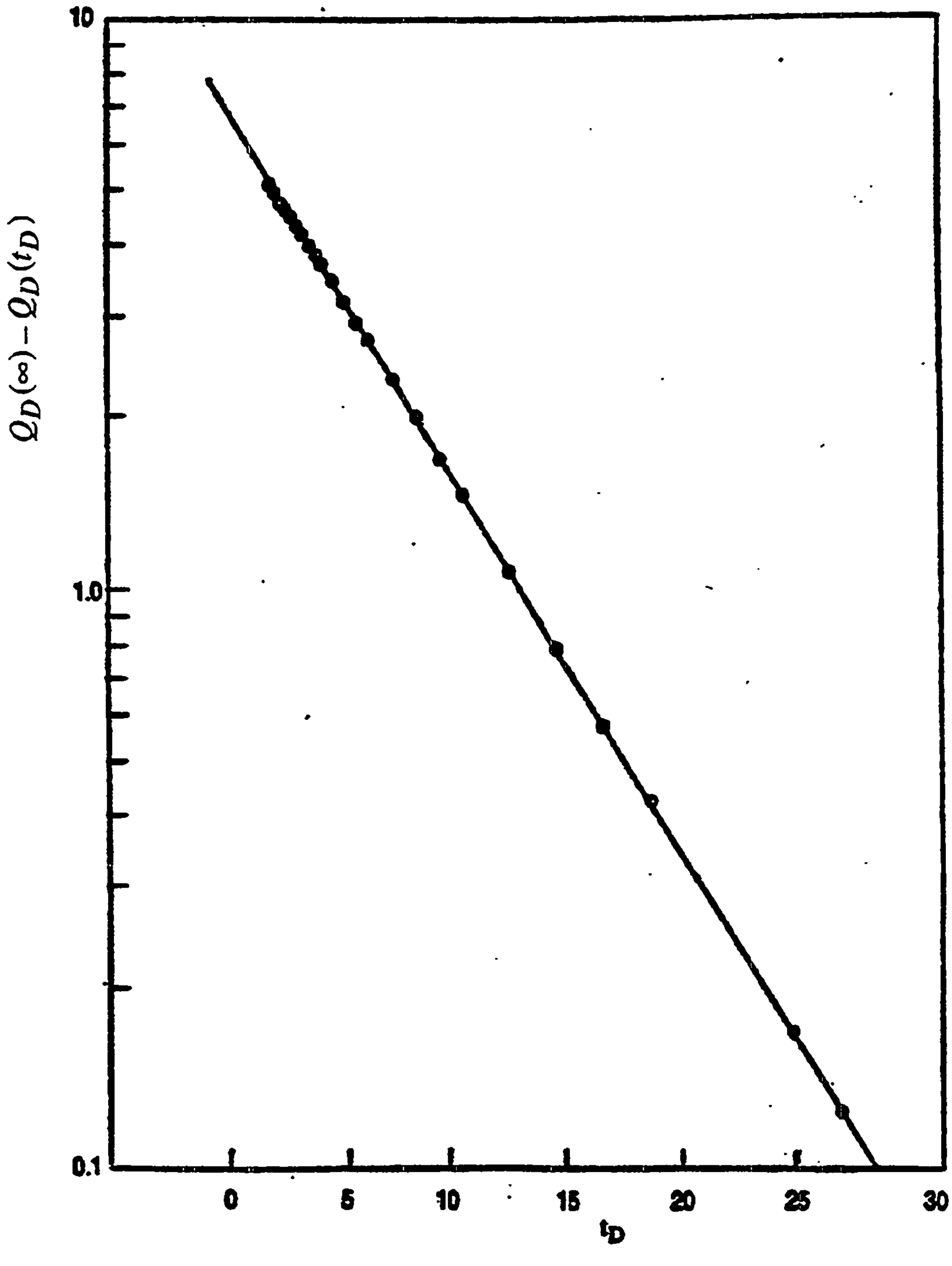

Figure 11. Exponential decline graph for constant pressure depletion, $r_D = 4.0$.

Thus the value of $Q_D(0)$ for this r_D ($r_D = 4.0$) is,

$$Q_D(0) = 7.500 - 6.8942 = 0.6058 \tag{45}$$

The values of $Q_D(0)$ for all the radii were correlated into an equation which will be discussed later.

Next I calculated the approximate value for $q_D(0)$ assuming the pseudo-steady state equation was valid. This equation is,

$$\frac{1}{q_D(0)} = \frac{r_D^2 \ln r_D}{r_D^2 - 1} - \frac{1}{2} = \frac{(4.0)^2 \ln(4)}{(4.0)^2 - 1} - \frac{1}{2}$$

$$= 0.9787 \tag{46}$$

Thus the approximate value for the slope is,

$$\frac{Q_D(\infty) - Q_D(0)}{q_D(0)} = 6.8942\,(0.9787) = 6.7474 \tag{47}$$

The actual slope is Eq. 43, while the approximate slope is Eq. 47. The error is thus,

$$\text{Slope Error} = \frac{6.7474}{6.4576} = 1.045 \tag{48}$$

The values of these errors were correlated into an equation for all radii. This correlation equation will be discussed later.

Note that there were two empirical equations developed to evaluate the parameters in the decline equations. The first one mentioned was for $Q_D(0)$, as discussed after Eq. 45. Values for $Q_D(0)$ were evaluated for all the r_D's in Chatas' Table 3. The results are shown in the table on the next page, along with some other columns of numbers, whose meaning will be discussed next.

Correlation for $Q_D(0)$

r_D	$r_D - 1$	From Chatas' Table 3, $Q_D(0)$	$Q_D(0) - 0.013$	Calc. $Q_D(0)$	% Error
1.5	0.5	0.0945	0.0815	0.0943	-0.21
2.0	1.0	0.1890	0.1760	0.1886	-0.21
2.5	1.5	0.2925	0.2795	0.2885	-1.37
3.0	2.0	0.3896	0.3766	0.3923	+0.69
3.5	2.5	0.5001	0.4871	0.4990	-0.22
4.0	3.0	0.6058	0.5928	0.6081	+0.38
4.5	3.5	0.7141	0.7011	0.7193	+0.73
5.0	4.0	0.814	0.802	0.8322	+2.24
6.0	5.0	1.064	1.051	1.063	-0.09
7.0	6.0	1.300	1.287	1.298	-0.15
8.0	7.0	1.540	1.527	1.539	-0.06
9.0	8.0	1.798	1.785	1.783	-0.83
10.0	9.0	2.050	2.037	2.030	-0.98

In the second column, are listed values of $r_D - 1$, for this was found to be the best way to correlate the data. The third column shows values of $Q_D(0)$ calculated by extrapolating Chatas' data from Table 3 to zero time. A log-log plot of $r_D - 1$ versus $Q_D(0)$ was almost a straight line, but curved slightly. By trial and error, I found that it could be straightened by subtracting 0.013 from $Q_D(0)$, and these values are tabulated in the fourth column, and graphed in Fig. 12, page 57, along with the empirical straight line found by least squares fitting of the data. The resulting equation is,

$$Q_D(0) = 0.013 + 0.1756\,(r_D - 1)^{1.111} \tag{49}$$

The next two columns show the calculated values of $Q_D(0)$ and the errors compared to the data used in Column 3. Note that the maximum error is 2.24%. This is very good indeed! Remember that it is not the value of $Q_D(0)$ that is needed, but rather the value

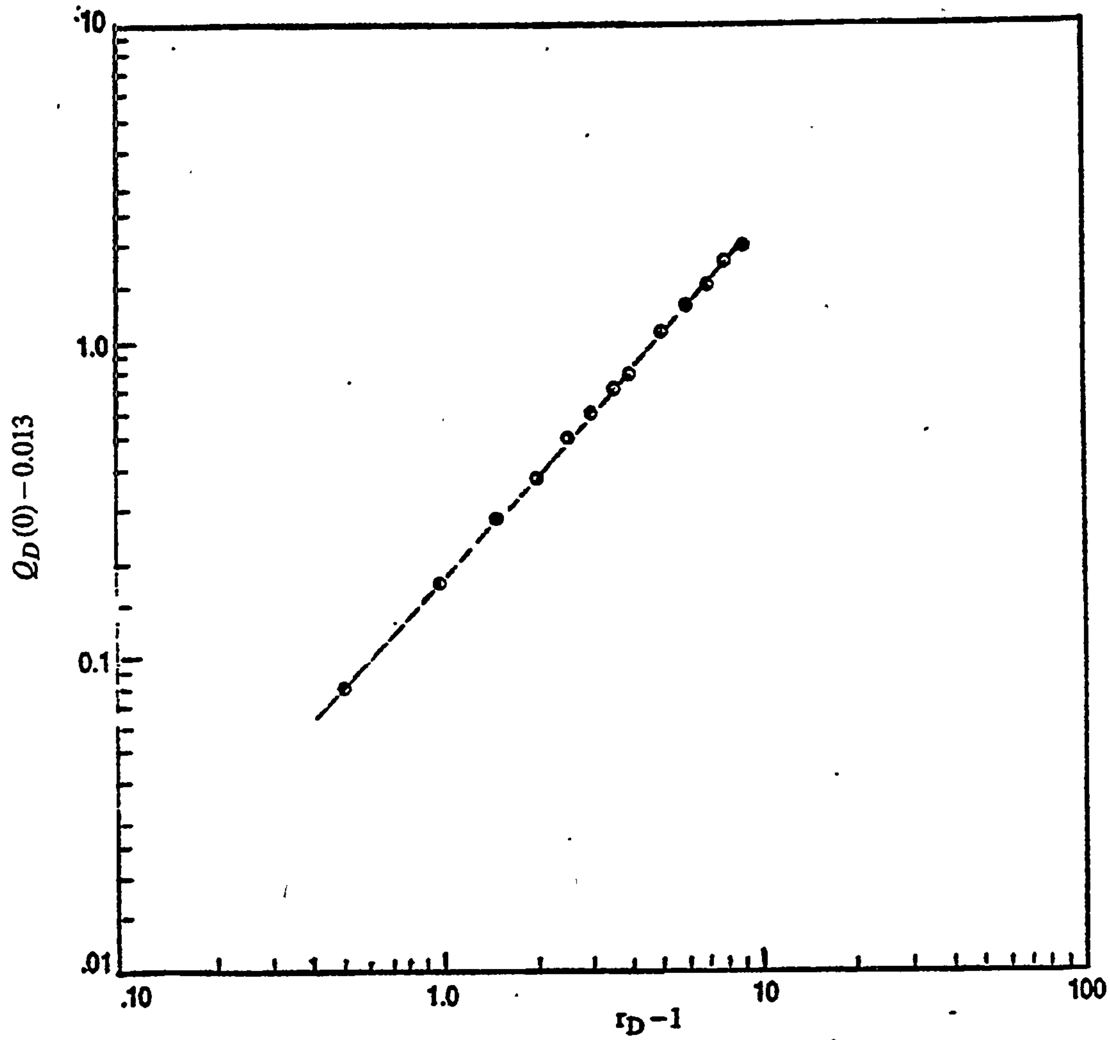

Figure 12. Correlation of $Q_D(0)$ versus r_D for constant pressure aquifer flow.

of $Q_D(\infty)-Q_D(0)$. At small r_D ($r_D=1.5$), $Q_D(0)$ is only about 15% of $Q_D(\infty)$, and the ratio decreases at higher r_D's, so that at $r_D=10$, $Q_D(0)$ is only about 4% of $Q_D(\infty)$. Thus the actual errors in $Q_D(\infty)-Q_D(0)$ are consistently below 1%.

Next, I looked at the errors in the slopes calculated using the pseudo-steady state approximation. For $r_D=4.0$, the value of $1/q_D(0)$ was 0.9787 (Eq. 46), the calculated slope was 6.7474 (Eq. 47), compared to the actual slope from Chatas' Table 3 of 6.4576 (Eq. 43). The ratio of these slopes (the error due to the pseudo-steady state assumption) was 1.045 (Eq. 48). This same procedure was carried out for all the r_D's in Chatas' Table 3, and the results are listed in the table below, along with some other columns whose meaning will be discussed next.

Exponential Decline Slopes

r_D	r_D^2-1	Error Ratio	$\frac{0.057}{\left(r_D^2-1\right)^{0.297}}$	Calculated Error Ratio (Eq. 50)	% Error in Approx. Eq.
1.5	1.25	1.021	0.0533	1.0167	-0.43
2.0	3.00	1.030	0.0411	1.0289	-0.11
2.5	5.25	1.033	0.0348	1.0352	+0.22
3.0	8.00	1.042	0.0307	1.0393	-0.27
3.5	11.25	1.042	0.0278	1.0422	+0.02
4.0	15.00	1.045	0.0255	1.0445	-0.05
4.5	19.25	1.049	0.0237	1.0463	-0.27
5.0	24.00	1.051	0.0222	1.0478	-0.32
6.0	35.0	1.051	0.0198	1.0502	-0.08
7.0	48.0	1.054	0.0181	1.0519	-0.21
8.0	63.0	1.052	0.0167	1.0533	+0.13
9.0	80.0	1.054	0.0155	1.0545	+0.05
10.0	99.0	1.057	0.0146	1.0554	-0.16

The second column in the table lists $r_D^2 - 1$, for this was the parameter that was found to best correlate the data. The third column lists the ratios of the slopes found when comparing the pseudo-steady state equation with the slopes from Chatas' Table 3. Remember that earlier I stated that the depletion rates using the pseudo-steady state approximation would be greater than what is actually taking place. The numbers in this column, ranging from 1.021 to 1.057, indicate the small size of this error.

Next, I correlated the size of this error, as a function of $r_D^2 - 1$, with the following equation.

$$\text{Error} = 1.070 - \frac{0.057}{(r_D^2 - 1)^{0.297}} \tag{50}$$

The power function portion of this equation is shown in the fourth column, and the calculated error ratios from Eq. 50 are shown in the fifth column. Finally the errors in the calculated slopes are shown in the sixth column. Note that the maximum difference is 0.43%, a remarkably accurate result! Thus we now can calculate all the decline portions of the finite constant pressure aquifers with considerable accuracy using simple equations.

In brief then, we now know we can calculate the early time constant pressure aquifer data using Eq. 28 or Eq. 30, depending on the time range required, and we can calculate the later time (depletion) history using Eq. 38e. It only remains to define the time to switch from infinite-acting to finite-acting (depletion) behavior. Again this required correlating the data in Chatas' Tables 2 and 3 as a function of r_D. The equation I came up with was,

$$(t_D)_{switch} = 0.1600\,(r_D - 1)^{2.21} \tag{51}$$

Equation 51 is not very accurate. The reason it is not, is that for all r_D's, the infinite-acting data and the finite-acting data were quite close to each other over a rather broad time range. Thus the precise times could not be defined very accurately. This, of course, is good news, for it almost guaranteed that all the resulting calculations would be reasonably accurate.

To evaluate the accuracy of these equations at the times when we switch from infinite acting to finite acting behavior, I have listed all the influx values from Chatas' tables and from my equations in the table below. In this table, the first column shows all the r_D's (r_e / r_w values) listed in Chatas' Table 3. The second lists the switchover times calculated by Eq. 51; while the third column shows the actual times used. These times were picked to be near the calculated times, and also compatible with the listings in Chatas' tables.

Influxes From Chatas' Tables 2 and 3
Compared to Approximate Equations

r_D	Calc. $(t_D)_{switch}$ Eq. 51	$(t_D)_{switch}$ Used	∞ Acting Q_D		Finite Acting Q_D		Max. Diff. (%)
			Eqs. 28 and 30	Chatas' Table 2	Eq. 38e	Chatas' Table 3	
1.5	0.035	0.050	0.2710	0.278	0.2753	0.276	2.58
2.0	0.160	0.15	0.5022	0.520	0.5064	0.507	3.54
2.5	0.392	0.40	0.8927	0.898	0.8940	0.897	0.59
3.0	0.740	0.70	1.255	1.251	1.257	1.256	0.46
3.5	1.212	1.00	1.568	1.569	1.574	1.571	0.56
4.0	1.814	2.00	2.448	2.447	2.443	2.442	0.24
4.5	2.55	2.50	2.836	*	2.836	2.835	0.04
5.0	3.43	3.50	3.554	*	3.552	2.542	0.34
6.0	5.61	6.0	5.150	5.153	5.144	5.148	0.17
7.0	8.39	9.0	6.859	6.869	6.853	6.861	0.23
8.0	11.80	12.0	8.446	8.457	8.436	8.431	0.31
9.0	15.85	15.0	9.970	9.949	9.932	9.945	0.38
10.0	20.6	20.0	12.36	12.32	12.29	12.30	0.57

The fourth and fifth columns compare the Q_D's for the infinite acting system: the fourth column is from my Eq. 28 for r_D's up to 7.0, and from Eq. 30 for the three larger r_D's; while the fifth column lists the results from Chatas' Table 2 for these same times.

Note that there are two blank spots in the Chatas' listings. This is because there were no listings for these times in his Table 2.

The sixth and seventh columns show the same kind of information for the finite systems. The sixth column shows the predicted values of Q_D from Eq. 38e, while the seventh column shows values listed in Chatas' Table 3. It is of interest to realize that, at any r_D , all four values of Q_D are very close to each other, as of course they should be. To compare them in detail, I've listed the maximum differences in the Q_D listings in the eighth column. Note that the first two show differences of 2.58 and 3.54%, while all the others are less than 1% in maximum difference. This is a remarkably accurate result! As I've said earlier, I have some doubts about Chatas' tables at small values of t_D , but even a 3.54% error would be satisfactory.

An indication of some of the inconsistencies in Chatas' tables can be seen by looking carefully at the table listings for $r_D = 3.0$ and 3.5. If $r_D = 3.0$, the t_D used was equal to 0.70. In Chatas' Table 2, the infinite system, the value for Q_D is 1.251, while for the finite system it is 1.256; a larger value, which of course, is impossible. The same behavior is seen at $r_D = 3.5$; the infinite system Q_D is 1.569 compared to 1.571 for the finite system.

The final evaluation is to compare the calculated exponential decline slopes (using all the material discussed here) with the slopes found from Chatas' Table 3. The equation for the decline using my method is as follows,

$$\text{Calculated Slope} = \frac{Q_D(\infty) - Q_D(0)}{q_D(0)\,(Error)} \tag{52}$$

In this equation, the term $Q_D(\infty) - Q_D(0)$ comes from combining Eqs. 34 and 49. The rate at $t_D = 0$, $q_D(0)$, comes from calculations similar to Eq. 46, and the error is Eq. 50.

In the table on page 62, I've compared the results from Eq. 52 with Chatas' slopes, using calculations similar to Eq. 43. In brief, the decline rates calculated for these systems are quite accurate.

Comparison of Slopes From Chatas' Table 3

With Slopes From Eq. 52

r_D	Decline Equation Slopes		Error %
	Eq. 52	Chatas' Table 3	
1.5	0.1199	0.1199	0.00
2.0	0.5406	0.5384	0.41
2.5	1.334	1.332	0.15
3.0	2.555	2.537	0.71
3.5	4.251	4.248	0.07
4.0	6.461	6.457	0.06
4.5	9.214	9.197	0.18
5.0	12.537	12.580	-0.34
6.0	21.02	21.01	0.05
7.0	32.07	32.03	0.12
8.0	45.87	45.91	-0.09
9.0	62.55	62.52	0.05
10.0	82.16	81.98	0.22

In general we can conclude that aquifer influx history can be calculated easily for any radial system, using simple equations rather than voluminous tables. Further, the process is easier. But probably the most important aspect of this rather voluminous exercise, was to show the nature of the aquifer influx equations and how they behave. For the infinite system, simple equations are valid, and they behave logically. At short times the influx history acts like an extension of the very short time equation; while for long times the influx history is semi-logarithmic in form, as we might have expected. In the finite systems, after a period of time, the systems show exponential decline behavior, and the values of the decline intercepts and slopes behave in the logical manner one would expect, based on the rate equations and on material balance principles. These are important ideas that need to be emphasized, for often such ideas become lost when results are expressed in infinite series equations or in tables.

Superposition

Chatas' tables are interesting and useful, but they normally cannot be used directly, for it is seldom true that either rate or pressure are held constant at the reservoir/aquifer boundary. This is not a serious problem, however, for we can invoke the concept of superposition, which I'll discuss next.

There is a general concept in mathematics relating the time integral of two variables called the Faltung Integral, Duhamel's Integral, or the convolation integral, as follows,

$$F_3(t) = \int_0^t F_1(t-\tau) F_2(\tau)\, d\tau \tag{53a}$$

$$= \int_0^t F_2(t-\tau) F_1(\tau)\, d\tau \tag{53b}$$

where either way of handling the integral gives identical results. We also commonly call this the superposition integral when handling well testing and aquifer flow problems.

The usual practical way of handling this integral for water influx is as follows.

$$Q_D(t_D) = \int_0^{t_D} \frac{\partial p_D}{\partial \tau} Q_D(t_D - \tau)\, d\tau \tag{54a}$$

Normally the pressure history is not known analytically, and Q_D is in tabular form, so this integral is handled numerically, as follows.

$$Q_D(t_D) = \sum_{i=0}^{n} [p_D(t_{Di}) - p_D(t_{Di-1})]\, Q_D(t_{Dn} - t_{Di}) \tag{54b}$$

Notice in Eqs. 54a and 54b, that the indicies on time are reversed on the p_D and Q_D terms in both the integral and the summation. This concept may be a bit confusing, so I'll attempt to clarify it graphically in Fig. 13.

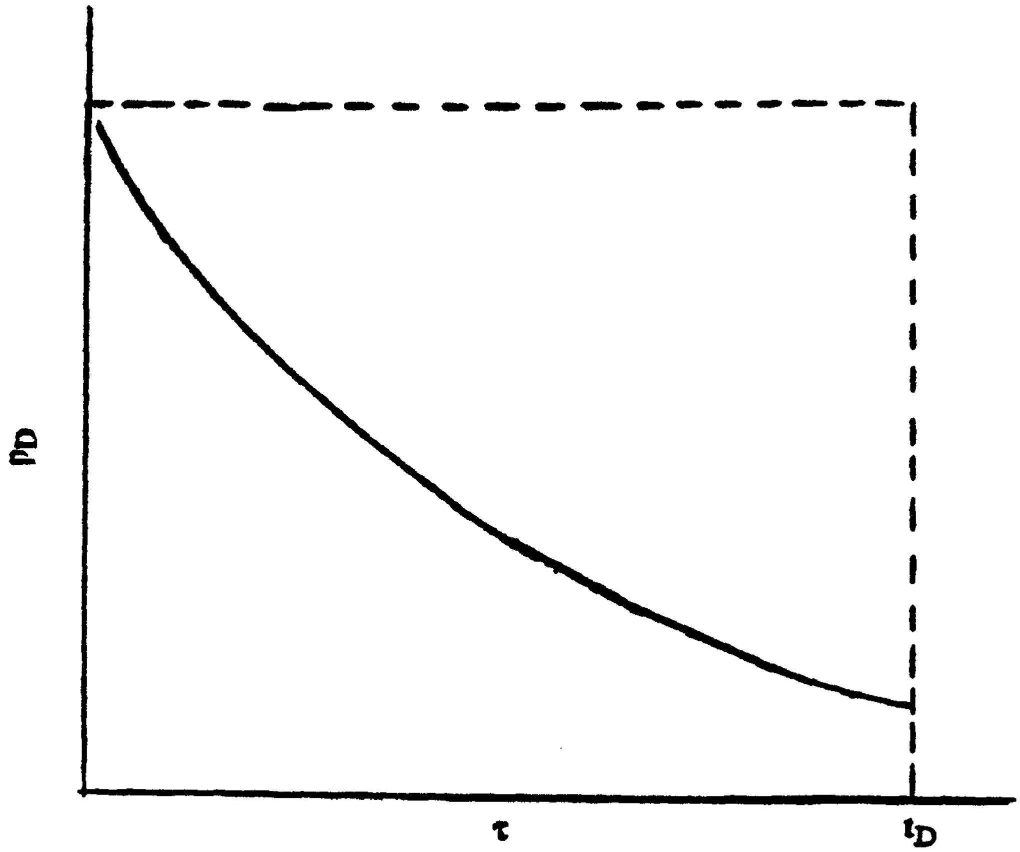

Figure 13. Example pressure history.

In this figure I've graphed pressure, p_D, against time, τ, for a total time, t_D Notice that the early pressure drop is small, but it is felt for the entire time. This is indicated in Eq. 54a as $\partial p_D / \partial \tau$ when τ is small, and the Q_D term is evaluated over the entire time, $t_D - \tau$. The same is true in Eq. 54b. The pressure drop is indicated at t_{Di}, with i small, and Q_D is evaluated at $t_{Dn} - t_{Di}$, with i small.

As time goes on, the pressure continues to drop, but the effect of each drop is felt for a shorter time. The pressure change is evaluated at this later time, τ, and the resulting Q_D is evaluated for a shorter time, $t_D - \tau$. All this is quite logical, and behaves as one might instinctively envision. I should also add that it isn't necessary that the pressures decrease with time. They can also increase, and the formal procedure will be the same. Some influx terms will be negative, as a result; but if the overall pressure is lower than the initial pressure, the summation will be positive, and correct.

To show how this is done in practice, I've made a similar graph in Fig. 14, page 66, but here also divided it into discreet stairsteps as implied by Eq. 54b. We presume that specific data are available at specific times; p_i at τ_0, p_1 at τ_1, p_2 at τ_2 and so on to p_6 at τ_6; the final time, t_D, when the total influx is to be evaluated.

To handle the summation of Eq. 54b, we first assume that over time, $\tau_1 - \tau_0$, that pressure actually dropped abruptly at time τ_0 to half the pressure drop [to $(p_i + p_1)/2$] that occurred over the first time period. This concept is continued over the rest of the time periods in steps. From τ_1 to τ_2, we assume the pressure drops abruptly to $(p_1 + p_2)/2$ at time τ_1. This, too, is shown in Fig. 14. This second pressure drop is assumed to last from τ_1 to total time, t_D (or τ_6, in the illustration). This sequence is followed for the remainder of the time history.

Notice, in Eq. 54b, that it is the individual pressure drops that are included in the summations, not the pressure levels themselves. So Δp_0 is defined as follows,

$$\Delta p_0 = p_i - \frac{(p_i + p_1)}{2} = \frac{p_i - p_1}{2} \tag{55}$$

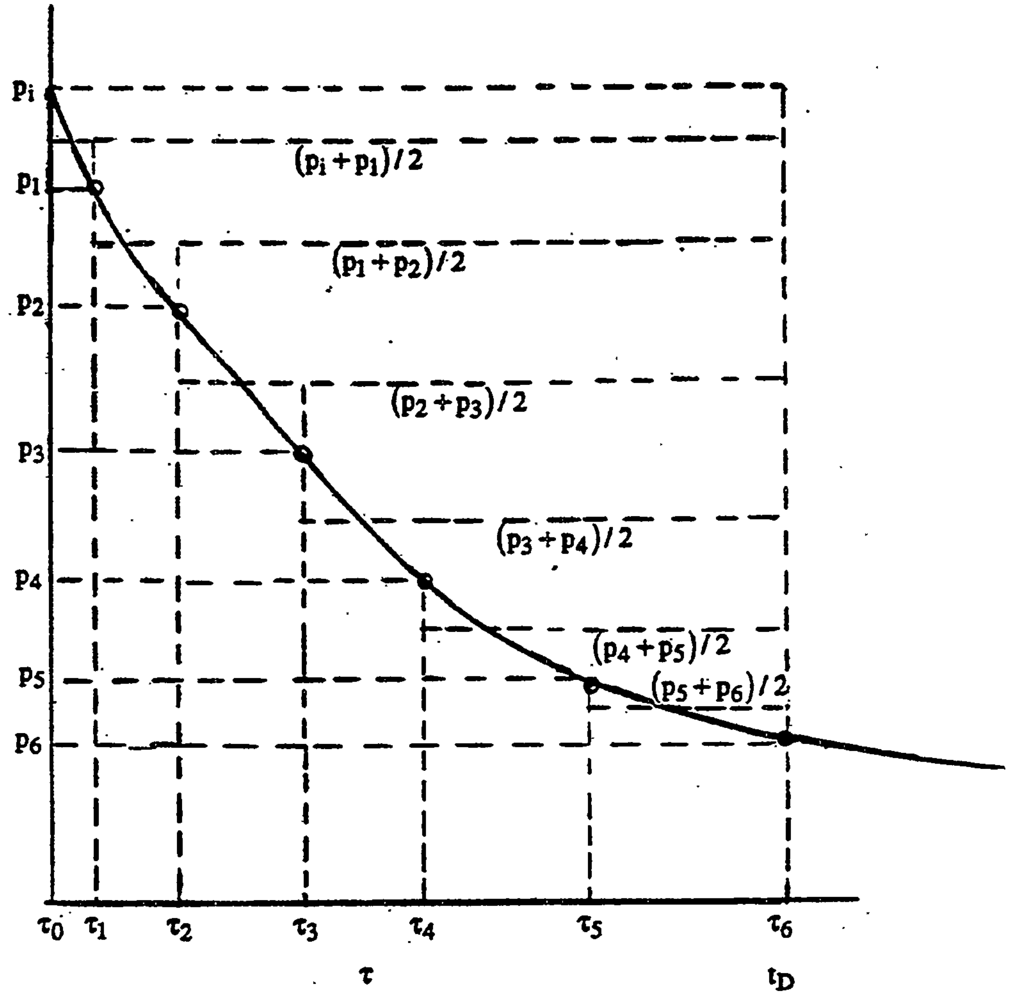

Figure 14. Approximation of pressure history.

In Eq. 54b, this pressure drop is evaluated for the entire time, t_D (or τ_6). For Δp_1 , the equation is,

$$\Delta p_1 = \overline{p}_i - \overline{p}_2 = \frac{p_i + p_1}{2} - \frac{p_1 + p_2}{2} = \frac{p_i - p_2}{2} \tag{56}$$

This pressure drop lasts for time $t_D - \tau_1$. For Δp_2 , the equation is,

$$\Delta p_2 = \overline{p}_2 - \overline{p}_3 = \frac{p_1 + p_2}{2} - \frac{p_2 + p_3}{2} = \frac{p_1 - p_3}{2} \tag{57}$$

This pressure drop lasts for time, $t_D - \tau_2$. The rest of the Δp 's follow the same logical order as Eqs. 56 and 57.

Note the interesting concept that the actual p_n (p_1, p_2 etc.) for the particular time step is not included when evaluating the effect of that pressure drop on that time step. There is no theoretical logic for this strange behavior; it merely falls out from the procedure used to discretize this summation.

One other important item concerns the sizes of the time and pressure steps taken. Notice in the illustration of Fig. 14, that they were not equal, either in pressure drop or in time step size. They don't need to be. However, in practice, when evaluating a number of water influx calculations with time, it is usually convenient to divide the calculations into equal sized time steps. This procedure makes the table lookup and the calculational procedures more convenient to handle. Also, it seems wise here to point out that this formal procedure is the same for any geometry and boundary condition.

In Eq. 54a I've shown one form of the more commonly used water influx superposition integral. Actually there are four different ways to write this equation. They are,

$$(W_e)_D = \int_0^{t_D} \Delta p_D(t_D - \tau) q_D(\tau) d\tau \tag{58a}$$

$$(W_e)_D = \int_0^{t_D} \Delta p_D(\tau) q_D(t_D - \tau) d\tau \tag{58b}$$

$$(W_e)_D = \int_0^{t_D} \frac{d\Delta p_D(\tau)}{d\tau} Q_D(t_D - \tau) d\tau \tag{58c}$$

and

$$(W_e)_D = \int_0^{t_D} \frac{d\Delta p_D(t_D-\tau)}{d(t_D-\tau)} Q_D(\tau)\,d\tau \tag{58d}$$

If what I've said earlier is correct, all four of these equations should produce the same result. To test this idea out, I've looked at the results using the following equation forms for the variables.

$$\Delta p_D(\tau) = a\tau^2 \qquad \Delta p_D(t_D-\tau) = a(t_D-\tau)^2$$

$$Q_D(\tau) = b\tau^m \qquad q_D(\tau) = mb\tau^{m-1}$$

$$\frac{d\Delta p_D(\tau)}{d\tau} = 2a\tau \qquad q_D(t_D-\tau) = mb(t_D-\tau)^{m-1}$$

$$\frac{d\Delta p_D(t_D-\tau)}{d(t_D-\tau)} = 2a(t_D-\tau)$$

We will evaluate $(W_e)_D(t_D)$ using these parameters, and all four equation forms, to test whether all four equations give the same result.

Using Eq. 58a, and substituting the definitions, we get,

$$(W_e)_D = \int_0^{t_D} a(t_D-\tau)^2 mb\tau^{m-1} d\tau \tag{59a}$$

$$= mab \int_0^{t_D} \left(t_D^2\,\tau^{m-1} - 2t_D\tau^m + \tau^{m+1}\right) d\tau$$

$$= mab \left| \frac{t_D^2\,\tau^m}{m} - \frac{2t_D\tau^{m+1}}{m+1} + \frac{\tau^{m+2}}{m+2} \right|_0^{t_D}$$

$$= mab\,t_D^{m+2}\left[\frac{1}{m} - \frac{2}{m+1} + \frac{1}{m+2}\right]$$

$$(W_e)_D = \frac{2ab\,t_D^{m+2}}{(m+1)(m+2)} \tag{59b}$$

By comparison, using Eq. 58b, and substituting the definitions, we get,

$$(W_e)_D = \int_0^{t_D} a\,\tau^2 mb(t-\tau)^{m-1} d\tau \tag{60a}$$

Equation 60a is more easily solved if we were to change the variables and integration limits as follows,

$$\text{call} \qquad t_D - \tau = y \quad , \qquad d\tau = -dy$$

$$\text{when} \quad \tau = t_D \quad , \quad y = 0 \quad \text{and when} \quad \tau = 0 \quad , \quad y = t_D$$

So the equation becomes,

$$(W_e)_D = -\int_{t_D}^{0} a\,(t_D - y)^2\, mby^{m-1} dy \tag{60b}$$

But Eq. 60b is identical to Eq. 59a! So its solution is also the same,

$$(W_e)_D = \frac{2ab\, t_D^{m+2}}{(m+1)\,(m+2)} \tag{60c}$$

Next we'll look at Eq. 58d. When we substitute the definitions for the pressure derivative and cumulative water influx terms, we get,

$$(W_e)_D = \int_0^{t_D} 2a\,(t_D - \tau)\, b\tau^m d\tau \tag{61a}$$

$$= 2ab\left|\frac{t_D\,\tau^{m+1}}{m+1} - \frac{\tau^{m+2}}{m+2}\right|_0^{t_D}$$

$$(W_e)_D = 2ab\; t_D^{m+2}\left[\frac{(m+2)-(m+1)}{(m+2)(m+1)}\right] = \frac{2ab\; t_D^{m+2}}{(m+2)(m+1)} \tag{61b}$$

Again, the result is identical to Eqs. 59b and 60c. Finally we'll look at Eq. 58c and substitute the appropriate definitions. The result is,

$$(W_e)_D = \int_0^{t_D} 2a\tau b\,(t_D - \tau)^{\,m} d\tau \tag{62a}$$

As before, we'll change variables and limits as follows,

$$\text{call} \qquad t_D - \tau = y \quad , \qquad d\tau = -dy$$

when $\tau = t_D$, $y = 0$, and when $\tau = 0$, $y = t_D$

And when these definitions are substituted into Eq. 60a, the result is,

$$(W_e)_D = -\int_{t_D}^{0} 2a(t_D - y)\, b y^m dy \tag{62b}$$

and, as we might have predicted, Eq. 62b is identical to Eq. 61a, thus its solution is the same as the others.

$$(W_e)_D = \frac{2ab\, t_D^{m+2}}{(m+2)(m+1)} \tag{62c}$$

These results are remarkable, but they have far greater implications than just for this specific case. To make these calculations, I used a general power function, m , on the Q_D term, and a power of 2.0 on the Δp_D term. I could have used any power I wished on the Δp_D term, but chose to use 2.0 to simplify the algebra. For example, suppose I had used an equation of the form,

$$\Delta p_D(\tau) = a\tau^3$$

for the pressure equation. Using this equation form, the resulting water influx equations would all have resulted in the following solution,

$$(W_e)_D = \frac{6ab\, t_D^{m+3}}{(m+1)(m+2)(m+3)} \tag{63}$$

I'll not bother to show the algebraic details necessary to prove this statement. The interested reader can prove it for himself.

Clearly then, if *any* power could be used on either term, then any function could be used on either term, for any function can be put into an infinite power series. Thus we can conclude that Eqs. 58a-d are always equal to each other for any superposition problem we wish to solve. This is true for any geometry and any boundary conditions we wish to use.

Normally we use Eq. 54a, which is the same as Eq. 58c, but sometimes one of the other equation forms will be more convenient.

In brief, due to variations in both pressure and aquifer flow rate with time, some superposition procedure must always be used in water influx calculations, as we'll see in later notes on application. This statement is true for whatever inner or outer boundary conditions are applicable, and for whatever geometry is appropriate. Next, however, I'll discuss the linear aquifer solutions.

Linear Geometry

The behavior of a linear aquifer is far simpler than that of a radial aquifer. The mathematics of the problem were first published by Miller in 1962, but shortly after that a quite elegant piece of work by Nabor and Barham (1964) presented the entire linear aquifer equations and curves in a three-page paper in the Journal of Petroleum Technology. The remarkable result of Nabor and Barham's work was to show that all six possible boundary conditions (Interior Boundary, constant pressure or constant rate; Outer Boundary, closed, constant pressure or infinite), could be shown with only three equations, or alternatively, three lines on a single graph. A copy of their paper is attached.

The reason for this behavior becomes obvious when one looks at their equations. Their Eq. 1 shows the pressure drop for the infinite system with a constant rate inner boundary, while their Eq. 4 shows the cumulative water influx for the infinite system with a constant pressure inner boundary. Notice that the time relationship is the same for both of them. It is,

$$\text{Time Function} = 2\sqrt{kt / \pi\phi\mu c_t} \tag{64}$$

The careful reader will notice that this time function is not dimensionless as one might have expected, but it is made dimensionless in their Eqs. 9 and 12, and defined by the general infinite acting function $F_{1/2}(t_D)$ as follows,

$$F_{1/2}(t_D) = 2\sqrt{t_D / \pi} \tag{65}$$

Linear Aquifer Behavior

G. W. NABOR
R. H. BARHAM
MEMBERS AIME

SOCONY MOBIL OIL CO., INC.
DALLAS, TEX.

INTRODUCTION

Linear aquifers, either limited or essentially infinite, may be encountered in reservoir engineering practice. In areas where faulting fixes reservoir boundaries, the fault block reservoir may have an aquifer of limited extent whose geometry is best approximated as linear. An infinite linear aquifer can occur as a regional feature whenever water movement through the aquifer member is constrained to one direction. Such constraints can arise from major faults, facies changes or pinchout of the member.

Miller* pointed out that linear aquifers have received only meager attention in the past. He analyzed the performance of finite and infinite aquifers, developed working equations and curves, and presented examples. While Miller's curves may be used fairly easily, a separate one is required for each size of aquifer. In this paper, Miller's equations have been used as a starting point. By modifying them slightly, they can be reduced to a form which yields a single working curve, applicable to any size of aquifer. Thus, interpolation between curves is eliminated and accuracy is improved.

Miller's results for finite aquifers covered only the boundary condition of no flow across the outer aquifer boundary. This paper also includes the case of constant pressure at the outer aquifer boundary.

DEVELOPMENT OF EQUATIONS FOR LINEAR AQUIFERS

Miller's equations give pressure drop or cumulative influx at the linear aquifer-reservoir boundary as a function of time for the boundary conditions of an infinite aquifer and a finite aquifer with sealed outer boundary. In addition to these equations, those appropriate for the boundary condition of a finite aquifer with constant pressure at the outer boundary have been developed. The approach used in developing these equations was the same as that used by Miller.

BOUNDARY CONDITION 1: CONSTANT RATE OF INFLUX ACROSS AQUIFER-RESERVOIR BOUNDARY

Infinite Linear Aquifer

$$\Delta p = \frac{q\mu}{kbh}\left[2\sqrt{\frac{kt}{\pi\phi\mu c_t}}\right] \quad . . . . (1)$$

Finite Linear Aquifer, Sealed Outer Boundary

$$\Delta p = \frac{q\mu}{kbh}\left[\left(\frac{L}{3}+\frac{kt}{\phi\mu c_t L}\right)-\frac{2L}{\pi^2}\sum_{n=1}^{\infty}\left(\frac{1}{n^2}\right)\exp\left(-\frac{n^2\pi^2 kt}{\phi\mu c_t L^2}\right)\right] \quad . . . . (2)$$

Finite Linear Aquifer, Constant Pressure at Outer Boundary

$$\Delta p = \frac{q\mu}{kbh}\left[L-\frac{8L}{\pi^2}\sum_{n\,odd}^{\infty}\left(\frac{1}{n^2}\right)\exp\left(-\frac{n^2\pi^2 kt}{4\phi\mu c_t L^2}\right)\right] \quad . . . . (3)$$

BOUNDARY CONDITION 2: CONSTANT PRESSURE AT AQUIFER-RESERVOIR BOUNDARY

Infinite Linear Aquifer

$$W_e = \phi\, bh\, c_t\,(\Delta p)\left[2\sqrt{\frac{kt}{\pi\phi\mu c_t}}\right] \quad . . . . (4)$$

Finite Linear Aquifer, Sealed Outer Boundary

$$W_e = \phi\, bh\, c_t\,(\Delta p)\left[L-\frac{8L}{\pi^2}\sum_{n\,odd}^{\infty}\left(\frac{1}{n^2}\right)\exp\left(-\frac{n^2\pi^2 kt}{4\phi\mu c_t L^2}\right)\right]. \quad . . . . . . (5)$$

Finite Linear Aquifer, Constant Pressure at Outer Boundary

$$W_e = \phi\, bh\, c_t\,(\Delta p)\left[\left(\frac{L}{3}+\frac{kt}{\phi\mu c_t L}\right)-\frac{2L}{\pi^2}\sum_{n=1}^{\infty}\left(\frac{1}{n^2}\right)\exp\left(-\frac{n^2\pi^2 kt}{\phi\mu c_t L^2}\right)\right]. \quad . (6)$$

These equations are usually put in a form where dimensionless time is defined by

$$t_D = \frac{kt}{\phi\mu c_t x_c^2} \quad . . . . (7)$$

Here, x_c is a reference distance and is usually taken to be a unit distance. However, the choice is really arbitrary, as long as consistency is maintained. We choose $x_c = L$; then

$$t_D = \frac{kt}{\phi\mu c_t L^2} \quad . . . . (8)$$

For finite aquifers, L is the length of aquifer; for infinite cases, it may be considered as an arbitrarily chosen length. The reason for this choice will be clear later when the performances of finite and infinite aquifers are compared.

Substituting t_D from Eq. 8, the first six equations become:

BOUNDARY CONDITION 1:

Infinite Linear Aquifer

$$\Delta p = \frac{q\mu L}{kbh}F_1(t_D) \quad . . . . (9)$$

Finite Linear Aquifer, Sealed Outer Boundary

$$\Delta p = \frac{q\mu L}{kbh}F_s(t_D) \quad . . . . (10)$$

Finite Linear Aquifer, Constant Pressure at Outer Boundary

$$\Delta p = \frac{q\mu L}{kbh}F_c(t_D) \quad . . . . (11)$$

BOUNDARY CONDITION 2:

Infinite Linear Aquifer

$$W_e = \phi\, bhL\, c_t\,(\Delta p)\,F_1(t_D) \quad . . . . . (12)$$

Original manuscript received in Society of Petroleum Engineers office Dec. 13, 1963.

*Miller, F. G.: "Theory of Unsteady-State Influx of Water in Linear Reservoirs", *Journal Institute of Petroleum* (Nov., 1962) 48, 365.

Finite Linear Aquifer, Sealed Outer Boundary

$$W_e = \phi\, bh\, L\, c_t\, (\Delta p)\, F_0\, (t_D) \quad \ldots\ldots \quad (13)$$

Finite Linear Aquifer, Constant Pressure at Outer Boundary

$$W_e = \phi\, bh\, L\, c_t\, (\Delta p)\, F_1\, (t_D) \quad \ldots\ldots \quad (14)$$

In these equations, the functions of dimensionless time are:

$$F_0\,(t_D) = 1 - \frac{8}{\pi^2} \sum_{n\,odd}^{\infty} \left(\frac{1}{n^2}\right) \exp\left(-\frac{n^2\pi^2 t_D}{4}\right) \quad (15)$$

$$F_{\frac{1}{2}}\,(t_D) = 2\sqrt{t_D/\pi} \quad \ldots\ldots \quad (16)$$

$$F_1\,(t_D) = \left(t_D + \frac{1}{3}\right) - \frac{2}{\pi^2} \sum_{n=1}^{\infty} \left(\frac{1}{n^2}\right) \exp\left(-n^2\pi^2 t_D\right) \quad \ldots\ldots \quad (17)$$

These functions are shown in Fig. 1. The subscripts 0, ½ and 1 correspond to the slopes of the curves as t_D approaches large values. Table 1 gives numerical values.

THE F-FUNCTIONS

The F-functions, in contrast to those used in Eqs. 1 through 6, do not depend explicitly on L, the aquifer length. This dependence has been removed by the particular definition used for dimensionless time.

The advantages are obvious. Only a single curve or table of values need be examined for a given boundary condition. Even in cases where L is not known precisely, it is easy to assume several trial values, calculate the corresponding t_D values, and read the required F-values from a single curve. All interpolation between curves is eliminated.

The behavior of the F-functions at small and large times is of interest. At $t_D = 0$, the summation appearing in $F_0\,(t_D)$ reduces to a summation of $(1/n^2)$, for odd values of n. The summation of $F_1\,(t_D)$ reduces to a summation of $(1/n^2)$, for all values of n. These sum to $(\pi^2/8)$ and $(\pi^2/6)$, so F_0 and F_1 both approach zero as t_D approaches zero. As t_D approaches infinity, $F_0\,(t_D)$ approaches 1, and $F_1\,(t_D)$ approaches $(t_D + 1/3)$; i.e., becomes linear with t_D. If the boundary conditions applying to Eqs. 9 through 14 are examined, it is apparent this must be the case. For example, in the constant rate case, with sealed outer boundary, we expect the total pressure drop to become linear with time as the quasi-steady-state condition is reached at large time.

It would be expected that finite linear aquifers would behave, at small times, just as infinite aquifers do. In other words, at low values of t_D, $F_0\,(t_D)$ and $F_1\,(t_D)$ should both approach $F_{\frac{1}{2}}\,(t_D)$. This is indeed the case, as a referral to Table 1 or Fig. 1 will show.

Table 1 was computed digitally and Fig. 1 was prepared from the results. Fig. 1 clearly indicates that the functions $F_0\,(t_D)$ and $F_1\,(t_D)$, for finite aquifers, begin to deviate from the infinite linear aquifer curve, $F_{\frac{1}{2}}\,(t_D)$, when t_D exceeds 0.25. When t_D exceeds 2.5, the finite aquifer functions may be very well approximated by their limiting forms. Hence,

$$\text{For } t_D \leqslant 0.25,\ F_0 = F_{\frac{1}{2}} = F_1 = 2\sqrt{t_D/\pi} \quad \ldots\ldots \quad (18)$$

For $0.25 < t_D < 2.5$, use Table 1 or Fig. 1 for F_0 and F_1

$$\text{For } t_D \geqslant 2.5,\ F_0 = 1 \quad \ldots\ldots \quad (19)$$

$$F_1 = t_D + \frac{1}{3} \quad \ldots\ldots \quad (20)$$

Eqs. 19 and 20 show, of course, that the finite systems have closely approached the steady or quasi-steady state at longer times.

APPLICATIONS

UNITS

The equations and graphs presented in this paper require that a dimensionally consistent set of units be used. This is perhaps an obvious point, but may easily be overlooked when attempting to work in terms of practical units.

The metric or cm-sec-cp-atm-darcy system is dimensionally consistent and applications can be carried out without difficulty.

The so-called practical system, which uses one basic unit, ft, for measuring length and area and another, bbl, for measuring volume, is subject to error in application. The most rational approach appears to be that of defining a special permeability unit (spu) such that

$$k_{spu} = 6.3283\ k_{darcies} \quad \ldots\ldots \quad (21)$$

Then, a consistent ft-day-cp-psi-spu system of units may be used, remembering that influx rates and volumes must be expressed in terms of cubic feet rather than barrels.

SUPERPOSITION

To calculate pressure drop when rate of influx has varied:

$$\Delta p = \frac{\mu L}{kbh}\left[q_0 F_k\,(t_D) + (q_1 - q_0)\, F_k\,(t_D - t_{D1}) + \ldots\right] \quad \ldots\ldots \quad (22)$$

To calculate influx for a series of pressure drops:

$$W_e = \phi\, bh\, L\, c_t\, [\Delta p_0 F_k\,(t_D) + \Delta p_1 F_k\,(t_D - t_{D1}) + \ldots] \quad \ldots\ldots \quad (23)$$

where

$$(\Delta p)_j = (p_{j-1} - p_{j+1})/2 \quad \ldots\ldots \quad (24)$$

In these equations, $F_k(t_D)$ refers to the particular F-function for boundary conditions appropriate to the case of interest.

Example No. 1

Over the months of April through June, the pressure of a reservoir dropped from 2,810 to 2,780 psi during initial production. The aquifer associated with this reservoir is estimated to have the properties in Table 2.

Estimate the water influx from the aquifer over this period of time, assuming (1) an infinite aquifer, (2) a finite, sealed aquifer 2 miles long, and (3) a finite aquifer 2 miles long with constant pressure at the outer boundary.

Since the data are given in practical units,

$$k_{spu} = 6.3283\ k_{darcies} = 6.3283\ (0.3) = 1.8985.$$

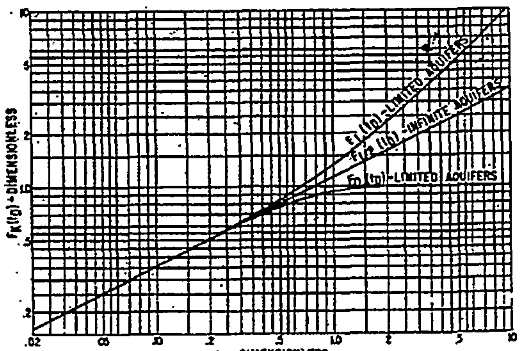

FIG. 1—PRESSURE DROP AND CUMULATIVE INFLUX FORMATIONS, LINEAR AQUIFERS.

TABLE 1—PRESSURE DROP AND CUMULATIVE INFLUX FUNCTIONS FOR LINEAR AQUIFERS

t_D	$F_0(t_D)$	$F_{1/2}(t_D)$	$F_1(t_D)$	t_D	$F_0(t_D)$	$F_{1/2}(t_D)$	$F_1(t_D)$
1.00(10^-2)	1.128379(10^-1)	1.128379(10^-1)	1.128379(10^-1)	3.10(10^-1)	6.226824(10^-1)	6.282549(10^-1)	6.338276(10^-1)
1.10(10^-2)	1.183454(10^-1)	1.183454(10^-1)	1.183454(10^-1)	3.50(10^-1)	6.581891(10^-1)	6.675581(10^-1)	6.769283(10^-1)
1.25(10^-2)	1.261566(10^-1)	1.261566(10^-1)	1.261566(10^-1)	4.00(10^-1)	6.978819(10^-1)	7.136496(10^-1)	7.294231(10^-1)
1.40(10^-2)	1.335116(10^-1)	1.335116(10^-1)	1.335116(10^-1)	4.50(10^-1)	7.329537(10^-1)	7.569398(10^-1)	7.809461(10^-1)
1.60(10^-2)	1.427299(10^-1)	1.427299(10^-1)	1.427299(10^-1)	5.00(10^-1)	7.639503(10^-1)	7.978846(10^-1)	8.318760(10^-1)
1.80(10^-2)	1.513880(10^-1)	1.513880(10^-1)	1.513880(10^-1)	5.60(10^-1)	7.964332(10^-1)	8.444016(10^-1)	8.925272(10^-1)
2.00(10^-2)	1.595769(10^-1)	1.595769(10^-1)	1.595769(10^-1)	6.20(10^-1)	8.244456(10^-1)	8.884866(10^-1)	9.528875(10^-1)
2.25(10^-2)	1.692569(10^-1)	1.692569(10^-1)	1.692569(10^-1)	7.00(10^-1)	8.558930(10^-1)	9.440697(10^-1)	10.331309(10^-1)
2.50(10^-2)	1.784124(10^-1)	1.784124(10^-1)	1.784124(10^-1)	8.00(10^-1)	8.874029(10^-1)	10.092530(10^-1)	11.332578(10^-1)
2.80(10^-2)	1.888139(10^-1)	1.888139(10^-1)	1.888139(10^-1)	9.00(10^-1)	9.120229(10^-1)	10.704744(10^-1)	12.333052(10^-1)
3.10(10^-2)	1.986717(10^-1)	1.986717(10^-1)	1.986717(10^-1)	1.00	9.312597(10^-1)	1.128379	1.333323
3.50(10^-2)	2.111004(10^-1)	2.111004(10^-1)	2.111004(10^-1)	1.10	9.462902(10^-1)	1.183454	1.433329
4.00(10^-2)	2.256758(10^-1)	2.256758(10^-1)	2.256758(10^-1)	1.25	9.629049(10^-1)	1.261566	1.583332
4.50(10^-2)	2.393654(10^-1)	2.393654(10^-1)	2.393654(10^-1)	1.40	9.743799(10^-1)	1.335116	1.733333
5.00(10^-2)	2.523133(10^-1)	2.523133(10^-1)	2.523133(10^-1)	1.60	9.843590(10^-1)	1.427299	1.933333
5.60(10^-2)	2.670232(10^-1)	2.670232(10^-1)	2.670232(10^-1)	1.80	9.904512(10^-1)	1.513880	2.133333
6.20(10^-2)	2.809641(10^-1)	2.809641(10^-1)	2.809641(10^-1)	2.00	9.941705(10^-1)	1.595769	2.333333
7.00(10^-2)	2.985411(10^-1)	2.985411(10^-1)	2.985411(10^-1)	2.25	9.968541(10^-1)	1.692569	2.583333
8.00(10^-2)	3.191537(10^-1)	3.191538(10^-1)	3.191539(10^-1)	2.50	9.983024(10^-1)	1.784124	2.833333
9.00(10^-2)	3.385133(10^-1)	3.385138(10^-1)	3.385141(10^-1)	2.80	9.991902(10^-1)	1.888139	3.133333
1.00(10^-1)	3.568234(10^-1)	3.568248(10^-1)	3.568262(10^-1)	3.10	9.996137(10^-1)	1.986717	3.433333
1.10(10^-1)	3.742370(10^-1)	3.742410(10^-1)	3.742451(10^-1)	3.50	9.998560(10^-1)	2.111004	3.833333
1.25(10^-1)	3.989280(10^-1)	3.989423(10^-1)	3.989566(10^-1)	4.00	9.999581(10^-1)	2.256758	4.333333
1.40(10^-1)	4.221615(10^-1)	4.222008(10^-1)	4.222401(10^-1)	4.50	9.999878(10^-1)	2.393654	4.833333
1.60(10^-1)	4.512368(10^-1)	4.513517(10^-1)	4.514665(10^-1)	5.00	9.999964(10^-1)	2.523133	5.333333
1.80(10^-1)	4.784617(10^-1)	4.787307(10^-1)	4.789997(10^-1)	5.60	9.999992(10^-1)	2.670232	5.933333
2.00(10^-1)	5.040878(10^-1)	5.046265(10^-1)	5.051652(10^-1)	6.20	9.999998(10^-1)	2.809641	6.533333
2.25(10^-1)	5.341424(10^-1)	5.352372(10^-1)	5.363320(10^-1)	7.00	10.000000(10^-1)	2.985411	7.333333
2.50(10^-1)	5.622335(10^-1)	5.641896(10^-1)	5.661456(10^-1)	8.00	10.000000(10^-1)	3.191538	8.333333
2.80(10^-1)	5.936127(10^-1)	5.970821(10^-1)	6.005516(10^-1)	9.00	10.000000(10^-1)	3.385138	9.333333

For all cases, $t = 91$ days and L is 2 miles $= 10{,}560$ ft.

$$t_D = \frac{kt}{\phi \mu c_t L^2}$$

$$= \frac{(1.8985)\ (91)}{(0.25)\ (1)\ (6.2)\ (10^{-4})\ (10{,}560)^2} = 1.0.$$

Since the pressure drop occurs over a period of time, superposition should be used. Assumption of a linear drop with time is shown in Table 3.

The water influx is given by Eq. 23:

$$W_e = \phi\, bh\, L\, c_t\, \Sigma_j \Delta p_j\, F_k\, (t_k - t_{Dj})$$

$$= (0.25)\ (2{,}000)\ (41)\ (10{,}560)\ (6.2)\ (10^{-4})\ (\Sigma)$$

$$= 1342.2\ (\Sigma).$$

Example No. 2

Assume an aquifer of the same properties as used in Example 1, Case (2). Estimate the pressure drop at the aquifer-reservoir boundary for a constant influx rate of 53.1 B/D over a 91 day time period.

$$q, \text{cu ft/D} = 5.6146\ (53.1)$$

$$= 298.1 \text{ cu ft/D}$$

Since the same t_D equation applies in this case as previously, $t_D = 1.0$. Also, $k_{spu} = 1.8985$. The pressure drop is given by Eq. 22:

$$\Delta p = \frac{q \mu L}{kbh} F_1(t_D)$$

$$= \frac{(298.1)\ (1)\ (10{,}560)}{(1.8985)\ (2{,}000)\ (41)} (1.333) = 27 \text{ psi.}$$

TABLE 2—AQUIFER PROPERTIES

$b = 2{,}000$ ft
$h = 41$ ft
$k = 300$ md
$\phi = 0.25$
$\mu_w = 1$ cp
$c_t = 6.2\ (10^{-4})$ psi^{-1} (rock & water)

TABLE 3—INFLUX FUNCTION CALCULATIONS

t_{Dj}	p_j	$t_D - t_{Dj}$	Δp_j	$F_0(t_D - t_{Dj})$	$F_{1/2}(t_D - t_{Dj})$	$F_1(t_D - t_{Dj})$
0.0	2810	1.0	3	.931	1.128	1.333
0.2	2804	0.8	6	.887	1.009	1.133
0.4	2798	0.6	6	.815	.870	.930
0.6	2792	0.4	6	.698	.714	.729
0.8	2786	0.2	6	.504	.505	.506
1.0	2780	0.0				
$\Sigma_j \Delta p_j F_k (t_D - t_{Dj})$				20.217	21.972	23.788

TABLE 4—WATER INFLUX RESULTS

Case	F_k	W_e (cu ft)	W_e (bbl)	Avg. q (B/D)
1	$F_{1/2}$	29,491	5,253	57.7
2	F_0	27,135	4,833	53.1
3	F_1	31,928	5,687	62.5

CONCLUSIONS

The equations describing linear aquifer behavior may be reduced, by a particular definition of dimensionless time, to three working curves. These curves are appropriate for both infinite and finite aquifers of any size, for all common boundary conditions.

A single curve applies for any given set of boundary conditions. This eliminates interpolation within a family of curves, and thereby improves the speed and accuracy of calculations.

Very simple limiting forms of the equations may be used in place of the working curves at short times ($t_D \leqslant 0.25$) and at long times ($t_D \geqslant 2.5$).

ACKNOWLEDGMENTS

The authors wish to thank the management of Socony Mobil Oil Co. for permission to publish this paper.

NOMENCLATURE*

b = Width of aquifer, cm or ft
c_t = Aquifer compressibility (total), atm^{-1} or psi^{-1}
h = Thickness of aquifer, cm or ft
k = Aquifer permeability, darcies or spu**
Δp = Pressure drop, atm or psi
q = Flow rate, cc/sec or cu ft/D
t = Time, sec or days
x_e = Unit distance, cm or ft
F = Function of t_D, dimensionless
L = Length of aquifer, cm or ft
W_e = Water influx volume, cc or cu ft
μ = Viscosity, cp
ϕ = Porosity, dimensionless

SUBSCRIPTS

j = index
k = index
D = dimensionless.

★★★

*Where two units are given, the metric system appears first followed by the practical system unit.

**spu = special permeability units
$k_{spu} = 6.2832\ k_{darcies}$

where $t_D = kt / \phi \mu c_t L^2$

and L = any arbitrary distance, for the infinite system

Other comparisons are also interesting. I'll address the dimensionless equations for this purpose. Note in Nabor and Barham's Eq. 11, for the finite aquifer with the constant pressure at the outer boundary at constant rate, the pressure drop behavior fits the $F_0(t_D)$ function. In their Eq. 13, for the finite aquifer with a closed outer boundary and constant pressure inner boundary, the cumulative water influx solution uses the same $F_0(t_D)$ function. $F_0(t_D)$ is defined in Eq. 15 by Nabor and Barham.

It is not too surprising that these two cases give the same result. For the pressure drop case, their Eq. 11, after a period of time the pressure drop follows Darcy's Law, and becomes constant. For the water influx case, Eq. 13, the total water influx must be limited to a finite value due to the sealed outer boundary. The dimensionless equations are defined so that these constants are both equal to 1.00.

The $F_0(t_D)$ function can be expressed almost exactly using simple analytic solutions. Remember earlier that I pointed out that the radial system exhibits exponential decline once the outer boundary is felt. Actually, this behavior is generally found for *any* bounded system, whatever its geometry. We can use this idea to test the data or Nabor and Barham's $F_0(t_D)$ function. Using ideas similar to those in Eqs. 38c, d and e, we would expect the tabulated data would be a straight line on semi-log paper. The table on the following page lists their data from $0.18 \le t_D \le 2.80$, and evaluates $1 - F_0(t_D)$, as suggested by the equation for exponential decline. The data are graphed in Fig. 15, page 77. These data veer away from the infinite acting data; but note the important concept that the first data point in this table fits the infinite aquifer solution, Eq. 65. So these data act in the same way as the radial data we discussed earlier. At early times they fit the infinite acting equation. Then they switch immediately to exponential decline at time, $t_D = 0.18$, as Fig. 15 shows.

$F_0(t_D)$ Data for Exponential Decline Graph

t_D	$F_0(t_D)$	$1-F_0(t_D)$
0.18	0.47846	0.52154
0.20	0.50409	0.49591
0.225	0.53414	0.46586
0.25	0.56223	0.43777
0.28	0.59361	0.40639
0.31	0.62268	0.37732
0.35	0.65819	0.34181
0.40	0.69788	0.30212
0.45	0.73295	0.26705
0.50	0.76395	0.20605
0.56	0.79643	0.20357
0.60	0.82445	0.17555
0.70	0.85539	0.14461
0.80	0.88740	0.11260
0.90	0.91202	0.08798
1.00	0.93126	0.06874
1.10	0.94629	0.05371
1.25	0.96290	0.03710
1.40	0.97438	0.02562
1.60	0.98436	0.01564
1.80	0.99045	0.00955
2.00	0.99417	0.00583
2.25	0.99685	0.00315
2.50	0.99830	0.00170
2.80	0.99919	0.00081

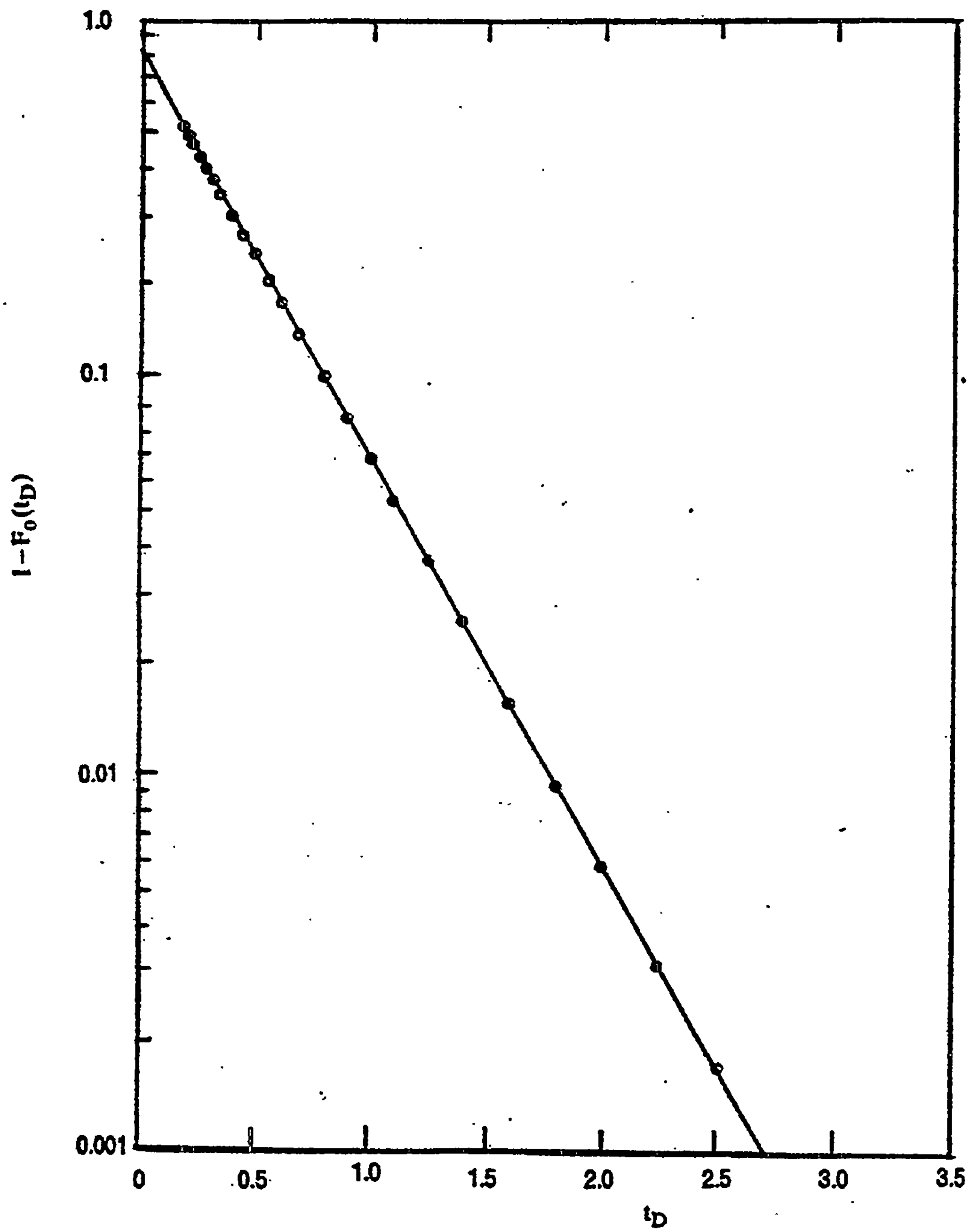

Figure 15. Exponential decline behavior for linear aquifers.

As expected, the data in Fig. 15 are a perfect straight line. So a simple equation could be used to predict the cumulative influx behavior with time. Since the pressure behavior for constant rate with a constant pressure outer boundary fit the same curve, we could also use this idea to predict the exponential pressure decline history for this case. However, there is an even easier (but somewhat less accurate) way to handle this problem, which I'll discuss next.

Notice in Nabor and Barham's Fig. 1 that, as a first approximation, the $F_0(t_D)$ curve can be treated as two straight lines. At early time $F_0(t_D)$ is proportional to the square root of t_D and is equal to $F_{1/2}(t_D)$. At late times it is 1.00. If we were to ignore the curvature and treat it as two straight lines, breaking at $t_D = \pi/4 = 0.785$, any calculations of water influx would be greatly simplified. An evaluation of this procedure shows that the maximum error occurs at $t_D = 0.785$ and it is about 12% too high. This concept was successfully used by Brigham and Neri (1979) and by Dee and Brigham (1985) using superposition calculations to simplify predictions of two geothermal systems which exhibited linear steam influx behavior.

The last two cases which fit together are the pressure drop prediction for the case with a constant rate and a sealed outer boundary, and the water influx prediction for constant pressure inner and outer boundaries. These both use the $F_1(t_D)$ equation, Nabor and Barham's Eq. 17. This behavior is also logical. With the closed outer boundary, after a period of time the system will reach pseudo-steady state and the pressure drop will become a linear function of time, just as it did for the radial system we discussed at length earlier in these notes. While, with the constant pressure boundaries, after a period of time the system reaches steady state and the cumulative water influx will rise linearly with time, also following the $F_1(t_D)$ function.

Notice in their Eq. 17, that the long time result for the $F_1(t_D)$ function is,

$$F_1(t_D) = t_D + 1/3 \tag{66}$$

This is the pseudo-steady state equation for linear systems,

$$\frac{kbh\Delta p}{q\mu L} = t_D + 1/3 \tag{67}$$

where $b =$ the width of the linear aquifer

$h =$ the height of the linear aquifer

And now all the pressure, geometric and rate terms on the left-hand side of Eq. 67 constitute the definition for p_D for linear systems.

Since a simplification of the $F_0(t_D)$ curve worked well, it seems logical that a similar approach would work for the $F_1(t_D)$ curve. To test this idea, I compared $F_1(t_D)$ for various times against the values of Eq. 66 and $F_{1/2}(t_D)$, Eq. 65, as shown on the following table.

Comparisons of $F_1(t_D)$ with Eq. 65 and Eq. 66

to Approximate $F_1(t_D)$

t_D	$F_1(t_D)$	Eq. 66 $t_D + 1/3$	Eq. 66 Error	Eq. 65 $F_{1/2}(t_D)$	Eq. 65 Error
0.225	0.536	0.558	0.022	0.535	-0.001
0.25	0.566	0.583	0.017	0.564	-0.002
0.28	0.601	0.613	0.012	0.597	-0.004
0.31	0.634	0.643	0.009	0.628	-0.006
0.35	0.677	0.683	0.006	0.668	-0.009
0.40	0.729	0.733	0.004	0.714	-0.015
0.45	0.781	0.783	0.002	0.757	-0.024
0.50	0.832	0.833	0.001	0.798	-0.034
0.56	0.893	0.893	0.000	0.844	-0.049

A comparison of the results in this table is similar to the behavior we saw earlier when looking at radial systems. At late time the pseudo-steady state assumption, Eq. 66, is valid, while at early time the infinite-acting equation (Eq. 65) is valid. The cross-over occurs at a time, t_D , between 0.31 and 0.35 with an error of about ± 0.008 or only about 1.4%. Clearly this procedure would simplify calculations one would need to make to predict influx of linear aquifers.

Superposition of Linear Systems

We've already discussed superposition in general, but let's look at it in particular for an infinite linear system. The reason is that we'll find that the integration can be handled quite easily. In general, the superposition integral can be written, as follows,

$$(W_e)_D = \int_0^{t_D} \Delta p_D\,(t_D-\tau)\frac{\partial Q_D(\tau)}{\partial \tau}d\tau \tag{58a}$$

For illustrative purposes let's assume the following relationships for pressure drop and cumulative water influx as functions of time,

$$\Delta p_D(\tau) = a\tau^2 \tag{68a}$$

$$\Delta p_D(t_D-\tau) = a(t_D-\tau)^2 \tag{68b}$$

$$Q_D(\tau) = b\tau^{1/2} \tag{69a}$$

$$\frac{\partial p_D(\tau)}{\partial \tau} = \frac{b(\tau)^{-1/2}}{2} = \frac{b}{2\tau^{1/2}} \tag{69b}$$

Equations 69a and 69b are Nabor and Barham's analytic solution for $Q_D(t_D)$ for an infinite linear system, while Eq. 68 is the arbitrary $\Delta p_D(\tau)$ function I chose to illustrate the behavior of the integrals. Substituting Eqs. 68b and 69b into Eq. 58a, we get,

$$(W_e)_D = \int_0^{t_D} \frac{a(t_D-\tau)^2 b d\tau}{2\tau^{1/2}} \tag{70a}$$

$$= \frac{ab}{2} \int_0^{t_D} \left(t_D^2 \tau^{-1/2} - 2t_D \tau^{1/2} + \tau^{3/2}\right) d\tau$$

$$= \frac{ab}{2} \left| 2t_D^2 \tau^{1/2} - \frac{4t_D \tau^{3/2}}{3} + \frac{2\tau^{5/2}}{5} \right|_0^{t_D}$$

$$(W_e)_D = \frac{8ab t_D^{\ 5/2}}{15} \tag{70b}$$

Alternatively we could look at this problem using Eq. 58d, as follows,

$$(W_e)_D = \int_0^{t_D} \frac{d\Delta p_D(t_D-\tau)}{d(t_D-\tau)} Q_D(\tau) d\tau \tag{58d}$$

with the following definitions:

$$\Delta p_D(t_D-\tau) = a(t_D-\tau)^2 \tag{68b}$$

$$\frac{\partial \Delta p_D(t_D-\tau)}{\partial(t_D-\tau)} = 2a(t_D-\tau) \tag{68c}$$

Substituting Eq. 68c and 69a into Eq. 58d, we get

$$(W_e)_D = \int_0^{t_D} 2a(t_D-\tau) b\tau^{1/2} d\tau \tag{71a}$$

$$= 2ab \left| \frac{2t_D \tau^{3/2}}{3} - \frac{2\tau^{5/2}}{5} \right|_0^{t_D}$$

$$= 2ab t_D^{5/2} \left[\frac{2(5)-2(3)}{15} \right] = \frac{8ab t_D^{5/2}}{15} \tag{71b}$$

Note that Eq. 71b is identical to Eq. 70b, just as we anticipated. Further it is clear that if the pressure history can be put into any analytic form, the water influx history can be easily calculated analytically. This concept bodes well for simplifying water influx calculations for linear systems.

Let us carry this idea further, and consider the implications of the approximations in the previous table on the F_1 function (page 79) that tell us we can use the infinite acting equation for early time data, and the pseudo-steady state equation for later time data. To do this we realize that at early times we get,

$$Q_D(\tau) = 2b(\tau / \pi)^{1/2} \tag{65}$$

While for late time we get,

$$Q_D(\tau) = b(\tau + 1/3) \tag{66}$$

To solve our equation we will again assume that the pressure drop is a quadratic,

$$\Delta p_D(t_D - \tau) = a(t_D - \tau)^2 \tag{68b}$$

$$\frac{\partial \Delta p_D(t_D - \tau)}{\partial (t_D - \tau)} = 2a(t_D - \tau) \tag{68c}$$

The superposition equations we will use for comparison are,

$$(W_e)_D = \int_0^{t_D} \frac{\partial \Delta p_D(t_D - \tau)}{\partial (t_D - \tau)} Q_D(\tau)\, d\tau \tag{58d}$$

and

$$(W_e)_D = \int_0^{t_D} \Delta p_D(t_D - \tau)\, q_D(\tau)\, d\tau \tag{58a}$$

For this purpose we will break these integrals up into two time periods as indicated by our geometry. A break occurs somewhere between $\tau = 0.31$ and 0.35. We'll look at both times for a total time, t_D , equal to an arbitrary value of 1.00. I've chosen this rather short total time purposely, for this will tend to exaggerate any differences due to the equation approximations. Thus we will get four different results, that theoretically should be identical, but which in practice we expect to differ slightly due to these approximations.

Looking at a break in time of $t_D = 0.31$, and using the definitions for $\partial \Delta p_D (t_D - \tau) / \partial (t_D - \tau)$ and for $Q_D(\tau)$, Eq. 58d becomes,

$$(W_e)_D = \int_0^{0.31} \frac{4ab(t_D - \tau)\tau^{1/2} d\tau}{\sqrt{\pi}} + \int_{0.31}^{1} 2ab(t_D - \tau)(\tau + 1/3)\, d\tau \quad (72a)$$

which, when evaluated, becomes.

$$(W_e)_D = 0.62717\, ab \quad (72b)$$

Using Eq. 58a instead, and differentiating Eqs. 65 and 66 to evaluate $q_D(\tau)$, we get,

$$(W_e)_D = \int_0^{0.31} \frac{ab(t_D - \tau)^2 \tau^{-1/2} d\tau}{\sqrt{\pi}} + \int_{0.31}^{1} ab(t_D - \tau)^2\, d\tau \quad (73a)$$

which, when evaluated, becomes,

$$(W_e)_D = 0.62000\, ab \quad (73b)$$

Notice that these two differ by only 1.16%. This is certainly within the accuracy of any field data one would normally find.

Instead if we were to break our time at $t_D = 0.35$, Eq. 72a will merely be changed by the integration limits. The resulting answer is,

$$(W_e)_D = 0.62634\, ab \quad (74)$$

Note that Eq. 74 is nearly identical to Eq. 72b. Similarly, if the integration switchover time of 0.35 is used in Eq. 73a, the result is,

$$(W_e)_D = 0.61970ab \tag{75}$$

Again note that Eq. 75 is almost identical to Eq. 73b. So it is clear that it is not the switch in integration crossover time that causes the slight differences, but rather the form of the superposition equation used. But in any case, it is also clear that these simplifications are quite adequate for the engineering accuracy required.

Spherical Geometry

As I mentioned earlier, the spherical geometry is not too commonly seen in water influx problems; but it can arise whenever there is a small oil "bubble" surrounded at the sides and bottom by a large aquifer. The enclosed paper by Chatas (1966) discusses the solution for this equation. It is far longer than it needs to be, for it could have been simplified in much the same way that Nabor and Barham simplified the linear systems.

One important point in spherical flow is the fact that the vertical permeability, k_v is often far less than the horizontal permeability, k_h . Chatas discusses this fact and his Eq. 10 is supposed to give us the correct value of average permeability, $\bar{k}$ to use when these permeabilities differ. This equation is wrong! The correct value for the average permeability is,

$$\bar{k} = \left(k_h^2 \, k_v\right)^{1/3} \tag{76}$$

To derive this equation, I used the same scaling law ideas discussed in my notes on injectivity (Brigham, 1985).

We also need to look at the transformed inner boundary that results from these scaling laws. The z direction coordinate will be elongated as a result of this transformation, while the x and y directions will be shrunk. As a result, the inner sphere will be changed into "rugby ball" shape, with the ball standing on its end, an

Unsteady Spherical Flow in Petroleum Reservoirs

A. T. CHATAS
MEMBER AIME

IRANIAN OIL EXPLORATION & PRODUCING CO.
TEHRAN, IRAN

ABSTRACT

A description of the geometrical characteristics of spherical reservoir systems, a discussion of unsteady-state flow of such systems and examples of engineering applications are presented as background material. The fundamental differential equation, a description of average spherical permeability and the introduction of the Laplace transformation serve as theoretical foundations. Engineering concepts are investigated to indicate particular solutions of interest, which are analytically obtained with the aid of the Laplace transform. These are numerically evaluated by computer, and presented in tabular form.

INTRODUCTION

A tractable mathematical analysis of unsteady fluid flow through porous media generally requires incorporation of a geometrical symmetry. The simplest forms include the linear, cylindrical (radial) and spherical. Most analytical endeavors have concentrated on cylindrical symmetry because it occurs more often in petroleum reservoirs. Nevertheless, some reservoir systems do exist that are better approximated by spherical geometry.

Review of technical literature revealed but a single reference to unsteady spherical flow in petroleum reservoirs.[1] The motive and purpose of the present work was to remove this gap in technical information, and to provide the practicing engineer with some useful analytical tools. The mathematical details associated with the particular solutions of interest involved use of the Laplace transformation. Hurst and van Everdingen previously demonstrated the efficacy of this operational technique, and in many respects the present treatment was patterned after their earlier work.[2]

PRELIMINARY CONSIDERATIONS

GEOMETRICAL CHARACTERISTICS

Geometrically, a spherical reservoir system is defined at any instant of time by two concentric hemispheres whose physical properties of interest vary only with the radial distance. Every physical property is thus restricted to be a space function of only one variable: the distance along a radius vector emanating from the center.

Such a system is composed of an outer region and an inner region, separated by a defined internal boundary. The inner region simply extends inward from this boundary, whereas the outer region extends outward from it to an external boundary. The position of the internal boundary is presumed fixed, so that the size of the inner region remains constant. On the other hand, the position of the external boundary at any given instant of time is determined by the distance into the system that a sensible pressure reaction has occurred. Thus, the external boundary may change position with time.

It initially emerges from the inner region and advances outward to its ultimate position. When this ultimate position coincides with a geometric limit, the reservoir system is said to be limited. When it coincides with points subject to pressure gradients furthest removed from the internal boundary, yet short of a geometric limit, the system is said to be unlimited. In this investigation two different boundary conditions are imposed at the ultimate boundaries of limited systems. The first requires that no fluid flow occur across this boundary; the second that the pressure remain fixed at this boundary.[3-5]

UNSTEADY-STATE FLOW

In a strict sense virtually all flow phenomena associated with a reservoir system are unsteady-state. The transient behavior of these phenomena requires accounting, however, only when time must be introduced as an explicit variable. Otherwise, steady-state mechanics may be used. Analytically, steady-state conditions prevail in a reservoir system only over that portion of its history when this relation is satisfied:

$$\frac{\phi c \mu}{k}\frac{\partial p}{\partial t} \doteq 0 \quad \ldots \ldots \ldots \ldots \ldots (1)$$

But to do this, a reservoir system must contain either an ideal fluid, which implies a vanishing viscosity, or an incompressible fluid, which

Original manuscript received in Society of Petroleum Engineers office Sept. 27, 1965. Revised manuscript of SPE 1305 received April 5, 1966.

[1]References given at end of paper.

implies a vanishing compressibility; or it must have pressures fixed with time such that the time-derivative vanishes. Evidently, strict steady-state conditions are virtually impossible to attain, since these provisions are abstractions of the mind and not properties of physical systems. From a practical standpoint, however, this fact does not exclude application of steady-state mechanics, because in many situations Eq. 1 is closely approximated.[3-5]

The significant physical properties that determine the extent of transient behavior in spherical reservoir systems are exhibited by the so-called readjustment time which is approximated by:

$$t_r = \frac{\phi c r_e^2}{2k/\mu} \quad . . . . (2)$$

These factors are the size of the system, its compressibility and its mobility. When they combine to yield a large readjustment time, unsteady-state mechanics should be used unless pressures are invariant.[3,5]

ENGINEERING APPLICATIONS

When a water drive field is characterized by bottom-water encroachment, the hydrocarbon accumulation usually fills only a portion of the total thickness of the reservoir formation and is entirely underlain by water. Flow of water into the pay zone results from a gradual and uniform rise of the underlying water.

Of particular interest to the reservoir engineer are methods, formally independent of material balance principles, for determining the water influx into bottom-water drive fields. First, these methods afford determination of a number of reservoir properties through an analysis of the past reservoir history by an adjunctive use with other relations. Secondly, by independently yielding the water influx they provide means of predicting future reservoir performance. Many bottom-water drive fields lend themselves to the imposition of spherical geometry; hence, solutions of the fundamental flow equations appropriate to this symmetry can be used to analytically determine the water influx for this class of reservoir.[4,6]

Although many wells are completed after the drill has passed entirely through the pay formation, some are purposely completed after only partial penetration has been effected. Sometimes such wells are completed after the top surface of the reservoir is merely tapped by the drill, in which case they are termed non-penetrating wells.

Non-penetrating wells that occur in a relatively thick formation can be treated as spherical systems. They can be analytically investigated by using appropriate solutions of the fundamental flow equations corresponding to spherical symmetry. These investigations include flow calculations, analysis of drawdown and build-up tests, determination of static bottom-hole pressure, productivity indices, effective permeabilities and evaluation of damaged sand conditions. Also, although the analytical solutions strictly apply only to the single-phase flow of compressible liquids, the results can sometimes be used (with proper interpretation) the flow of gases when pressure drops are small, and to the simultaneous flow of oil and gas upon imposition of drastic assumptions.[3,4,7]

THEORETICAL CONSIDERATIONS

FUNDAMENTAL DIFFERENTIAL EQUATION

The fundamental differential equation governing the dynamics of the flow of compressible liquids through spherical reservoir systems can be written as:

$$\frac{\partial^2 p}{\partial r^2} + \frac{2}{r}\frac{\partial p}{\partial r} = \frac{\phi c \mu}{k}\frac{\partial p}{\partial t}, \quad . . . . (3)$$

where the porosity, compressibility and mobility are interpreted as fixed averages, and where the effects of gravity are neglected. Define a dimensionless length ratio, time ratio and pressure-drop ratio, respectively, as follows:

$$r_D = \frac{r}{r_w} \quad . . . . (4)$$

$$t_D = \frac{kt}{\phi \mu c r_w^2} \quad . . . . (5)$$

$$p_D = p_D(r_D, t_D) = \frac{p_i - p(r_D, t_D)}{p_i - p(1, t'_D)} \quad . . . . . (6)$$

Introduction of these relations into Eq. 3 permits it to be rewritten as:

$$\frac{\partial^2 p_D}{\partial r_D^2} + \frac{2}{r_D}\frac{\partial p_D}{\partial r_D} = \frac{\partial p_D}{\partial t_D}, \quad . . . . (7)$$

which represents the fundamental differential equation in dimensionless form appropriate to reservoir systems characterized by spherical symmetry.[2-5,8]

AVERAGE SPHERICAL PERMEABILITY

Available evidence indicates that the permeability of porous media constituting reservoir systems is not isotropic in character. As a rule the vertical permeability is less than the horizontal, and in some instances the difference is profound. Since spherical symmetry embraces a three-dimensional geometric space, it was felt necessary to include the effects of this anistropy here. The radial permeability in a spherical porous medium characterized by uniform vertical and horizontal permeability components can be analytically described by:

$$\frac{1}{k_r} = \frac{1}{k_h}\sin^2\alpha + \frac{1}{k_v}\cos^2\alpha \quad . . . . (8)$$

The average spherical permeability can then be obtained with the volume integral:

$$\bar{k}_r = k = \frac{(2/3)\,\pi(r_e^3 - r_w^3)}{\int_0^{\pi}\int_0^{\pi}\int_{r_w}^{r_e} \frac{r^2}{k_r}\sin\alpha\, dr\, d\alpha\, d\theta} \quad . \; . \; . \; . \; (9)$$

which, upon evaluation, gives:

$$k = \frac{3k_h k_v}{k_h + 2k_v}, \quad . \; . \; . \; . \; . \; . \; . \; . \; . \; . \; . \; (10)$$

the average spherical permeability.

APPLICATION OF THE LAPLACE TRANSFORMATION

The fundamental differential equation for a spherical reservoir system has been expressed in dimensionless form by Eq. 7. Define the product:

$$b = r_D p_D \quad . \; . \; . \; . \; . \; . \; . \; . \; . \; . \; . \; . \; . \; . \; . \; . \; (11)$$

Then Eq. 7 can be written in the alternative form:

$$\frac{\partial^2 b}{\partial r_D^2} = \frac{\partial b}{\partial t_D} \quad . \; . \; . \; . \; . \; . \; . \; . \; . \; . \; . \; . \; . \; . \; (12)$$

The Laplace transform of b is given by the definite integral:

$$\bar{b} = \int_0^{\infty} b \exp(-s t_D)\, dt_D \quad . \; . \; . \; . \; . \; . \; . \; . \; (13)$$

Multiplication by the nucleus of the transform and integration over all time converts Eq. 12 from a partial to the ordinary differential equation:

$$\frac{d^2 \bar{b}}{dr_D^2} = s\bar{b}. \quad . \; . \; . \; . \; . \; . \; . \; . \; . \; . \; . \; . \; . \; . \; . \; (14)$$

The general solution of this subsidiary equation can be written at once:

$$\bar{b} = C_1 \exp(-r_D\sqrt{s}) + C_2 \exp(r_D\sqrt{s}) \;, \quad . \; . \; . \; (15)$$

where C_n is an arbitrary constant.[2,9-11]

Particular solutions to the subsidiary equation corresponding to specifically imposed boundary conditions are obtained upon appropriate evaluation of the constants that appear in its general solution. These particular solutions would represent the Laplace transforms of the required particular solutions to Eq. 12. The latter are determined by effecting the inverse transformations of their Laplace transforms. This procedure will be used to develop the particular solutions of interest.

SELECTION OF PARTICULAR SOLUTIONS

Reduction of Eq. 3 to the dimensionless form depicted by Eq. 7 was effected, because the complete dimensionlessness of Eq. 7 renders the numerical values associated with its particular solutions entirely independent of the actual magnitudes of the physical properties of any given reservoir system. But due to the generality introduced, it becomes necessary to relate certain physical quantities associated with absolute units of measurement to functions of the dimensionless variables in Eq. 7.[2,5]

The macroscopic radial velocity at the internal boundary of a spherical reservoir system is given by Darcy's law:[2-4]

$$u = -\frac{k}{\mu}\left(\frac{\partial p}{\partial r}\right)_{r_w}. \quad . \; . \; . \; . \; . \; . \; . \; . \; . \; . \; . \; . \; (16)$$

Introduction of the relations defined by Eqs. 4 through 6 yields:

$$u = \frac{k}{\mu r_w}\,\Delta p(r_w, t')\left(\frac{\partial p_D}{\partial r_D}\right)_1, \quad . \; . \; . \; . \; . \; . \; . \; (17)$$

which relates the actual velocity with the dimensionless function $(\partial p_D/\partial r_D)_1$. The rate of fluid influx at the internal boundary is given by:[3,4]

$$e = -\int_0^{\pi}\int_0^{\pi} r^2 u \sin\alpha\, d\alpha\, d\theta = 2\pi r_w^2 \frac{k}{\mu}\left(\frac{\partial p}{\partial r}\right)_{r_w} \quad . \; . \; . \; . \; . \; . \; . \; . \; . \; . \; . \; . \; . \; . \; . \; . \; (18)$$

Then, introduction of Eqs. 4 through 6 yields:

$$e = -2\pi r_w \frac{k}{\mu}\,\Delta p(r_w, t')\left(\frac{\partial p_D}{\partial r_D}\right)_1, \quad . \; . \; . \; . \; (19)$$

which relates the actual fluid influx rate with the dimensionless function $-(\partial p_D/\partial r_D)_1$.

The cumulative fluid influx at the internal boundary up to any time t is given by:[2]

$$F = \int_0^t e\, dt = 2\pi r_w^2 \frac{k}{\mu}\int_0^t \left(\frac{\partial p}{\partial r}\right)_{r_w} dt \quad . \; . \; . \; . \; (20)$$

Similarly, introduction of Eqs. 4 through 6 yields:

$$F = -2\pi\phi c r_w^3\,\Delta p(r_w, t')\int_0^{t_D}\left(\frac{\partial p_D}{\partial r_D}\right)_1 dt_D \quad . \; . \; . \; (21)$$

which relates the actual cumulative fluid influx with the time integral of the dimensionless function $-(\partial p_D/\partial r_D)_1$. Upon proper interpretation, Eqs. 17, 19 and 21 can be used to determine the fluid flow and pressure behavior in a spherical reservoir system, and also to indicate the appropriate choice of particular solutions to Eq. 7. Two distinct cases arise: the so-called pressure and rate cases.[2,5]

The Pressure Case

The pressure case presumes knowledge of the pressure conditions at the internal boundary of a reservoir system and permits determination of the fluid flow behavior. Consider a spherical reservoir system characterized by dimensionless properties. Let this system be charged to a unit dimensionless pressure, and at zero time let the pressure at the internal boundary vanish and remain zero. This condition represents the distinctive feature of the pressure case. The problem then remains to determine the dimensionless rate and cumulative fluid influx at the internal boundary as functions of dimensionless time. This dimensionless description of the fluid flow behavior and its translation into absolute units of measurement constitutes the pressure case.[2,5]

Under the precepts of the pressure case, the dimensionless fluid influx rate is defined by:

$$e_D = e_D(1, t_D) = -\left(\frac{\partial p_D}{\partial r_D}\right)_1 , \quad \ldots \ldots \ldots (22)$$

and the dimensionless cumulative fluid influx by:

$$F_D = F_D(1, t_D) = -\int_0^{t_D} \left(\frac{\partial p_D}{\partial r_D}\right)_1 dt_D \quad \ldots \ldots (23)$$

Symbolically, the actual velocity, rate and cumulative fluid influx may now be expressed in terms of e_D and F_D as follows:

$$u = u(r_w, t) = -\frac{k}{\mu r_w} \Delta p(r_w, 0)\, e_D(1, t_D). \quad . (24)$$

$$e = e(r_w, t) = 2\pi r_w \frac{k}{\mu} \Delta p(r_w, 0)\, e_D(1, t_D). \quad . (25)$$

$$F = F(r_w, t) = 2\pi \phi c r_w^3 \Delta p(r_w, 0) F_D(1, t_D). \quad . (26)$$

Eqs. 24 through 26 express the facets of fluid flow behavior in terms of field data and the *dimensionless* functions e_D and F_D. By application of the superposition principle (Duhamel's theorem) these functions can also be used to treat *time-varying* pressure histories.

The Rate Case

The rate case presumes knowledge of the fluid flow conditions at the internal boundary and permits determination of the pressure behavior. Consider a dimensionless spherical reservoir system charged to a unit dimensionless pressure, and from zero-time onward let a unit dimensionless fluid influx rate be imposed. This condition, which expressed analytically is:

$$-\left(\frac{\partial p_D}{\partial r_D}\right)_1 = 1 , \quad \ldots \ldots \ldots \ldots (27)$$

for all time t_D, represents the distinctive feature of the rate case. The problem here is to determine the dimensionless pressure drop distribution in the system, and the pressure drop at the internal boundary under the conditions prescribed by Eq. 27. This dimensionless description of pressure behavior and its translation into absolute units of measurement constitutes the rate case.[2,5]

Under the precepts of the rate case, the actual pressure distribution in the system is given by:

$$p(r,t) = p_i - \frac{e\mu}{2\pi k r_w} p_D(r_D, t_D). \quad \ldots \ldots (28)$$

Similarly, the actual pressure at the internal boundary is given by:

$$p = p(r_w, t) = p_i - \frac{e\mu}{2\pi k r_w} p_D(1, t_D) \quad \ldots (29)$$

These symbolic relations express the pressure behavior in terms of field data and the dimensionless functions $p_D(r_D, t_D)$ and $p_D(1, t_D)$. Likewise, by application of the superposition principle, these functions can be used to treat time-varying rate histories.

DESCRIPTION OF PARTICULAR SOLUTIONS

UNLIMITED SYSTEM

By definition the external boundary of an unlimited system continuously recedes from the internal boundary without reaching a geometric limit. Under these conditions the product $r_D p_D$ vanishes and Eq. 15 becomes:

$$\bar{b} = C_1 \exp(-r_D\sqrt{s}). \quad \ldots \ldots \ldots \ldots (30)$$

The precepts of the pressure case require that a dimensionless pressure drop of unity be maintained at the internal boundary, and since the Laplace transform of unity is $1/s$, it follows that:

$$\bar{b} = \frac{1}{s} \exp\left[-\sqrt{s}\,(r_D - 1)\right] , \quad \ldots \ldots \ldots (31)$$

which is the subsidiary equation appropriate to the pressure case for an unlimited system. The dimensionless fluid influx rate e_D can be rewritten in terms of b:

$$e_D = -\left(\frac{\partial p_D}{\partial r_D}\right)_1 = -\left(\frac{\partial b}{\partial r_D} - b\right)_1 \quad \ldots \ldots (32)$$

Then the Laplace transfom of e_D, utilizing Eqs. 31 and 32, is:

$$\bar{e}_D = \frac{1}{\sqrt{s}} + \frac{1}{s} , \quad \ldots \ldots \ldots \ldots \ldots (33)$$

whose inverse transformation can be written at once as:

$$e_D = 1 + (\pi t_D)^{-1/2}, \quad \ldots \ldots \ldots \ldots (34)$$

rate

which is the dimensionless fluid influx rate of an unlimited system. The Laplace transform of F_D (dimensionless cumulative fluid influx) is simply:

$$\bar{F}_D = \frac{\bar{e}_D}{s} = \frac{1}{s^{3/2}} + \frac{1}{s^2} \quad \ldots \ldots \ldots (35)$$

whose inverse transformation can likewise be written at once as:

$$F_D = t_D + 2\left(\frac{t_D}{\pi}\right)^{1/2}, \quad \ldots\ldots\ldots\ldots (36)$$

CUMULATIVE INFLUX

which is the dimensionless cumulative fluid influx of an unlimited system.[9,11,13,14]

The precepts of the rate case require that a dimensionless rate of unity be maintained at the internal boundary, which can be written in terms of b as:

$$-\left(\frac{\partial p_D}{\partial r_D}\right)_1 = -\left(\frac{\partial b}{\partial r_D} - b\right)_1 = 1 \quad \ldots\ldots (37)$$

Using Eq. 30 it follows that:

$$b = \frac{\exp\left[-\sqrt{s}\,(r_D - 1)\right]}{s\,(1 + \sqrt{s})}, \quad \ldots\ldots\ldots (38)$$

which is the subsidiary equation appropriate to the rate case for an unlimited system. The inverse transformation is available from integral transform tables. This result divided by r_D yields:

$$p_D(r_D, t_D) = \frac{1}{r_D}\left[\operatorname{erfc}\left(\frac{r_D - 1}{2\sqrt{t_D}}\right) - \exp(t_D + r_D - 1)\,\operatorname{erfc}\left(\frac{r_D - 1}{2\sqrt{t_D}} + \sqrt{t_D}\right)\right], \quad \ldots (39)$$

which is the dimensionless pressure-drop distribution of an unlimited system. Upon placing r_D at unity, Eq. 39 reduces to:

$$p_D = 1 - \exp(t_D)\,\operatorname{erfc}(t_D^{1/2}), \quad \ldots\ldots\ldots (40)$$

PRESSURE DROP

which is the dimensionless pressure drop at the internal boundary of an unlimited system.[2,9,11,13,14]

At this juncture some significant observations can be made. First, the least upper bound of the dimensionless pressure drop is unity. Consequently, under the conditions of constant rate the pressure drop at the internal boundary of an unlimited spherical system can never exceed a fixed finite value. Secondly, the greatest lower bound of the dimensionless rate is also unity. Hence, the rate engendered by a single pressure drop imposed at zero time at the internal boundary of an unlimited spherical system can never be less than a fixed non-vanishing value. In either situation, it appears that an unlimited spherical reservoir system approaches steady-state conditions as dimensionless time assumes excessively large values. This property, strangely enough, is not enjoyed by unlimited linear or cylindrical (radial) systems.[2,5]

LIMITED SYSTEM WITH CLOSED EXTERNAL BOUNDARY

In a limited reservoir system the external boundary eventually coincides with a geometric limit. At this limit, a system with a closed external boundary can sustain no fluid flow across it. Hence, the normal pressure derivative there must vanish. Introduction of this condition into Eq. 15 gives:

$$\bar{b} = C_1\left[\exp(-r_D\sqrt{s}) + \left(\frac{r_D'\sqrt{s}+1}{r_D'\sqrt{s}-1}\right)\exp\sqrt{s}\,(r_D - 2r_D')\right] \quad \ldots\ldots (41)$$

Under the precepts of the pressure case and by subsequent conversion to hyperbolic functions, Eq. 41 becomes:

$$\bar{b} = \frac{\sinh[\sqrt{s}(r_D' - r_D)] - \sqrt{s}\,r_D'\cosh[\sqrt{s}(r_D' - r_D)]}{s\{\sinh[\sqrt{s}(r_D' - 1)] - \sqrt{s}\,r_D'\cosh[\sqrt{s}(r_D' - 1)]\}}, \quad \ldots\ldots (42)$$

which is the subsidiary equation appropriate to the pressure case for a closed limited system. The Laplace transform of e_D, using Eqs. 32 and 42, is:

$$\bar{e}_D = \frac{\sqrt{s}(r_D' - 1)\cosh[\sqrt{s}(r_D' - 1)] + (s r_D' - 1)\sinh[\sqrt{s}(r_D' - 1)]}{s\{\sqrt{s}\,r_D'\cosh[\sqrt{s}(r_D' - 1)] - \sinh[\sqrt{s}(r_D' - 1)]\}} \quad \ldots\ldots (43)$$

The inverse transformation of the relation may be obtained with the aid of Mellin's inversion theorem, and is given by the following integral in the complex plane:

$$e_D = \frac{1}{2\pi i}\lim_{\delta\to\infty}\int_{\gamma - i\delta}^{\gamma + i\delta}\exp(z t_D)\,\bar{e}_D\,dz, \quad \ldots (44)$$

which for the function at hand may be evaluated by converting it to a closed contour integral and then applying the calculus of residues. Thus, by virtue of Cauchy's integral formula:

$$\frac{1}{2\pi i}\lim_{\delta\to\infty}\int_{\gamma - i\delta}^{\gamma + i\delta} e^{z t_D}\bar{e}_D\,dz = \frac{1}{2\pi i}\int_c e^{z t_D}\bar{e}_D\,dz = R_0 + \sum_{n=1}^{\infty} R_n, \quad \ldots (45)$$

where R_0 is the residue corresponding to the singularity at the origin and R_n the residues corresponding to the other singular points. Evaluation of Eq. 45 yields the dimensionless fluid influx rate for a closed limited spherical system, as follows:

$$e_D = \frac{2}{(r_D' - 1)}\sum_{n=1}^{\infty}\frac{w_n^2 r_D'^2 + (r_D' - 1)^2}{w_n^2 r_D'^2 - (r_D' - 1)}\exp\left[-\frac{w_n^2 t_D}{(r_D'^2 - 1)}\right], \quad \ldots\ldots (46)$$

where w_n are the roots of the equation:

$$\frac{\tan w}{w} = \frac{r_D'}{(r_D' - 1)} \quad \ldots\ldots\ldots (47)$$

The Laplace transform of F_D is:

$$\bar{F}_D = \frac{\bar{e}_D}{s} = \frac{\sqrt{s}(r_D'-1)\cosh\sqrt{s}(r_D'-1) + (sr_D'-1)\sinh\sqrt{s}(r_D'-1)}{s^2[\sqrt{s}\,r_D'\cosh\sqrt{s}\,(r_D'-1) - \sinh\sqrt{s}\,(r_D'-1)]} \quad \ldots \ldots (48)$$

By virtue of previous arguments, the inverse transformation of Eq. 48 yields the dimensionless cumulative fluid influx for a closed limited system:

$$F_D = R_0 + \sum_{n=1}^{\infty} R_n = \frac{1}{3}(r_D'^3-1) - 2(r_D'-1)\sum_{n=1}^{\infty}\frac{1}{w_n^2}\left[\frac{w_n^2 r_D' + (r_D'-1)^2}{w_n^2 r_D' - (r_D'-1)}\right] e^{-\frac{w_n^2 t_D}{(r_D'-1)^2}}, \quad \ldots \ldots (49)$$

where w_n are also the roots of Eq. 47.[2,10,11,13-18]

Under the precepts of the rate case, Eq. 41 becomes, upon conversion to hyperbolic functions:

$$\bar{b} = \frac{\sqrt{s}\,r_D'\cosh\sqrt{s}\,(r_D'-r_D) - \sinh\sqrt{s}\,(r_D'-r_D)}{s[\sqrt{s}(r_D'-1)\cosh\sqrt{s}(r_D'-1) + (sr_D'-1)\sinh\sqrt{s}(r_D'-1)]}, \quad \ldots \ldots (50)$$

which is the subsidiary equation appropriate to the rate case for a closed limited system. As before, the inverse transformation of Eq. 50 is given by the sum of the residues, and since b is $r_D p_D$, there follows:

TABLE 1 — UNLIMITED SYSTEM

Dimensionless Time (t_D)	Dimensionless Rate (e_D)	Dimensionless Influx (F_D)	Dimensionless Pressure-Drop (p_D)	Dimensionless Time (t_D)	Dimensionless Rate (e_D)	Dimensionless Influx (F_D)	Dimensionless Pressure-Drop (p_D)
0.001	18.84124	0.03668	0.03471	60.0	1.07284	68.7	0.92595
0.002	13.61566	0.05246	0.04853	70.0	1.06743	79.4	0.93103
0.003	11.30065	0.06480	0.05892	80.0	1.06308	90.1	0.93512
0.004	9.92062	0.07536	0.06755	90.0	1.05947	100.7	0.93851
0.005	8.97885	0.08479	0.07504	100.0	1.05642	111.0	0.94139
0.006	8.28366	0.09340	0.08174	200.0	1.03989	216.0	0.95703
0.007	7.74336	0.10141	0.08782	300.0	1.03257	320.0	0.96408
0.008	7.30783	0.10893	0.09343	400.0	1.02821	423.0	0.96835
0.009	6.94708	0.11606	0.09865	500.0	1.02523	525.0	0.97131
0.01	6.64190	0.12284	0.10354	600.0	1.02303	628.0	0.97352
0.02	4.98942	0.17958	0.14152	700.0	1.02132	730.0	0.97526
0.03	4.25735	0.22544	0.16894	800.0	1.01995	832.0	0.97668
0.04	3.82095	0.26568	0.19098	900.0	1.01881	934.0	0.97787
0.05	3.52313	0.30231	0.20962	1,000.0	1.01784	1,036.0	0.97888
0.06	3.30329	0.33640	0.22588	2,000.0	1.01262	2,050.0	0.98453
0.07	3.13244	0.36854	0.24036	3,000.0	1.01030	3,062.0	0.98714
0.08	2.99471	0.39915	0.25345	4,000.0	1.00892	4,071.0	0.98874
0.09	2.88063	0.42851	0.26540	5,000.0	1.00798	5,080.0	0.98984
0.10	2.78412	0.45682	0.27642	6,000.0	1.00728	6,087.0	0.99067
0.20	2.26157	0.70463	0.35621	7,000.0	1.00674	7,094.0	0.99132
0.30	2.03006	0.91804	0.40798	8,000.0	1.00631	8,101.0	0.99185
0.40	1.89206	1.11365	0.44639	9,000.0	1.00595	9,107.0	0.99229
0.50	1.79788	1.29788	0.47684	10,000.0	1.00564	10,113.0	0.99267
0.60	1.72837	1.47404	0.50198	20,000.0	1.00399	20,160.0	0.99473
0.70	1.67434	1.64407	0.52330	30,000.0	1.00326	30,195.0	0.99566
0.80	1.63078	1.80925	0.54175	40,000.0	1.00282	40,226.0	0.99623
0.90	1.59471	1.97047	0.55798	50,000.0	1.00252	50,252.0	0.99662
1.0	1.56419	2.12830	0.57242	60,000.0	1.00230	60,276.0	0.99690
2.0	1.39894	3.59577	0.66380	70,000.0	1.00213	70,299.0	0.99713
3.0	1.32574	4.95441	0.71266	80,000.0	1.00199	80,319.0	0.99731
4.0	1.28209	6.25676	0.74460	90,000.0	1.00188	90,339.0	0.99746
5.0	1.25231	7.52313	0.76765	100,000.0	1.00178	100,357.0	0.99759
6.0	1.23033	8.76395	0.78534	200,000.0	1.00126	200,505.0	0.99829
7.0	1.21324	9.98541	0.79946	300,000.0	1.00103	300,618.0	0.99860
8.0	1.19947	11.19154	0.81109	400,000.0	1.00089	400,714.0	0.99878
9.0	1.18006	12.38514	0.82088	500,000.0	1.00080	500,798.0	0.99891
10.0	1.17841	13.56825	0.82927	600,000.0	1.00073	600,874.0	0.99900
20.0	1.12616	25.04626	0.87624	700,000.0	1.00067	700,944.0	0.99908
30.0	1.10301	36.18039	0.89770	800,000.0	1.00063	801,009.0	0.99914
40.0	1.08921	47.13650	0.91060	900,000.0	1.00059	901,070.0	0.99919
50.0	1.07979	57.97885	0.91943	1,000,000.0	1.00056	1,001,128.0	0.99923

$$p(r_D,t_D) =$$

$$\frac{[3r_D' + (r_D'-1)^2]\left[\frac{1}{6}(r_D'-r_D)^2(2r_D'+r_D)+r_D t_D\right] - \frac{1}{2}(r_D'-1)^2\left[\frac{1}{5}(r_D'-1)^2+r_D'\right]r_D}{(r_D'-1)\left[\frac{1}{5}(r_D'-1)^4+2r_D'(r_D'-1)^2+3r_D'^2\right]r_D}$$

$$-\frac{2(r_D'-1)^2}{r_D}\sum_{n=1}^{\infty}$$

$$\times\frac{\left[\frac{r_D' w_n}{r_D'-1}\cos\left(w_n\frac{r_D'-r_D}{r_D'-1}\right)-\sin\left(w_n\frac{r_D'-r_D}{r_D'-1}\right)\right]e^{-\frac{w_n^2 t_D}{(r_D'-1)^2}}}{w_n^2(w_n r_D'\cos w_n+(r_D'^2+1)\sin w_n)},$$

$$\ldots\ldots\ldots\ldots\ldots\ldots\ldots\ldots (51)$$

where w_n are here the roots of:

$$\frac{ctn\,w}{w}-\frac{1}{w^2}=\frac{r_D'}{(r_D'-1)^2}\ldots\ldots\ldots\ldots (52)$$

The expression embodied by Eq. 51 represents the dimensionless pressure-drop distribution for a closed limited spherical system. Upon placing r_D at unity and simplifying, there follows at once the dimensionless pressure-drop at the internal boundary:

$$p_D =$$

$$\frac{[(r_D'-1)^2+3r_D']\left[\frac{1}{6}\left(r_D'-1\right)^2(2r_D'+1)+t_D\right] - \frac{1}{2}(r_D'-1)^2\left[\frac{1}{5}(r_D'-1)^2+r_D'\right]}{(r_D'-1)\left[\frac{1}{3}(r_D'-1)^4+2(r_D'-1)^2 r_D'+3r_D'^2\right]}$$

$$-2(r_D'-1)\sum_{n=1}^{\infty}\frac{[w_n^2 r_D'^2+(r_D'-1)^2]}{w_n^2[w_n^2 r_D'^2+(r_D'^2+r_D'+1)(r_D'-1)^2]}$$

$$\times e^{-\frac{w_n^2 t_D}{(r_D'-1)^2}},\ \ldots\ldots\ldots\ldots\ldots (53)$$

where w_n are still the roots of Eq. 52.

LIMITED SYSTEM WITH OPEN EXTERNAL BOUNDARY

It will be recalled that a limited reservoir system is characterized by the arrestment of growth of the external boundary when the latter coincides with the geometric limit of the system. For the case of an open boundary it is presumed that at this limit (r_D') the system suffers no pressure drop. Introduction of this condition into Eq. 15 gives:

$$\bar{b}=C_1[\exp(-r_D\sqrt{s})-\exp(r_D-2r_D')\sqrt{s}]\quad\ldots (54)$$

Under the precepts of the pressure case and conversion to hyperbolic functions, Eq. 54 becomes:

$$\bar{b}=\frac{\sinh\sqrt{s}\,(r_D'-r_D)}{s\,[\sinh\sqrt{s}\,(r_D'-1)]},\ \ldots\ldots\ldots (55)$$

which is the subsidiary equation appropriate to the pressure case for an open limited system. The Laplace transform of e_D using Eq. 55, is:

$$\bar{e}_D=\frac{1}{s}+\frac{\cosh\sqrt{s}\,(r_D'-1)}{\sqrt{s}\,[\sinh\sqrt{s}\,(r_D'-1)]}\ \ldots\ldots (56)$$

The inverse transformation is available from integral tables in the form:

$$e_D=1+\frac{1}{(r_D'-1)}\,\theta_4\left[\frac{1}{2}\middle|\frac{i\pi t_D}{(r_D'-1)^2}\right],\ \ldots (57)$$

and upon expanding the Theta function this becomes:

$$e_D=\frac{r_D'}{r_D'-1}+\frac{2}{r_D'-1}\sum_{n=1}^{\infty}\exp\left[-\frac{\pi^2 n^2 t_D}{(r_D'-1)^2}\right],\ \ldots (58)$$

which is the dimensionless rate for an open limited system. As before, the Laplace transforms of F_D is:

$$\bar{F}_D=\frac{\bar{e}_D}{s}=\frac{1}{s^2}+\frac{\cosh\sqrt{s}\,(r_D'-1)}{s^{3/2}\,[\sinh\sqrt{s}\,(r_D'-1)]},\ \ldots (59)$$

whose inverse transformation was obtained with the aid of the Faltung convolution theorem as:

$$F_D=\frac{r_D' t_D}{r_D'-1}+\frac{1}{3}(r_D'-1)$$

$$-\frac{2(r_D'-1)}{\pi^2}\sum_{n=1}^{\infty}\frac{1}{n^2}\exp\left[-\frac{\pi^2 n^2 t_D}{(r_D'-1)^2}\right],\ \ldots (60)$$

the dimensionless cumulative fluid influx for an open limited system.[9-11,13-20]

Under the precepts of the rate case, Eq. 54 becomes:

$$\bar{b}=\frac{\sinh\sqrt{s}\,(r_D'-r_D)}{s[\sqrt{s}\cosh\sqrt{s}\,(r_D'-1)+\sinh\sqrt{s}\,(r_D'-1)]},\ \ldots (61)$$

which is the subsidiary equation appropriate to the rate case for a limited system with a fixed pressure at the external boundary. The inverse transformation of Eq. 61 was again obtained by Mellin's inversion theorem, as previously explained. Thus, the pressure-drop distribution is given by:

TABLE 2 — LIMITED SYSTEMS
Closed External Boundary

Time (t_D)	Rate (q_D)	Influx (F_D)	Pressure Drop (p_D)
Dimensionless External Radius $r_D' = 2$			
0.07	3.1324	0.3685	0.2404
0.08	2.9947	0.3992	0.2534
0.09	2.8806	0.4285	0.2654
0.10	2.7839	0.4568	0.2764
0.20	2.2411	0.7040	0.3567
0.30	1.9342	0.9120	0.4120
0.40	1.6858	1.0927	0.4591
0.50	1.4713	1.2503	0.5033
0.60	1.2844	1.3879	0.5467
0.70	1.1212	1.5080	0.5897
0.80	0.9788	1.6128	0.6326
0.90	0.8544	1.7044	0.6755
1.0	0.7459	1.7843	0.7184
2.0	0.1916	2.1921	1.1469
3.0	0.0491	2.2970	1.5755
4.0	0.0127	2.3240	2.0041
5.0	0.0033	2.3309	2.4327
6.0	0.0008	2.3327	2.8612
7.0	0.0002	2.3332	3.2898
8.0	0.0001	2.3333	3.7184
9.0	0.0000	2.3333	4.1469
10.0	0.0000	2.3333	4.5755
Dimensionless External Radius $r_D' = 3$			
0.2	2.2616	0.7046	0.3562
0.3	2.0301	0.9180	0.4080
0.4	1.8920	1.1136	0.4464
0.5	1.7972	1.2978	0.4769
0.6	1.7261	1.4739	0.5021
0.7	1.6688	1.6435	0.5236
0.8	1.6199	1.8079	0.5425
0.9	1.5764	1.9677	0.5595
1.0	1.5363	2.1233	0.5750
2.0	1.2114	3.4891	0.7012
3.0	0.9586	4.5692	0.8171
4.0	0.7586	5.4239	0.9325
5.0	0.6004	6.1004	1.0479
6.0	0.4751	6.6356	1.1633
7.0	0.3760	7.0591	1.2787
8.0	0.2975	7.3944	1.3941
9.0	0.2354	7.6598	1.5095
10.0	0.1863	7.8698	1.6249
20.0	0.0180	8.5899	2.7787
30.0	0.0017	8.6593	3.9325
40.0	0.0002	8.6659	5.0864
50.0	0.0000	8.6666	6.2402
60.0	0.0000	8.6667	7.3941
Dimensionless External Radius $r_D' = 4$			
0.7	1.6743	1.644	0.5233
0.8	1.6308	1.809	0.5418
0.9	1.5946	1.970	0.5580
1.0	1.5640	2.128	0.5724
2.0	1.3869	3.592	0.6655
3.0	1.2755	4.921	0.7234
4.0	1.1780	6.147	0.7734
5.0	1.0878	7.279	0.8216
6.0	1.0049	8.325	0.8693
7.0	0.9283	9.291	0.9170
8.0	0.8576	10.184	0.9646
9.0	0.7922	11.008	1.0122
10.0	0.7318	11.770	1.0599
20.0	0.3311	16.822	1.5361
30.0	0.1498	19.110	2.0122
40.0	0.0678	20.144	2.4884
50.0	0.0307	20.613	2.9646
60.0	0.0139	20.825	3.4408
70.0	0.0063	20.921	3.9170
80.0	0.0028	20.964	4.3932
90.0	0.0013	20.984	4.8694
100.0	0.0006	20.993	5.3456
200.0	0.0000	21.000	10.1076
Dimensionless External Radius $r_D' = 5$			
1.0	1.5642	2.128	0.5724
2.0	1.3986	3.596	0.6638
3.0	1.3216	4.953	0.7133
4.0	1.2673	6.246	0.7479
5.0	1.2203	7.490	0.7764
6.0	1.1766	8.688	0.8024
7.0	1.1348	9.843	0.8273
8.0	1.0946	10.958	0.8518
9.0	1.0558	12.033	0.8761
10.0	1.0184	13.070	0.9004
20.0	0.7103	21.621	1.1424
30.0	0.4954	27.885	1.3843
40.0	0.3455	31.744	1.6262
50.0	0.2410	34.646	1.8682
60.0	0.1680	36.669	2.1101
70.0	0.1172	38.080	2.3520
80.0	0.0818	39.064	2.5940
90.0	0.0570	39.751	2.8359
100.0	0.0398	40.230	3.0778
200.0	0.0000	41.333	5.5068
Dimensionless External Radius $r_D' = 6$			
2.0	1.3989	3.596	0.6638
3.0	1.3255	4.954	0.7127
4.0	1.2807	6.256	0.7449
5.0	1.2477	7.520	0.7687
6.0	1.2201	8.753	0.7881
7.0	1.1951	9.961	0.8051
8.0	1.1714	11.144	0.8207
9.0	1.1487	12.304	0.8356
10.0	1.1265	13.441	0.8501
20.0	0.9283	23.683	0.9903
30.0	0.7650	32.123	1.1298
40.0	0.6304	39.078	1.2693
50.0	0.5195	44.810	1.4089
60.0	0.4281	49.534	1.5484
70.0	0.3528	53.426	1.6879
80.0	0.2907	56.634	1.8275
90.0	0.2396	59.277	1.9670
100.0	0.1974	61.455	2.1065
200.0	0.0285	70.191	3.5019
300.0	0.0041	71.453	4.8972
400.0	0.0006	71.636	6.2926
500.0	0.0001	71.662	7.6879
600.0	0.0000	71.666	9.0833
700.0	0.0000	71.666	10.4786
800.0	0.0000	71.667	11.8740
Dimensionless External Radius $r_D' = 7$			
3.0	1.3257	4.95	0.7127
4.0	1.2820	6.26	0.7446
5.0	1.2519	7.52	0.7678
6.0	1.2289	8.76	0.7857
7.0	1.2099	9.98	0.8004
8.0	1.1933	11.18	0.8131
9.0	1.1780	12.37	0.8244
10.0	1.1636	13.54	0.8348
20.0	1.0354	24.52	0.9255
30.0	0.9223	34.30	1.0133
40.0	0.8216	43.01	1.1010
50.0	0.7318	50.76	1.1887
60.0	0.6518	57.68	1.2765
70.0	0.5806	63.83	1.3642
80.0	0.5172	69.31	1.4519
90.0	0.4607	74.20	1.5396
100.0	0.4104	78.55	1.6273
200.0	0.1290	102.86	2.5045
300.0	0.0406	110.51	3.3817
400.0	0.0127	112.91	4.2598
500.0	0.0040	113.66	5.1361
600.0	0.0012	113.90	6.0133
700.0	0.0004	113.97	6.8905
800.0	0.0001	113.99	7.7677
900.0	0.0000	114.00	8.6449
1,000.0	0.0000	114.00	9.5221

TABLE 2—LIMITED SYSTEMS (continued)

Dimensionless External Radius $r_D' = 8$

Time (t_D)	Rate (q_D)	Influx (F_D)	Pressure Drop (p_D)
4.0	1.2821	6.26	0.7446
5.0	1.2523	7.52	0.7678
6.0	1.2302	8.76	0.7854
7.0	1.2128	9.98	0.7996
8.0	1.1983	11.19	0.8115
9.0	1.1859	12.38	0.8216
10.0	1.1747	13.56	0.8306
20.0	1.0860	24.85	0.8971
30.0	1.0078	35.31	0.9561
40.0	0.9354	45.02	1.0148
50.0	0.8681	54.04	1.0735
60.0	0.8056	62.40	1.1322
70.0	0.7477	70.17	1.1910
80.0	0.6939	77.37	1.2497
90.0	0.6440	84.06	1.3084
100.0	0.5976	90.26	1.3671
200.0	0.2832	132.37	1.9542
300.0	0.1342	152.34	2.5412
400.0	0.0637	161.80	3.1283
500.0	0.0302	166.29	3.7154
600.0	0.0143	168.41	4.3025
700.0	0.0068	169.42	4.8896
800.0	0.0032	169.90	5.4767
900.0	0.0015	170.13	6.0638
1,000.0	0.0007	170.24	6.6508
2,000.0	0.0000	170.33	12.5218

Dimensionless External Radius $r_D' = 9$

Time (t_D)	Rate (q_D)	Influx (F_D)	Pressure Drop (p_D)
5.0	1.2523	7.52	0.7676
6.0	1.2303	8.76	0.7853
7.0	1.2132	9.99	0.7995
8.0	1.1993	11.19	0.8112
9.0	1.1877	12.38	0.8211
10.0	1.1776	13.57	0.8296
20.0	1.1094	24.98	0.8848
30.0	1.0539	35.70	0.9271
40.0	1.0015	46.04	0.9684
50.0	0.9518	55.83	1.0096
60.0	0.9045	65.11	1.0508
70.0	0.8596	73.92	1.0920
80.0	0.8169	82.30	1.1332
90.0	0.7763	90.27	1.1745
100.0	0.7378	97.84	1.2157
200.0	0.4433	155.64	1.6278
300.0	0.2663	190.37	2.0398
400.0	0.1600	211.24	2.4519
500.0	0.0962	223.79	2.8640
600.0	0.0578	231.32	3.2761
700.0	0.0347	235.85	3.6882
800.0	0.0209	238.57	4.1003
900.0	0.0125	240.21	4.5124
1,000.0	0.0075	241.19	4.9245
2,000.0	0.0000	242.67	9.0455

Dimensionless External Radius $r_D' = 10$

Time (t_D)	Rate (q_D)	Influx (F_D)	Pressure Drop (p_D)
6.0	1.2303	8.76	0.7853
7.0	1.2132	9.99	0.7995
8.0	1.1995	11.19	0.8112
9.0	1.1880	12.38	0.8210
10.0	1.1783	13.57	0.8295
20.0	1.1196	25.02	0.8797
30.0	1.0783	36.01	0.9124
40.0	1.0398	46.60	0.9427
50.0	1.0027	56.81	0.9728
60.0	0.9669	66.66	1.0028
70.0	0.9325	76.15	1.0329
80.0	0.8992	85.31	1.0629
90.0	0.8672	94.14	1.0929
100.0	0.8362	102.66	1.1229
200.0	0.5816	172.78	1.4232
300.0	0.4045	221.56	1.7235
400.0	0.2813	255.48	2.0238
500.0	0.1956	279.07	2.3241
600.0	0.1361	295.49	2.6244
700.0	0.0947	306.90	2.9247
800.0	0.0659	314.85	3.2250
900.0	0.0458	320.37	3.5253
1,000.0	0.0319	324.22	3.8256
2,000.0	0.0008	332.77	6.8287
3,000.0	0.0000	332.99	9.8317
4,000.0	0.0000	333.00	12.8347

Dimensionless External Radius $r_D' = 20$

Time (t_D)	Rate (q_D)	Influx (F_D)	Pressure Drop (p_D)
30.0	1.1030	36.2	0.8977
40.0	1.0892	47.1	0.9106
50.0	1.0796	58.0	0.9199
60.0	1.0724	68.7	0.9270
70.0	1.0664	79.4	0.9328
80.0	1.0611	90.1	0.9378
90.0	1.0562	100.7	0.9423
100.0	1.0516	111.2	0.9465
200.0	1.0088	214.2	0.9851
300.0	0.9681	313.0	1.0229
400.0	0.9291	407.9	1.0604
500.0	0.8916	498.9	1.0979
600.0	0.8557	586.2	1.1354
700.0	0.8212	670.1	1.1729
800.0	0.7881	750.5	1.2104
900.0	0.7563	827.7	1.2479
1,000.0	0.7259	901.8	1.2854
2,000.0	0.4810	1,496.9	1.6604
3,000.0	0.3187	1,891.2	2.0355
4,000.0	0.2111	2,152.4	2.4105
5,000.0	0.1400	2,325.7	2.7856
6,000.0	0.0929	2,440.5	3.1606
7,000.0	0.0616	2,516.7	3.5357
8,000.0	0.0408	2,567.1	3.9107
9,000.0	0.0270	2,600.6	4.2858
10,000.0	0.0179	2,622.7	4.6608
20,000.0	0.0000	2,666.3	8.4113

Dimensionless External Radius $r_D' = 30$

Time (t_D)	Rate (q_D)	Influx (F_D)	Pressure Drop (p_D)
80.0	1.0631	90.1	0.9351
90.0	1.0595	100.7	0.9385
100.0	1.0564	111.3	0.9414
200.0	1.0381	215.9	0.9600
300.0	1.0254	319.1	0.9724
400.0	1.0133	421.0	0.9840
500.0	1.0014	521.7	0.9954
600.0	0.9895	621.3	1.0068
700.0	0.9780	719.7	1.0179
800.0	0.9665	816.9	1.0290
900.0	0.9552	913.0	1.0401
1,000.0	0.9439	1,007.9	1.0512
2,000.0	0.8388	1,898.3	1.1623
3,000.0	0.7453	2,689.4	1.2735
4,000.0	0.6622	3,392.4	1.3846
5,000.0	0.5884	4,017.0	1.4957
6,000.0	0.5228	4,572.0	1.6068
7,000.0	0.4646	5,065.2	1.7179
8,000.0	0.4128	5,503.4	1.8290
9,000.0	0.3668	5,892.7	1.9401
10,000.0	0.3259	6,238.6	2.0513
20,000.0	0.1000	8,153.6	3.1624
30,000.0	0.0307	8,739.1	4.2736
40,000.0	0.0094	8,919.7	5.3847
50,000.0	0.0029	8,975.1	6.4959
60,000.0	0.0009	8,992.1	7.6070
70,000.0	0.0003	8,997.3	8.7182
80,000.0	0.0001	8,998.9	9.8293
90,000.0	0.0000	8,999.4	10.9405
100,000.0	0.0000	8,999.6	12.0516

Dimensionless External Radius $r_D' = 40$

Time (t_D)	Rate (q_D)	Influx (F_D)	Pressure Drop (p_D)
100.0	1.0564	111.0	0.9416
200.0	1.0398	216.0	0.9570
300.0	1.0320	320.0	0.9653
400.0	1.0262	422.0	0.9715
500.0	1.0210	525.0	0.9769
600.0	1.0160	627.0	0.9820
700.0	1.0110	728.0	0.9871
800.0	1.0060	829.0	0.9925
900.0	1.0011	929.0	0.9972
1,000.0	0.9962	1,029.0	1.0019
2,000.0	0.9485	2,001.0	1.0488
3,000.0	0.9031	2,927.0	1.0957
4,000.0	0.8598	3,808.0	1.1425
5,000.0	0.8186	4,647.0	1.1894
6,000.0	0.7794	5,446.0	1.2363
7,000.0	0.7421	6,207.0	1.2832
8,000.0	0.7066	6,931.0	1.3301
9,000.0	0.6727	7,620.0	1.3769
10,000.0	0.6405	8,277.0	1.4238
20,000.0	0.3920	13,339.0	1.8926
30,000.0	0.2400	16,436.0	2.3613
40,000.0	0.1472	18,333.0	2.8301
50,000.0	0.0901	19,496.0	3.2988
60,000.0	0.0552	20,208.0	3.7676
70,000.0	0.0338	20,644.0	4.2363
80,000.0	0.0207	20,911.0	4.7051
90,000.0	0.0127	21,075.0	5.1739
100,000.0	0.0078	21,175.0	5.6426
200,000.0	0.0000	21,333.0	10.3302

TABLE 2—LIMITED SYSTEMS (continued)

Time (t_D)	Rate (q_D)	Influx (F_D)	Pressure Drop (p_D)
Dimensionless External Radius $r_D^* = 50$			
200.0	1.0319	216.0	0.9570
300.0	1.0325	320.0	0.9641
400.0	1.0280	422.0	0.9693
500.0	1.0246	525.0	0.9732
600.0	1.0217	628.0	0.9763
700.0	1.0190	730.0	0.9795
800.0	1.0164	831.0	0.9823
900.0	1.0139	933.0	0.9856
1,000.0	1.0113	1,034.0	0.9880
2,000.0	0.9865	2,033.0	1.0130
3,000.0	0.9622	3,007.0	1.0360
4,000.0	0.9385	3,958.0	1.0600
5,000.0	0.9155	4,884.0	1.0840
6,000.0	0.8930	5,787.0	1.1080
7,000.0	0.8710	6,671.0	1.1320
8,000.0	0.8496	7,531.0	1.1560
9,000.0	0.8287	8,370.0	1.1800
10,000.0	0.8083	9,188.0	1.2040
20,000.0	0.6301	16,344.0	1.4440
30,000.0	0.4912	21,921.0	1.6840
40,000.0	0.3828	26,269.0	1.9240
50,000.0	0.2984	29,658.0	2.1640
60,000.0	0.2326	32,299.0	2.4040
70,000.0	0.1818	34,357.0	2.6440
80,000.0	0.1418	35,967.0	2.8840
90,000.0	0.1106	37,222.0	3.1240
100,000.0	0.0862	38,201.0	3.3640
200,000.0	0.0072	41,378.0	5.7641
300,000.0	0.0006	41,642.0	8.1641
400,000.0	0.0000	41,664.0	10.5641
500,000.0	0.0000	41,666.0	12.9641
Dimensionless External Radius $r_D^* = 60$			
300.0	1.0326	320.0	0.9641
400.0	1.0282	423.0	0.9684
500.0	1.0232	525.0	0.9717
600.0	1.0220	628.0	0.9743
700.0	1.0209	730.0	0.9765
800.0	1.0192	832.0	0.9784
900.0	1.0176	934.0	0.9801
1,000.0	1.0160	1,035.0	0.9818
2,000.0	1.0015	2,044.0	0.9969
3,000.0	0.9872	3,038.0	1.0117
4,000.0	0.9732	4,019.0	1.0256
5,000.0	0.9594	4,985.0	1.0395
6,000.0	0.9457	5,937.0	1.0533
7,000.0	0.9323	6,876.0	1.0672
8,000.0	0.9190	7,802.0	1.0811
9,000.0	0.9060	8,714.0	1.0950
10,000.0	0.8931	9,614.0	1.1089
20,000.0	0.7739	17,935.0	1.2478
30,000.0	0.6706	25,145.0	1.3867
40,000.0	0.5811	31,393.0	1.5256
50,000.0	0.5036	36,808.0	1.6645
60,000.0	0.4363	41,499.0	1.8034
70,000.0	0.3780	45,564.0	1.9422
80,000.0	0.3275	49,086.0	2.0811
90,000.0	0.2838	52,137.0	2.2200
100,000.0	0.2458	54,781.0	2.3589
200,000.0	0.0590	67,879.0	3.7478
300,000.0	0.0141	71,014.0	5.1367
400,000.0	0.0034	71,764.0	6.5256
500,000.0	0.0008	71,943.0	7.9145
600,000.0	0.0002	71,986.0	9.3034
700,000.0	0.0000	71,996.0	10.6923
800,000.0	0.0000	72,000.0	12.0812
Dimensionless External Radius $r_D^* = 70$			
700.0	1.0213	730.0	0.9753
800.0	1.0190	832.0	0.9769
900.0	1.0185	934.0	0.9785
1,000.0	1.0174	1,036.0	0.9799
2,000.0	1.0079	2,048.0	0.9906
3,000.0	0.9989	3,052.0	1.0005
4,000.0	0.9899	4,046.0	1.0093
5,000.0	0.9811	5,032.0	1.0180
6,000.0	0.9723	6,008.0	1.0268
7,000.0	0.9636	6,976.0	1.0355
8,000.0	0.9550	7,936.0	1.0443
9,000.0	0.9465	8,886.0	1.0530
10,000.0	0.9380	9,829.0	1.0618
20,000.0	0.8575	18,800.0	1.1492
30,000.0	0.7838	27,002.0	1.2367
40,000.0	0.7165	34,498.0	1.3241
50,000.0	0.6549	41,351.0	1.4116
60,000.0	0.5987	47,615.0	1.4991
70,000.0	0.5472	53,341.0	1.5865
80,000.0	0.5002	58,575.0	1.6740
90,000.0	0.4572	63,359.0	1.7615
100,000.0	0.4179	67,732.0	1.8489
200,000.0	0.1701	95,296.0	2.7236
300,000.0	0.0692	106,570.0	3.5982
400,000.0	0.0280	111,168.0	4.4728
500,000.0	0.0113	113,042.0	5.3475
600,000.0	0.0045	113,807.0	6.2221
700,000.0	0.0018	114,118.0	7.0968
800,000.0	0.0007	114,245.0	7.9714
900,000.0	0.0003	114,297.0	8.8460
1,000,000.0	0.0001	114,318.0	9.7207
2,000,000.0	0.0000	114,333.0	12.4677
Dimensionless External Radius $r_D^* = 80$			
900.0	1.0188	934.0	0.9779
1,000.0	1.0178	1,036.0	0.9791
2,000.0	1.0103	2,050.0	0.9875
3,000.0	1.0047	3,057.0	0.9944
4,000.0	0.9987	4,059.0	1.0009
5,000.0	0.9927	5,055.0	1.0068
6,000.0	0.9863	6,045.0	1.0127
7,000.0	0.9809	7,028.0	1.0185
8,000.0	0.9750	8,006.0	1.0244
9,000.0	0.9692	8,978.0	1.0302
10,000.0	0.9634	9,945.0	1.0361
20,000.0	0.9073	19,275.0	1.0947
30,000.0	0.8545	28,102.0	1.1533
40,000.0	0.8048	36,396.0	1.2119
50,000.0	0.7579	44,207.0	1.2705
60,000.0	0.7138	51,564.0	1.3291
70,000.0	0.6723	58,493.0	1.3877
80,000.0	0.6331	65,018.0	1.4463
90,000.0	0.5963	71,163.0	1.5049
100,000.0	0.5616	76,950.0	1.5634
200,000.0	0.3081	119,176.0	2.1494
300,000.0	0.1697	142,333.0	2.7353
400,000.0	0.0933	155,096.0	3.3213
500,000.0	0.0512	162,112.0	3.9072
600,000.0	0.0281	165,967.0	4.4931
700,000.0	0.0155	168,084.0	5.0791
800,000.0	0.0085	169,248.0	5.6650
900,000.0	0.0047	169,887.0	6.2510
1,000,000.0	0.0026	170,238.0	6.8369
2,000,000.0	0.0000	170,666.0	12.6963
Dimensionless External Radius $r_D^* = 90$			
1,000.0	1.0178	1,036.0	0.9789
2,000.0	1.0119	2,050.0	0.9864
3,000.0	1.0075	3,060.0	0.9914
4,000.0	1.0033	4,065.0	0.9965
5,000.0	0.9991	5,066.0	1.0006
6,000.0	0.9949	6,063.0	1.0047
7,000.0	0.9907	7,056.0	1.0088
8,000.0	0.9866	8,045.0	1.0129
9,000.0	0.9824	9,029.0	1.0170
10,000.0	0.9783	10,010.0	1.0212
20,000.0	0.9381	19,590.0	1.0623
30,000.0	0.8995	28,776.0	1.1035
40,000.0	0.8625	37,585.0	1.1446
50,000.0	0.8270	46,031.0	1.1858
60,000.0	0.7930	54,129.0	1.2269
70,000.0	0.7603	61,895.0	1.2681
80,000.0	0.7291	69,341.0	1.3092
90,000.0	0.6991	76,480.0	1.3504
100,000.0	0.6703	83,326.0	1.3915
200,000.0	0.4402	138,050.0	1.8031
300,000.0	0.2890	173,987.0	2.2146
400,000.0	0.1905	197,575.0	2.6261
500,000.0	0.1253	213,137.0	3.0376
600,000.0	0.0824	223,370.0	3.4491
700,000.0	0.0541	230,097.0	3.8607
800,000.0	0.0356	234,519.0	4.2722
900,000.0	0.0234	237,425.0	4.6837
1,000,000.0	0.0154	239,335.0	5.0952
2,000,000.0	0.0000	243,000.0	9.2104
Dimensionless External Radius $r_D^* = 100$			
1,000.0	1.0178	1,036.0	0.9789
2,000.0	1.0123	2,050.0	0.9853
3,000.0	1.0090	3,061.0	0.9894
4,000.0	1.0058	4,068.0	0.9930
5,000.0	1.0028	5,073.0	0.9964
6,000.0	0.9997	6,074.0	1.0000
7,000.0	0.9967	7,072.0	1.0030
8,000.0	0.9936	8,067.0	1.0060
9,000.0	0.9906	9,059.0	1.0090
10,000.0	0.9876	10,048.0	1.0120
20,000.0	0.9578	19,775.0	1.0420
30,000.0	0.9290	29,208.0	1.0720
40,000.0	0.9010	38,358.0	1.1020
50,000.0	0.8739	47,232.0	1.1320
60,000.0	0.8476	55,839.0	1.1620
70,000.0	0.8221	64,187.0	1.1920
80,000.0	0.7974	72,283.0	1.2220
90,000.0	0.7733	80,136.0	1.2520
100,000.0	0.7501	87,753.0	1.2820
200,000.0	0.5525	152,377.0	1.5820
300,000.0	0.4068	199,972.0	1.8820
400,000.0	0.2995	235,018.0	2.1820
500,000.0	0.2210	260,815.0	2.4820
600,000.0	0.1633	279,849.0	2.7820
700,000.0	0.1203	293,918.0	3.0820
800,000.0	0.0887	304,287.0	3.3820
900,000.0	0.0653	311,928.0	3.6820
1,000,000.0	0.0482	317,558.0	3.9820
2,000,000.0	0.0000	333,333.0	6.9820

TABLE 3 — LIMITED SYSTEMS
Open External Boundary

Time (t_D)	Rate (q_D)	Influx (F_D)	Pressure Drop (p_D)
Dimensionless External Radius $r_D' = 2$			
0.07	3.1324	0.3685	0.2404
0.08	2.9947	0.3992	0.2534
0.09	2.8807	0.4285	0.2654
0.10	2.7843	0.4568	0.2764
0.20	2.2786	0.7052	0.3558
0.30	2.1036	[illegible]	0.4048
0.40	2.0386	1.1294	0.4370
0.50	2.0144	1.3319	0.4582
0.60	2.0054	1.5328	0.4723
0.70	2.0020	1.7331	0.4817
0.80	2.0007	1.9333	0.4878
0.90	2.0003	2.1333	0.4919
1.00	2.0001	2.3333	0.4947
2.00	2.0000	4.3333	0.4999
3.00	2.0000	6.3333	0.5000
Dimensionless External Radius $r_D' = 3$			
0.2	2.2616	0.7046	0.3562
0.3	2.0301	0.9180	0.4080
0.4	1.8921	1.1137	0.4464
0.5	1.7984	1.2979	0.4768
0.6	1.7302	1.4742	0.5019
0.7	1.6788	1.6445	0.5230
0.8	1.6393	1.8103	0.5412
0.9	1.6087	1.9727	0.5568
1.0	1.5849	2.1323	0.5704
2.0	1.5072	3.6638	0.6407
3.0	1.5006	5.1664	0.6397
4.0	1.5001	6.6666	0.6648
5.0	1.5000	8.1667	0.6661
6.0	1.5000	9.6667	0.6665
7.0	1.5000	11.1667	0.6666
Dimensionless External Radius $r_D' = 4$			
0.7	1.6743	1.6441	0.5233
0.8	1.6308	1.8093	0.5418
0.9	1.5948	1.9705	0.5580
1.0	1.5643	2.1284	0.5724
2.0	1.4078	3.5988	0.6625
3.0	1.3582	4.9773	0.7054
4.0	1.3416	6.3258	0.7272
5.0	1.3361	7.6641	0.7383
6.0	1.3343	8.9992	0.7440
7.0	1.3336	10.3331	0.7469
8.0	1.3334	11.6666	0.7484
9.0	1.3334	13.0000	0.7492
10.0	1.3333	14.3333	0.7496
20.0	1.3333	27.6667	0.7500
Dimensionless External Radius $r_D' = 5$			
1.0	1.5642	2.1284	0.5724
2.0	1.3992	3.5958	0.6638
3.0	1.3289	4.9558	0.7121
4.0	1.2924	6.2646	0.7422
5.0	1.2729	7.5462	0.7618
6.0	1.2623	8.8133	0.7748
7.0	1.2567	10.0725	0.7833
8.0	1.2536	11.3275	0.7890
9.0	1.2519	12.5802	0.7927
10.0	1.2510	13.8316	0.7952
20.0	1.2500	26.3333	0.7999
30.0	1.2500	38.8333	0.8000
Dimensionless External Radius $r_D' = 6$			
2.0	1.3989	3.5958	0.6638
3.0	1.3259	4.9545	0.7126
4.0	1.2832	6.2573	0.7444
5.0	1.2557	7.5258	0.7649
6.0	1.2375	8.7718	0.7834
7.0	1.2252	10.0028	0.7957
8.0	1.2170	11.2236	0.8050
9.0	1.2115	12.4377	0.8119
10.0	1.2077	13.6471	0.8172
20.0	1.2001	25.6663	0.8324
30.0	1.2000	37.6667	0.8333
40.0	1.2000	49.6667	0.8333
Dimensionless External Radius $r_D' = 7$			
3.0	1.3257	4.9544	0.7127
4.0	1.2822	6.2568	0.7446
5.0	1.2527	7.5234	0.7676
6.0	1.2315	8.7649	0.7851
7.0	1.2157	9.9881	0.7988
8.0	1.2039	11.1977	0.8098
9.0	1.1950	12.3969	0.8187
10.0	1.1882	13.5883	0.8258
20.0	1.1681	25.3283	0.8531
30.0	1.1668	37.0000	0.8566
40.0	1.1667	48.6666	0.8571
50.0	1.1667	60.3333	0.8571
Dimensionless External Radius $r_D' = 8$			
4.0	1.2821	6.2568	0.7446
5.0	1.2523	7.5231	0.7676
6.0	1.2305	8.7640	0.7853
7.0	1.2136	9.9857	0.7944
8.0	1.2003	11.1925	0.8109
9.0	1.1897	12.3873	0.8205
10.0	1.1811	13.5725	0.8285
20.0	1.1479	25.1652	0.8653
30.0	1.1435	36.6157	0.8730
40.0	1.1429	48.0472	0.8746
50.0	1.1429	59.4761	0.8749
60.0	1.1429	70.9048	0.8750
70.0	1.1429	82.3333	0.8750
Dimensionless External Radius $r_D' = 9$			
5.0	1.2523	7.5231	0.7676
6.0	1.2303	8.7640	0.7853
7.0	1.2133	9.9854	0.7995
8.0	1.1996	11.1917	0.8111
9.0	1.1884	12.3855	0.8209
10.0	1.1790	13.5690	0.8292
20.0	1.1364	25.0925	0.8717
30.0	1.1274	36.4008	0.8838
40.0	1.1255	47.6633	0.8874
50.0	1.1251	58.9159	0.8884
60.0	1.1250	70.1665	0.8888
70.0	1.1250	81 1166	0.8889
80.0	1.1250	92.6667	0.8889
Dimensionless External Radius $r_D' = 10$			
6.0	1.2303	8.764	0.7853
7.0	1.2132	9.985	0.7994
8.0	1.1995	11.192	0.8111
9.0	1.1881	12.385	0.8209
10.0	1.1785	13.568	0.8293
20.0	1.1306	25.063	0.8747
30.0	1.1169	36.286	0.8906
40.0	1.1128	47.431	0.8965
50.0	1.1116	58.551	0.8987
60.0	1.1113	69.665	0.8995
70.0	1.1112	80.777	0.8998
80.0	1.1111	91.889	0.8999
90.0	1.1111	103.000	0.9000
Dimensionless External Radius $r_D' = 20$			
30.0	1.1030	36.180	0.8977
40.0	1.0892	47.137	0.9106
50.0	1.0799	57.980	0.9193
60.0	1.0732	68.743	0.9261
70.0	1.0682	79.449	0.9312
80.0	1.0645	90.112	0.9351
90.0	1.0616	100.741	0.9382
100.0	1.0595	111.346	0.9406
200.0	1.0531	216.843	0.9486
300.0	1.0527	322.122	0.9495
400.0	1.0526	427.386	0.9497
500.0	1.0526	532.649	0.9499
600.0	1.0526	637.912	0.9500

$$p_D(r_D,t_D) = \frac{r_D' - r_D}{r_D' r_D} + \frac{2(r_D'-1)}{r_D} \sum_{n=1}^{\infty} \times \frac{\exp\left[-\frac{w_n^2 t_D}{(r_D'-1)^2}\right] \sin\left[w_n\left(\frac{r_D'-r_D}{r_D'-1}\right)\right]}{w_n[r_D'(r_D'-1)+w_n^2]\cos w_n}, \quad \ldots\ldots (62)$$

where w_n are the roots of the equation:

$$\frac{\tan w}{w} = -\frac{1}{r_D'-1} \quad \ldots\ldots (63)$$

Upon placing r_D at unity in Eq. 62 and simplifying, the dimensionless pressure drop is obtained:

$$p_D = \frac{r_D'-1}{r_D'} - 2(r_D'-1) \sum_{n=1}^{\infty} \frac{\exp\left[-\frac{w_n^2 t_D}{(r_D'-1)^2}\right]}{r_D'(r_D'-1)+w_n^2}, \quad \ldots (64)$$

which is the concluding result.[9-11,17]

NUMERICAL COMPUTATION OF PARTICULAR SOLUTIONS

Nine particular solutions to Eq. 7 obtained with the aid of the Laplace transformation were numerically computed. Specifically, these included the functions defined by Eqs. 34, 36, 40, 46, 49, 53, 58, 60 and 64.

The numerical computations were carried out with the aid of IBM 1401 and 1620 computer systems. Programming was in FORTRAN. The functions for

TABLE 3 — LIMITED SYSTEMS (Continued)

Dimensionless Functions			
Time (t_D)	Rate (e_D)	Influx (F_D)	Pressure Drop (p_D)
Dimensionless External Radius $r_D' = 30$			
80.0	1.0631	90.093	0.9351
90.0	1.0595	100.705	0.9385
100.0	1.0564	111.284	0.9414
200.0	1.0411	216.001	0.9576
300.0	1.0365	319.838	0.9629
400.0	1.0351	423.406	0.9649
500.0	1.0347	526.891	0.9656
600.0	1.0345	630.351	0.9660
700.0	1.0345	733.803	0.9662
800.0	1.0345	837.252	0.9664
900.0	1.0345	940.701	0.9665
1,000.0	1.0345	1,044.149	0.9667
Dimensionless External Radius $r_D' = 40$			
100.0	1.0564	111.28	0.9414
200.0	1.0399	215.96	0.9570
300.0	1.0330	319.56	0.9646
400.0	1.0295	422.67	0.9686
500.0	1.0276	525.51	0.9708
600.0	1.0267	628.22	0.9721
700.0	1.0262	730.86	0.9729
800.0	1.0259	833.47	0.9734
900.0	1.0258	936.05	0.9737
1,000.0	1.0257	1,038.63	0.9739
2,000.0	1.0256	2,064.28	0.9750
Dimensionless External Radius $r_D' = 50$			
200.0	1.0399	215.96	0.9570
300.0	1.0326	319.54	0.9641
400.0	1.0283	422.58	0.9688
500.0	1.0256	525.27	0.9718
600.0	1.0239	627.74	0.9739
700.0	1.0227	730.06	0.9754
800.0	1.0219	832.29	0.9764
900.0	1.0214	934.46	0.9771
1,000.0	1.0211	1,036.58	0.9776
2,000.0	1.0204	2,057.15	0.9794
3,000.0	1.0204	3,077.56	0.9800
Dimensionless External Radius $r_D' = 60$			
300.0	1.0326	319.54	0.9641
400.0	1.0282	422.57	0.9684
500.0	1.0253	525.23	0.9716
600.0	1.0232	627.63	0.9740
700.0	1.0216	729.89	0.9758
800.0	1.0205	831.99	0.9772
900.0	1.0196	933.99	0.9783
1,000.0	1.0189	1,035.91	0.9792
2,000.0	1.0171	2,053.52	0.9822
3,000.0	1.0170	3,070.51	0.9829
4,000.0	1.0169	4,087.46	0.9833
Dimensionless External Radius $r_D' = 70$			
700.0	1.0213	730.0	0.9753
800.0	1.0200	832.0	0.9767
900.0	1.0190	934.0	0.9781
1,000.0	1.0181	1,036.0	0.9795
2,000.0	1.0150	2,052.0	0.9838
3,000.0	1.0146	3,066.0	0.9848
4,000.0	1.0145	4,081.0	0.9853
5,000.0	1.0145	5,095.0	0.9857
6,000.0	1.0145	6,110.0	0.9857
Dimensionless External Radius $r_D' = 80$			
900.0	1.0188	934.0	0.9779
1,000.0	1.0179	1,036.0	0.9794
2,000.0	1.0137	2,051.0	0.9847
3,000.0	1.0129	3,064.0	0.9862
4,000.0	1.0127	4,077.0	0.9868
5,000.0	1.0127	5,090.0	0.9872
6,000.0	1.0127	6,102.0	0.9875
7,000.0	1.0127	7,115.0	0.9875
Dimensionless External Radius $r_D' = 90$			
1,000.0	1.0178	1,036.0	0.9789
2,000.0	1.0131	2,051.0	0.9850
3,000.0	1.0118	3,063.0	0.9870
4,000.0	1.0114	4,074.0	0.9878
5,000.0	1.0113	5,086.0	0.9883
6,000.0	1.0112	6,097.0	0.9886
7,000.0	1.0112	7,108.0	0.9889
8,000.0	1.0112	8,120.0	0.9889
Dimensionless External Radius $r_D' = 100$			
1,000.0	1.0178	1,036.0	0.9789
2,000.0	1.0128	2,051.0	0.9846
3,000.0	1.0111	3,062.0	0.9874
4,000.0	1.0105	4,073.0	0.9885
5,000.0	1.0102	5,083.0	0.9891
6,000.0	1.0101	6,094.0	0.9894
7,000.0	1.0101	7,104.0	0.9897
8,000.0	1.0101	8,114.0	0.9899
9,000.0	1.0101	9,124.0	0.9900

the unlimited system were computed first over the dimensionless time range 0.001 to 1,000,000. Then tables of the trigonometric relations described by Eqs. 47, 52 and 63 were developed from which the roots w_n (with $n = 6$) were obtained. Finally, numerical values of the functions for limited systems were computed over the range of external radii (r_D') 2 to 100. The range of dimensionless time (t_D) for these functions was chosen to begin with the points of divergence from the unlimited system envelope and to end with steady-state values. These numerical results are included in tabular form to foster practical application of this work.

NOMENCLATURE

C_1, C_2 = arbitrary constants
F = cumulative fluid influx
F_D = dimensionless cumulative fluid influx
$\bar{F}_D$ = Laplace transform of F_D
R_0 = residue of singularity at origin
R_n = residues of singularities at z_n
b = dimensionless product of pressure drop and radial distance
$\bar{b}$ = Laplace transform of b
c = compressibility
e = rate of fluid influx or fluid rate
e_D = dimensionless rate of fluid influx
$\bar{e}_D$ = Laplace transform of e_D
k = permeability
k_h = horizontal permeability
k_r = radial permeability in spherical system
k_v = vertical permeability
n = element of domain of positive integers
p = pressure
p_i = initial pressure
p_D = dimensionless pressure drop
r = radial distance, length of radius vector of sphere
r_e = radius of external boundary
r_w = radius of internal boundary
r_D = dimensionless radial distance
r_D' = dimensionless radius of external boundary
s = Laplace transform parameter, a complex variable
t = time
t_r = readjustment time
t_D = dimensionless time
t' = maximum time
u = macroscopic velocity in porous media
w = arbitrary real variable
z = complex variable
α = colatitude angle, spherical coordinates
γ = abscissa of convergence
δ = arbitrary parameter
θ = longitudinal angle, spherical coordinates
θ_4 = Jacobian theta function, also denoted by θ_0 or θ
μ = viscosity
ϕ = porosity
Δp = cumulative pressure drop

ACKNOWLEDGMENTS

Grateful acknowledgment is made to A. S. Odeh of Mobil Oil Co.'s Field Research Laboratories who reviewed this work, critically checked the mathematics and offered some valuable criticisms. The author wishes to express his appreciation to Deno Ladas of IBM Corp. for his help in programming the analytic functions and to William Chichester for his help in their computation. Thankful acknowledgment is also made to H. L. Smith of the U. S. Corps of Engineers for his practical suggestions and encouragement to publish this paper.

REFERENCES

1. Hurst, W.: "Water Influx into a Reservoir and Its Application to the Equation of Volumetric Balance", *Trans.*, AIME (1943) Vol. 151, 57.
2. Hurst, W. and van Everdingen, A. F.: "The Application of the Laplace Transformation to Flow Problems in Reservoirs", *Trans.*, AIME (1949) Vol. 186, 305.
3. Muskat, M.: *The Flow of Homogeneous Fluids Through Porous Media*, J. W. Edwards, Ann Arbor (1946).
4. Muskat, M.: *Physical Principles of Oil Production*, McGraw-Hill Book Co., New York, N. Y. (1949).
5. Chatas, A. T.: "A Practical Treatment of Nonsteady-State Flow Problems in Reservoir Systems", *Pet. Eng.* (May, June and Aug., 1953) 25.
6. Muskat, M.: "The Performance of Bottom-Water Drive Reservoirs", *Trans.*, AIME (1947) Vol. 170, 81.
7. Hurst, W.: "The Skin Effect and Its Impediment to Fluid Flow into a Wellbore", *Pet. Eng.* (Oct., 1953) Vol. 25, B-6.
8. Eisenhart, L. P.: *An Introduction to Differential Geometry with the Use of the Tensor Calculus*, Princeton U. Press, Princeton, N. J. (1947).
9. Churchill, R. V.: *Modern Operational Mathematics in Engineering*, McGraw-Hill Book Co., New York, N.Y. (1944).
10. Widder, D. V.: *The Laplace Transform*, Princeton U. Press, Princeton, N. J. (1946).
11. Carslaw, H. S. and Jaeger, J. C.: *Operational Methods in Applied Mathematics*, Dover, New York (1963).
12. Bush, V.: *Operational Circuit Analysis*, John Wiley & Sons, Inc., New York, N. Y. (1929).
13. Abramowitz, M. and Stegun, I. A.: *Handbook of Mathematical Functions*, U. S. Government Printing Office, Washington, D. C. (1964).
14. Erdelyi, A. *et al.*: *Tables of Integral Transforms*, McGraw-Hill Book Co., New York, N.Y. (1954) Vol. 1.
15. Hildebrand, F. B.: *Advanced Calculus for Engineers*, Prentice-Hall, Inc., Inglewood Cliffs, N. J. (1948).
16. Murnaghan, F. D.: *Introduction to Applied Mathematics*, Dover, New York (1963).
17. Churchill, R. V.: *Introduction to Complex Variables and Applications*, McGraw-Hill Book Co., New York, N. Y. (1948).
18. Korn, G. A. and Korn, T. M.: *Mathematical Handbook for Scientists and Engineers*, McGraw-Hill Book Co., New York, N. Y. (1961).
19. Erdelyi, A. *et al.*: *Higher Transcendental Functions*, McGraw-Hill Book Co., New York, N.Y. (1953) Vol. II.
20. Carslaw, H. S. and Jaeger, J. C.: *Conduction of Heat in Solids*, Oxford U. Press, Oxford, England (1959).

***

ellipsoid. The equivalent inner radius of this "rugby ball" will depend on the dimensionless time. At early time, it will be a function of its surface area, just as it is for all other geometries, while at later times it will depend on the equivalent flow resistance of an ellipsoid. To the best of my knowledge, these equations have not been worked out for this geometry.

Chatas' solutions are listed in voluminous tables. Some of the nomenclature in his tables is different than we now use. His rate of influx is labeled, e_D, while we now use $q_D(t_D)$. His cumulative influx is labeled F_D, while we now use $Q_D(t_D)$. In his table for the infinite system, he lists e_D, which is $q_D(t_D)$, F_D, which is $Q_D(t_D)$, and p_D. He shows that there are simple equations for these terms. They are,

$$q_D(t_D) = 1 + (\pi t_D)^{-1/2} \tag{77}$$

$$Q_D(t_D) = t_D + 2(t_D / \pi)^{1/2} \tag{78}$$

and

$$p_D(t_D) = 1 - \exp(t_D)\, erfc\left(t_D^{1/2}\right) \tag{79}$$

So it really wasn't necessary to list these values. Equations 77 and 78 are very easy to evaluate. Equation 79, the most complex one, can be evaluated using various simple closed form approximations which are valid at various times, and which are listed in Abramowitz and Stegun's book (1964).

Chatas also lists results for finite systems with closed exterior boundaries in his Table 2, and constant pressure exterior boundaries in Table 3. Based on the work we have done for the linear and radial systems, we would expect that these tables could also be handled with simple analytic solutions. For example, in his Table 2, the closed boundary influx rates and cumulative influxes follow the exponential decline equation. While at constant rate the pressure drop increases linearly with time, according to material balance principles. His Table 3 lists the results for the constant pressure external boundary. Those, too, behave as we would anticipate, obeying Darcy's Law at late times.

I am positive that it would be possible to develop simple appropriate equations to handle these closed systems, just as we did for the linear and radial cases. However, I am not going to do this, for I've seldom seen field cases where the spherical geometry is required. If any reader does run into this geometry, it would be wise to spend the time needed to develop the appropriate approximate equations for his system, for this effort would greatly simplify his resulting calculational procedures.

Conclusions

We've seen that the results of all three geometries (linear, radial and spherical) can be put into simple approximately exact equation forms. These equation forms are all logical, based on an analysis of the physics of flow in the systems. Thus for all the possible inner and outer boundary conditions (Inner Boundary; constant rate or constant pressure: Outer Boundary; infinite, constant pressure or closed) the solutions all behave in a logical manner.

The linear and spherical systems behave in similar ways. The reason is that the spherical equation can be transformed into a differential equation form that is identical to the linear system. A new variable, b_D , which is defined as follows, $b_D = r_D p_D$, changes the spherical differential equation into the same format as the linear equation. As a result both geometries show a square root of time relationship for the infinite system for predicting cumulative encroachment with time. For the linear system, the pressure prediction is also proportional to the square root of time. While for the spherical system, the equation is slightly more complex, but still simple.

For the infinite radial systems, the very early time data also follow square root of time behavior. For a limited time, simple empirical extensions of this idea are valid for either the constant pressure or constant flow rate inner boundary.

The very long time behavior of the infinite radial systems are also logical, being functions of the logarithm of time. Simple empirical adjustements to these late time results are shown for both the constant pressure and constant flow rate inner boundary.

For all the finite systems, either a constant pressure or a closed outer boundary can be assumed. The early time data for these systems all follow the infinite curves. It's possible to define simple equations for the times when this short time behavior is no longer valid. As might be expected, these equations are functions of the sizes of the systems.

Once the outer boundary begins to be felt, the equations, for all practical purposes, jump immediately to the long time form expected for that geometry and boundary condition. For example, for a constant pressure inner and outer boundary, the cumulative influx varies linearly with time, following the steady state Darcy equation. Similarly, for the constant rate inner boundary and a closed outer boundary, the pseudosteady state equations define the linear pressure decline behavior. These statements are true for all three geometries.

By comparison, for a constant rate inner boundary and constant pressure outer boundary, exponential decline behavior is seen. The pressure history is a logarithmic function of dimensionless time. At infinite time the pressure drop is constant, fitting Darcy's Law. Thus on the logarithmic coordinate we graph, $p_D(\infty) - p_D(t_D)$, to depict this exponential behavior.

Similarly, for the constant pressure inner boundary and the closed outer boundary, we also see exponential behavior. This, too, has a limit at infinite time, $Q_D(\infty)$, which is defined by the geometry. The variable graphed on the arithmetic coordinate is again the dimensionless time, while the logarithmic coordinator is $Q_D(\infty) - Q_D(t_D)$.

Thus we've seen that the exact infinite series solutions can be transformed into very accurate closed form approximations which make calculations much easier, and which also give great insight into the behavior of the various solutions. We've also seen that superposition is an important way of handling real data which vary both in pressure and flow rate with time. Many times, the approximate equations can be used to greatly simplify the superposition calculations. Further notes on this subject will discuss how to relate these ideas to reservoir/aquifer combinations, the ultimate goal for reservoir engineering applications.

References

1. Abramowitz, M. and Stegun, I.A.:. Handbook of Mathematical Functions with Formulas, Graphs, and Mathematical Tables, Dover, New York, (1964) pp. 1043.
2. Al-Hussainy, R., Ramey, H.J., Jr., and Crawford, P.B.: "The Flow of Real Gases Through Porous Media," *J. Pet. Tech.* (May 1966) 624-636.
3. Aziz, K. and Flock, D.L.: "Unsteady State Gas Flow -- Use of Drawdown Data in the Prediction of Gas Well Behaviour," *J. Can. Pet. Tech.* 2, (1), (1963) 9-15.
4. Brigham, W.E.: "Injectivity Calculations for Various Flooding Patterns," class notes, PE 270A, Stanford University (1985).
5. Brigham, W.E.: "Pseudo-Steady State Equations," class notes, PE 270A, Stanford University, (1988).
6. Brigham, W.E. and Neri, G.: "Preliminary Results on a Depletion Model for the Gabbro Zone (Northern Part of Larderello Field)," Proceedings, Fifth workshop on Geothermal Reservoir Engineering (December 12-14, 1979), SGP-TR-40, 229-240.
7. Chatas, A.T.: "A Practical Treatment of Nonsteady-State Flow Problems in Reservoir Systems," Petroleum Engineer Series, Part 3, (May 1953), 14-19.
8. Chatas, A.T.: "Unsteady Spherical Flow in Petroleum Reservoirs," SPE 1305, *SPEJ* (June 1966), 102-114.
9. Dee, J.F. and Brigham, W.E.: "A Reservoir Engineering Analysis of a Vapor-Dominated Geothermal Field," *Geothermal Resources Counsel, Trans.* Part II (August 1985).
10. Ehlig-Economides, Christine: "Well Test Analysis for Wells Produced at a Constant Pressure," Ph.D. thesis, Stanford University (June 1979).
11. Katz, Donald L., Cornell, David, Kobayashi, Riki L., Poettmann, Fred H., Vary, John A., Elenbaas, John R., and Weinaug, Charles F.: Underground Storage of Fluids, Ulrich's Books, Inc., Ann Arbor, Michigan (1968) 575 pp.
12. Miller, F.G.: "Theory of Unsteady-State Influx of Water in Linear Reservoirs," *Jour. Inst. of Pet.* 48 (November 1962) 365.
13. Mueller, T.D. and Witherspoon, P.A.: "Pressure Interference Effects Within Reservoirs and Aquifers," *J. Pet. Tech.* 17, 471-474.

14. Nabor, G.W. and Barham, R.H.: "Linear Aquifer Behavior," *Jour. Pet. Tech.* (May 1964) 561-563.

15. Samaniego, V., Brigham, W.E., and Miller, F.G.: "A Performance Prediction Procedure for Transient Flow of Fluids Through Pressure Sensitive Formations," SPE 6051, paper presented at the 51st Annual Fall Meeting, Soc. of Pet. Engr. of AIME, New Orleans, LA (October 3-6, 1976); also *J. Pet. Tech.* (June 1979), 779-786.

16. van Everdingen, A.F. and Hurst, W.: "The Application of the Laplace Transformation to Flow Problems in Reservoirs," *Trans. AIME.* 186 (1949) 305-324.